Multilevel study of nickel oxide nanoparticles-associated effects in Ni hyperaccumulator *Odontarrhena lesbiaca*

Ph.D. Thesis

Selahattin Kondak

Supervisor:

Dr. Zsuzsanna Ördögné Kolbert

associate professor

Doctoral School of Biology

Department of Plant Biology

University of Szeged

Faculty of Science and Informatics

Szeged

2025

Table of Contents

1. List of Abbreviations

ANOVA: Analysis of Variance
APX: Ascorbate peroxidase
AsA: Ascorbic acid
BET: Brunauer–Emmett–Teller
BSA: Bovine Serum Albumin
b-NiO: Bulk nickel oxide
Ca: Calcium
Ca^{2+}: Calcium ion
CAT: Catalase
Cort: Cortex
Cu Kα: Copper K-alpha radiation
Cu^{2+}: Copper ion
DAF-FM DA: 4-amino-5-methylamino 2′,7′-difluorofluorescein diacetate
DHR: Dihydrorhodamine 123
DNA: Deoxyribonucleic acid
ED: Electron Diffraction
EDTA: Ethylenediaminetetraacetic Acid
EDS: Energy Dispersive X-ray Spectroscopy
En: Endodermis
Ex: Exodermis
Fe: Iron
FITC: Fluorescein Isothiocyanate
GR: Glutathione reductase
GSNO: *S*-nitrosoglutathione
GSNOR: GSNO reductase
H_2O_2: Hydrogen Peroxide
HCl: Hydrochloric Acid
He: Helium
HMA4: Heavy Metal ATPase 4
HNO_3: Nitric Acid

H^+-ATPase: Proton-ATPase enzyme
ICP-MS: Inductively Coupled Plasma Mass Spectrometry
IgG: Immunoglobulin G
K: Potassium
LIBS: Laser-induced breakdown spectroscopy
Mg: Magnesium
Mg^{2+}: Magnesium ion
MYB: A family of transcription factors
N_2: Nitrogen
Na: Sodium
NA: Nicotinamine
NADH: Nicotinamide Adenine Dinucleotide
NBP/BCIP: 5-bromo-4-chloro-3-indolylphosphate
NCs: Nanocomposites
Ni: Nickel
Ni^{2+}: Nickel ion
Ni-CHT NPs: Nickel-chitosan nanoparticles
NiCNC: Nickel-chitosan nanoconjugates
$NiCl_2$: Nickel(II) chloride
$NiFe_2O_4$: Nickel ferrite nanoparticles
Ni NPs: Nickel nanoparticles
NiO NPs: Nickel oxide nanoparticles
Ni_2O_3: Nickel(III) oxide
$Ni(OH)_2$: Nickel(II) hydroxide
$NiSO_4$: Nickel sulfate
NMs: Nanomaterials
NO: Nitric oxide
NO_2-BSA: Nitrated Bovine Serum Albumin
NOS-like: Nitric Oxide Synthase-like
NPs: Nanoparticles
NRAMP: Natural Resistance-Associated Macrophage Proteins
$O_2^{\bullet-}$: Superoxide anion
$ONOO^-$: Peroxynitrite

PBS: Phosphate-Buffered Saline

PGPB: Plant Growth-Promoting Bacteria

PTFE: Polytetrafluoroethylene

RNS: Reactive nitrogen species

ROS: Reactive oxygen species

RR: Ruthenium Red

Sc: Scandium

SEM: Scanning Electron Microscopy

SiO_2: Silicon dioxide

SOD: Superoxide dismutase

SDS-PAGE: Sodium Dodecyl Sulfate Polyacrylamide Gel Electrophoresis

TB: Toluidine Blue

TEM: Transmission electron microscopy

Tris: Tris(hydroxymethyl)aminomethane

XRD: X-ray Diffraction

ZIP: Zinc-regulated transporter, Iron-regulated transporter-like Protein

Zn^{2+}: Zinc ion

Xyl: Xylem

2. Introduction

Nickel (Ni) is a naturally present micronutrient that plays a crucial role in plant biology, supporting essential physiological and biochemical processes. Under natural conditions, soil Ni concentrations typically remain below 100 mg/kg. However, industrial activities such as stainless steel and heat-resistant steel manufacturing have substantially increased Ni levels in the environment. This rise poses potential ecological and agricultural concerns, particularly in relation to plant health and development.

Nickel oxide nanoparticles (NiO NPs, 1-100 nm at least in one dimension) have gained considerable interest due to their distinct physicochemical attributes, including high surface area, stability, and antimicrobial properties. These characteristics make them highly valuable in diverse industrial and consumer applications, ranging from metallurgy to electronics. However, large-scale production and utilization of NiO NPs raise concerns about their environmental implications and interactions with biological systems, particularly plants.

Excess Ni accumulation in non-accumulator plants disrupts essential metabolic functions, inhibits enzyme activity, and impairs photosynthesis, leading to visible symptoms such as chlorosis, necrosis, and stunted growth. Additionally, Ni exposure promotes excessive reactive oxygen species (ROS) production, resulting in oxidative stress that compromises membrane stability and overall cellular function. While the impact of Ni on ROS balance in plants has been extensively studied, its influence on reactive nitrogen species (RNS) metabolism remains relatively unexplored. RNS, including nitric oxide (NO) and *S*-nitrosoglutathione (GSNO), play fundamental roles in plant physiology, particularly in stress signaling and regulatory mechanisms. Investigating Ni's effects on RNS metabolism may provide deeper insights into its broader biological consequences.

Serpentine soils, which are characterized by high Ni concentrations and low essential nutrient availability, create challenging conditions for most plant species. However, Ni hyperaccumulators have developed specialized mechanisms that enable them to thrive in such environments by efficiently absorbing, translocating, and sequestering Ni without exhibiting toxicity symptoms. Among the known Ni hyperaccumulators, members of the genus *Odontarrhena* are particularly noteworthy.

One such species, *Odontarrhena lesbiaca*, native to the serpentine soils of Lesbos, Greece, exhibits varying Ni accumulation capacities depending on soil composition.

This study examines three ecotypes of *Odontarrhena lesbiaca* (Ampeliko, Loutra, and Olympos) to explore their responses to NiO NPs. It specifically investigates Ni accumulation, microelement homeostasis, root structure modifications, and nitro-oxidative processes, addressing a critical gap in research on hyperaccumulator interactions with engineered nanoparticles (NPs). Given the increasing prevalence of NiO NPs in the environment and their potential interactions with plant systems, this study aims to improve our understanding of plant-nanoparticle dynamics and contribute to the development of more sustainable nanoparticle applications.

3. Literature Review

3. 1. Nickel: Properties, occurrence, industrial applications, environmental impact, and human exposure

Nickel (Ni; atomic number 28, atomic weight 58.6934; density 8.902 (25 °C); melting point 1453 °C (2647 °F); boiling point 2732 °C (4950 °F); electronic configuration [Ar] $3d^8 4s^2$) is the 24th most abundant element in the Earth's crust and the fifth most abundant by weight after iron, oxygen, magnesium, and silicon. The majority of nickel on Earth is located in the molten outer core, which is composed of an iron-nickel alloy that accounts for about 10% of its composition, lying between the solid inner core and the mantle. Naturally, nickel is found in various forms, often combined with other elements like arsenic, sulfur, and antimony. Nickel metal itself is silver-white, highly conductive in terms of both heat and electricity, and is most commonly found in the +2 oxidation state, though +3 and +4 states can also occur, albeit infrequently (Schaumlöffel, 2012) (**Fig. 1**).

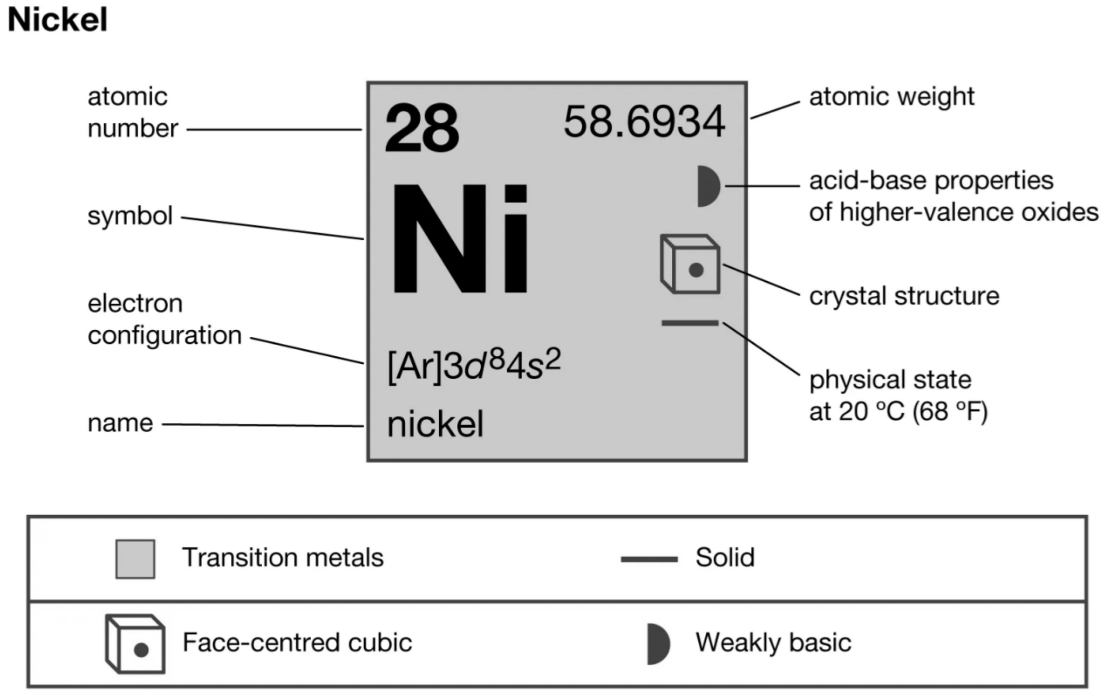

© Encyclopædia Britannica, Inc.

Fig. 1. Definition and properties of Nickel element. Image sourced from Encyclopaedia Britannica.

Ni is a metal that falls under the ferromagnetic category and is primarily found in the Earth's crust. It is most commonly combined with oxygen and sulfur in the form of oxides and sulfides. Besides the Earth’s crust, nickel can also be found in meteorites, soil, and is released through volcanic eruptions. It is estimated that there are about eight billion tons of nickel present in the oceans (Genchi *et al*., 2020). In typical soils, the Ni concentration averages less than 100 mg/kg (Shahzad *et al*., 2018). Thanks to its exceptional physical and chemical properties, nickel is used extensively in modern metallurgy across various processes, such as in the production of alloys, electroplating, manufacturing of nickel-cadmium batteries, and as a catalyst in both chemical and food industries. The widespread usage of nickel-containing products has led to environmental pollution during manufacturing, recycling, and disposal processes (Song *et al*., 2017; Genchi *et al*., 2020).

It is resistant to corrosion, oxidation, and high temperatures, and it is highly ductile and easily alloyed. These features make it ideal for producing items such as inexpensive jewelry, keys, paper clips, fasteners (*e.g*., zippers, snap buttons, belt buckles), stainless steel kitchenware, electrical components, armaments, coins, and alloys, as well as in the metallurgy and food processing sectors. Nickel Raney, in powdered or granular form, is widely used as a catalyst in chemical reactions, such as hydrogenation. Nickel alloys are incorporated into surgical tools, white gold, German silver, sterling silver (Denkhaus and Salnikow, 2002), and various other products.

Nickel compounds are frequently employed in electroplating, electroforming, as well as in the production of nickel-cadmium batteries and other electronic devices. Stainless steel and other nickel-based alloys are also crucial in the production of tools, machinery, armaments, aerospace equipment, and medical devices. Both natural processes and human activities contribute to nickel’s presence in the environment. Sources of nickel emissions include fossil fuel combustion, volcanic eruptions, forest fires, and wind-blown dust from weathered rock. Other sources include the incineration of waste, coal, and fuel oils.

While there is no clear evidence indicating the nutritional importance of nickel in humans, it has been identified as an essential element for certain microorganisms, plants, and animals (Song *et al*., 2017; Genchi *et al*., 2020). For plants, small amounts of nickel is vital for growth and development, influencing critical processes such as seed germination and overall productivity. However, excessive nickel concentrations can negatively affect plants by disrupting metabolic functions, including inhibiting enzyme activity, photosynthetic electron flow, and chlorophyll synthesis (Sreekanth *et al*., 2013).

Dietary intake is a significant route of nickel exposure in humans. Certain foods, such as spinach, asparagus, carrots, broccoli, green beans, tomatoes, cocoa, chocolate, and nuts, may naturally contain high levels of this metal (Carocci *et al*., 2016; Lavinia *et al*., 2018). Additionally, nickel can unintentionally enter the diet through food processing involving stainless steel equipment or *via* hand-to-mouth contact (Vasiluk *et al*., 2019).

Ni is a vital micronutrient for plants, playing a fundamental role in key enzymes such as urease, hydrogenase, and Ni-superoxide dismutase (Mustafa *et al*., 2023). Beyond its enzymatic functions, Ni contributes to plant health by stimulating the glyoxalase enzyme and maintaining cellular glutathione balance (Fabiano *et al*., 2015). When supplied at optimal levels, Ni has been found to enhance plant growth (Zulfiqar *et al*., 2019). On the other hand, a deficiency of Ni can result in excessive urea accumulation, leading to leaf tissue necrosis (Ahmad *et al*., 2011). Conventional fertilizers often release nutrients too quickly, surpassing the plant's uptake capacity and reducing nutrient use efficiency. Utilizing Ni and other nutrients in nano form as fertilizers presents a promising alternative, as it allows for controlled nutrient release and improved absorption efficiency (Zulfiqar *et al*., 2019).

3. 2. NiO NPs: Properties, synthesis, and applications

Nanotechnology is a field within science and engineering that explores materials with dimensions in the nanometer range, typically 1-100 nm at least in one dimension (Salata, 2004; Tailor *et al*., 2023). Nanomaterials (NMs) differ significantly from bulk materials, not only in terms of size but also in their morphology, chemical composition, redox properties, biodegradability, aggregation tendency, concentration, stability, surface characteristics, solubility, and colloidal behavior (Gnach *et al*., 2015).

NMs are currently applied in various disciplines such as biology, medicine, electronics, energy production, and environmental sciences (Pakzad *et al*., 2019; Ahmad *et al*., 2022). Their future potential is substantial, with many promising applications on the horizon. Based on their structural composition, NMs can be categorized into carbon-based (*e.g.*, fullerenes, nanotubes), organic (*e.g.*, liposomes, dendrimers), inorganic (*e.g.*, metal-based and metal oxide) nanomaterials, and nanocomposites (NCs) (Mekuye and Abera, 2023) (**Fig. 2**).

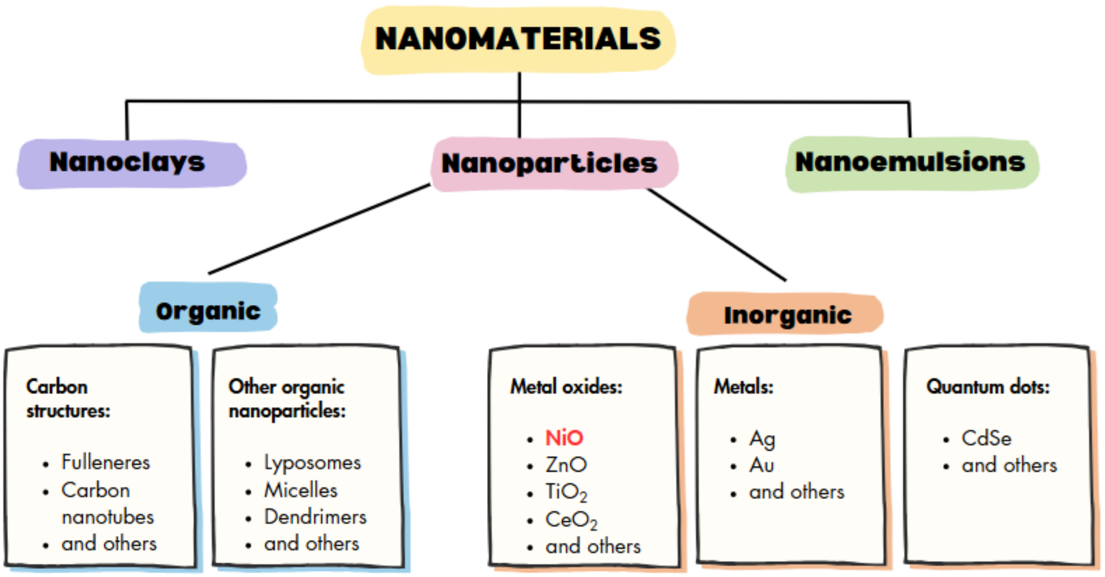

Fig. 2. Systematic categorization of distinct nanomaterial (NM) groups (adapted from Mageswari *et al*., 2016; Szőllősi *et al*., 2020) with modifications. Abbreviations: NiO=nickel oxide, ZnO=zinc oxide, TiO_2= titanium dioxide, CeO_2=cerium dioxide, Ag=silver, Au=gold, CdSe=cadmium selenide.

Among metal-based and metal oxide NMs, those containing Ni are particularly notable, with Ni-based NCs also being recognized. As nanotechnology advances, large quantities of Ni-based NMs are being synthesized mainly by traditional chemical and physical approaches.

These approaches, while effective, are associated with drawbacks such as energy-intensive processes, toxic by-products, and the use of hazardous chemicals, which can harm both the environment and living organisms (Nasrollahzadeh and Sajadi, 2015). Nanoparticles synthesized using these methods may retain harmful residues on their surfaces, reducing their compatibility with biological systems. In response, green synthesis techniques have emerged as sustainable alternatives. These methods utilize plant parts, extracts, or other biomaterials as reducing and stabilizing agents, offering an environmentally friendly, cost-effective, and straightforward approach (Khan *et al*., 2021). Plant-based green synthesis methods leverage bioactive phytocomponents such as enzymes, aldehydes, flavonoids, terpenoids, and phenolic compounds, which act as natural reducing and capping agents. This approach not only prevents nanoparticle aggregation but also enhances their chemical and biological stability. For example, plant extracts from diverse species like *Opuntia ficus indica*, *Peumus boldus*, *Berberis balochistanica*, *Gymnema sylvestre*, and even the hyperaccumulator *Lactuca sativa* have been successfully used to synthesize NiO NPs (Gebretinsae *et al*., 2021; Taş *et al*., 2021; Uddin *et al*., 2021; Bhoye *et al*., 2023; Hamdan *et al*., 2024). Despite these advancements, challenges persist in optimizing plant-mediated NiO NP synthesis. Key issues include the difficulty in reducing Ni(II) to Ni(0) under mild conditions and the susceptibility of the resulting nanoparticles to oxidation, leading to the formation of nickel oxides or hydroxides such as NiO, Ni_2O_3, and $Ni(OH)_2$ (Chen and Wu, 2000). These challenges highlight the need for further research to refine the synthesis process and address the parameters affecting nanoparticle properties and large-scale applicability.

By focusing on green synthesis techniques, researchers can mitigate the environmental risks associated with NiO NP production while unlocking their full potential for industrial and biological applications.

NiO NPs are increasingly utilized in various heavy industries and consumer products, such as smelting, coinage, and electrical goods, due to their unique physicochemical properties. These include a high surface area, stability, hardness, and specific optical, magnetic, and antimicrobial characteristics, which make them suitable for diverse applications (Danjumma *et al*., 2019; Manna *et al*., 2021; Kolbert *et al*., 2022). The growing production and use of NiO NPs raise concerns about their potential environmental release and interactions with plants.

3. 2. 1. Uptake and characterization of NiO NPs in plants

Plants are continuously exposed to NPs, which are widely distributed in soil, water, and aerosols (Mustafa and Komatsu, 2016). Similar to their bulk counterparts, heavy metal nanoforms can easily enter plants *via* endocytosis, pore formation, and plasmodesmata or by hitchhiking on carrier proteins (Pérez-de-Luque, 2017). This process is further facilitated by sorption under low pH conditions (Järup, 2003), enhancing the sorption and cellular sequestration of metallic nanoparticles.

The root system of plants primarily absorbs Ni through both active transport and passive diffusion (Seregin and Kozhevnikova, 2006). The balance between active and passive uptake of Ni varies depending on factors such as plant species, presence of organic matter, ionic form of Ni, pH of the growth medium, and concentrations of Ni and other ions in the soil solution (Chen *et al*., 2009). The absorbed Ni^{2+} is transported to the xylem through the transpiration stream and delivered to the shoots in association with various chelate complexes (Mustafa *et al*., 2023). Plants primarily regulate Ni uptake and transport to maintain photosynthetic activity. Molas (1998) emphasized that even small amounts of the metal can lead to significant anatomical changes in leaves, such as reduced thickness and smaller leaf area, especially in *Brassica oleracea*.

It is now recognized that plants play a role in the dispersion of NPs into the environment and contribute to their accumulation in the food chain (De Souza-Torres *et al*., 2021). The interaction between NPs and plants not only affects plant function but also influences food quality. NPs can adhere to plant surfaces, causing physical or chemical damage, or they may enter plant tissues through cell wall pores, depending on their size (Kurczyńska *et al*., 2021). The cell wall acts as a selective barrier, generally limiting the entry of NPs to those smaller than 20 nm. However, some nanomaterials have been found to alter the chemical composition of the cell wall, increasing pore size or creating new pores (Oliveira *et al*., 2023). NPs can penetrate the root system through lateral root junctions, move through the cortex and pericycle, and eventually reach the xylem (Hossain *et al*., 2015). Nevertheless, the uptake and in-plant movement of NPs are influenced by multiple factors, including size, shape, chemical composition, type, concentration, surface charge, plant species, growth stage, and environmental exposure conditions (Singh *et al*., 2021).

Parsons et al. (2010) analyzed the presence of Ni within mesquite seedling tissues exposed to uncoated and sodium citrate-coated Ni hydroxide NPs. Their findings revealed that in plants exposed to uncoated Ni NPs, the nanoparticles were present in both roots and shoots, while in plants treated with coated NPs, Ni nanoparticles were only found in the roots. The study by Manna et al. (2021) revealed that hydroponically administered FITC-tagged aminopropyl triethoxysilane-functionalized NiO NPs (<50 nm particle size) penetrate the epidermis in *Allium cepa* roots. The NPs enter individual cells, dispersing within the cytoplasm or clustering around the nuclear membrane.

More recently, the uptake of Ni in soybean seeds treated with nanodisperse $Ni(OH)_2$ was analyzed (de Oliveira *et al*., 2022). The findings indicate that Ni mainly accumulates in the seed coat, particularly in the hilum, and is not transported to the emerging cotyledons. Instead, it is released into the rhizosphere, where it is ultimately absorbed by the radicle or primary roots (de Oliveira *et al*., 2022).

NiO NPs interact with plant systems in complex ways, influencing not only cellular structures but also physiological and biochemical processes. Advanced analytical and imaging techniques have proven indispensable in elucidating these interactions, particularly in understanding the uptake, distribution, and effects of NiO NPs in plant tissues. These tools enable researchers to investigate how NiO NPs accumulate in specific plant organs and tissues. To monitor Ni NP uptake and distribution, high-resolution imaging and chemical mapping techniques such as transmission electron microscopy (TEM), laser-induced breakdown spectroscopy (LIBS), and single-particle inductively coupled plasma mass spectrometry (sp-ICP-MS) have been utilized. Among these, TEM stands out for its ability to visualize nanoparticles within plant tissues at the sub-cellular level. This technique has provided direct evidence of NiO NP accumulation in plant cells, revealing their localization within root cell walls and vacuoles (Malatesta, 2021). Such findings highlight the role of NiO NPs in altering cellular structures, including their potential to induce organelle-level disruptions like peroxisome proliferation and nuclear condensation (Faisal *et al*., 2013). Elemental mapping techniques like LIBS further enhance our understanding of NiO NP-induced changes in plants. LIBS allows for the detection of NiO NP aggregates and their associated effects on the distribution of macro- and microelements, providing a broader view of how these nanoparticles influence overall plant physiology. Similarly, sp-ICP-MS has been applied to quantify NiO NP concentrations in plant tissues, offering insights into their uptake efficiency and the barriers to their translocation (Zhou *et al*., 2023).

3. 2. 2. NiO NPs: Applications and environmental impact in agriculture

Recent studies have explored the potential of various nickel nanoforms to enhance plant growth and productivity. A comprehensive study by Zhou *et al*. (2023) investigated the effects of NiO NPs, bulk NiO (b-NiO), and nickel sulfate ($NiSO_4$) on *Glycine max* (soybean). The study demonstrated that NiO NPs can be absorbed directly by plants and transferred to soybean seeds in particulate form. An optimal dosage of NiO NPs significantly improved soybean yield and nutritional content, including higher fatty acid and starch levels, by promoting photosynthesis and regulating nitrogen metabolism and hormone balance. In another recent study, biodegradable Ni NPs coated with starch, polyvinyl alcohol, gum arabica, gelatin, molasses, and paraffin wax, have been prepared and applied for the soil treatment of *Chloris gayana* (Beig *et al.*, 2023). This research showed that the application of encapsulated Ni NPs significantly enhanced nitrogen availability, which led to an increase in dry matter production of Rhode grass. Furthermore, $NiFe_2O_4$ nanoparticles (12.5 ± 0.5 nm) were absorbed by barley (*Hordeum vulgare* L.) roots and transported to shoots, resulting in increased concentrations of calcium, magnesium, potassium, sodium, manganese, chlorophyll, carotenoids, and soluble proteins, though no significant increase in biomass was observed (Tombuloglu *et al.*, 2019). Nickel-chitosan nanoconjugates (NiCNC), with particle sizes ranging from 300 to 400 nm, have been shown to exert antifungal effects in vitro against *Fusarium solani*. These effects include reduced mycelium radial growth, inhibition of spore germination and sporulation, and decreased spore viability, likely due to ROS-mediated lipid peroxidation. In *F. solani*-inoculated wheat seedlings, NiCNC supplementation resulted in decreased disease incidence, increased shoot and root growth, and a higher vigor index compared to untreated seedlings (Chouhan *et al.*, 2022).

Beyond nanofertilization, there are attempts to discover the beneficial effects of Ni NPs in plant protection. The smaller nickel-chitosan nanoparticles (Ni-CHT NPs, spherical 20–70 nm) have been explored as a potential alternative to fungicides for combating rice blast caused by *Pyricularia oryzae*. Application of Ni-CHT NPs significantly improved seed germination and promoted better shoot and root growth in *Oryza sativa*. This improvement was partially attributed to the Ni NP-induced synthesis of new polypeptides, such as RuBisCO, which enhanced photosynthetic activity. Rice plants treated with Ni-CHT NPs displayed fewer symptoms of blast disease on their leaves, and Ni NPs inhibited mycelial growth in laboratory conditions (Parthasarathy *et al.*, 2023). Moreover, Ni NPs have shown potential in alleviating plant stress and providing other beneficial effects, such as managing Fusarium wilt and other fungal diseases (Ahmed *et al.*, 2016; Sharma *et al.*, 2017; Chouhan *et al.*, 2022). As the use of Ni NPs as nanofertilizers continues to grow, further studies are essential to fully unlock their potential to enhance plant stress tolerance and overall health.

3. 3. Toxicity and physiological impact of NiO NPs in agriculture

The potential toxicity of NiO NPs in agriculture has raised considerable concerns due to their effects on physiology of non-accumulator plant species. While Ni is an essential plant micronutrient in small quantities, excessive accumulation can disrupt various metabolic processes, hinder enzymatic functions, and interfere with chlorophyll production and photosynthetic electron transport (Sreekanth *et al.*, 2013; Genchi *et al.*, 2020). Plants, being stationary organisms, are particularly vulnerable to high Ni concentrations in the soil. The unique characteristics of Ni nanoparticles further amplify these toxic effects, making them a significant concern for plant health.

The toxicity of NiO NPs in plants is influenced by factors such as particle size, concentration, and chemical composition (Dietz and Herth, 2011; Chahardoli *et al.*, 2020). Smaller nanoparticles tend to exhibit higher toxicity due to their larger surface area, which increases their interaction potential with plant cells (Yin *et al.*, 2011; Scherer *et al.*, 2019; Yan and Chen, 2019). This increased interaction can cause substantial cellular disturbances, such as chromosomal abnormalities and disruptions in the cell cycle (Manna *et al.*, 2022).

Plant cell walls, primarily composed of polysaccharides and structural proteins, play a crucial role in defining plant morphology and providing protection against environmental stressors. These walls are highly dynamic, continuously adapting in response to plant growth, development, and external stimuli. Such flexibility allows for rapid cell elongation and enhances stress tolerance (Caffall *et al.*, 2009; Voxeur & Höfte, 2016; Liu *et al.*, 2021). Exposure to heavy metals, particularly Ni, can significantly compromise the integrity and functionality of plant cell walls. Ni stress has been shown to reduce wall elasticity (Shi & Cai, 2009) and alter its chemical composition (Kolbert *et al.*, 2020). Ni can inhibit cell elongation by interacting with cell wall polysaccharides, which contain functional groups that serve as binding sites for divalent and trivalent metal ions. Specifically, Ni^{2+} ions preferentially bind to the carboxyl groups of polygalacturonic acids and hydroxycinnamic acids, with binding affinity influenced by the pH of the root apoplast and plant species (Meychik *et al.*, 2014). In some plants, the cell wall even acts as the primary compartment for Ni sequestration (Krämer *et al.*, 2000; Redjala *et al.*, 2010). While metal binding to the cell wall can enhance tolerance to certain heavy metals, it may also lead to increased wall rigidity and, in extreme cases, cell rupture (Lešková *et* *al*., 2020). Furthermore, Ni exposure induces structural modifications such as lignin accumulation, suberin alteration, and thickening of the root endodermal cell wall, all of which impact overall plant development (Yadav *et al*., 2021; Mustafa *et al*., 2023).

A primary mechanism behind Ni toxicity is the disruption of ion homeostasis and membrane stability (Saad *et al*., 2016). Elevated Ni levels can lead to excessive production of ROS, such as hydrogen peroxide (H_2O_2) and hydroxyl radicals, which cause oxidative stress (Halliwell and Gutteridge, 1984). Despite Ni's lack of direct involvement in redox reactions, it plays a crucial role in triggering ROS accumulation, which has been widely studied in various plant species (Gajewska *et al*., 2006; Khaliq *et al*., 2015; Khair *et al*., 2020; Kumar *et al*., 2022; Bhat *et al*., 2023).

Regarding NiO NP-tiggered affects, NiO NPs have been shown to promote NO production, likely through enhanced nitrate reductase activity, which subsequently impacts nitrosative signaling pathways (Manna *et al*., 2021). Exposure to these nanoparticles induces oxidative stress, which subsequently triggers an increase in the activities of key antioxidant enzymes such as ascorbate peroxidase (APX), catalase (CAT), superoxide dismutase (SOD), glutathione peroxidase, and glutathione reductase (GR) as part of the plant's defense response (Faisal *et al*., 2013; Abdel-Salam *et al*., 2018; Chung *et al*., 2019; Pinto *et al*., 2019; Saleh *et al*., 2019; Chahardoli *et al*., 2020; Besharat *et al*., 2021; Chahardoli, 2023; Manna & Bandyopadhyay, 2023). In addition to enzyme activity changes, NiO NPs also influence oxidative stress-related gene expression, MYB transcription factors, and phenolic compound biosynthesis (Soares *et al*., 2018; Chung *et al*., 2019; Manna *et al*., 2021). One of the key consequences of oxidative stress induced by NiO NPs is the accumulation of H_2O_2, which contributes to cellular damage in multiple plant species (Oukarroum *et al*., 2015; Abdel-Salam *et al*., 2018; Baskar *et al*., 2018; Saleh *et al*., 2019; Chung *et al*., 2019; Pinto *et al*., 2019; Chahardoli *et al*., 2020; Manna *et al*., 2021; Manna & Bandyopadhyay, 2023). Additionally, oxidative stress caused by NiO NPs is linked to lipid peroxidation, evidenced by increased levels of malondialdehyde (Manna and Bandyopadhyay, 2017a; Abdel-Salam *et al*., 2018; Saleh *et al*., 2019; Baskar *et al*., 2018; Chung *et al*., 2019; Pinto *et al*., 2019; Besharat *et al*., 2021).

Despite numerous studies addressing Ni's role in disrupting ROS balance in plants, its impact on RNS metabolism remains underexplored (Kolbert *et al*., 2020).

Biologically active RNS, such as NO, GSNO, and peroxynitrite ($ONOO^-$), play key roles in plant systems (Corpas *et al*., 2022; Liao *et al*., 2023; Khan *et al*., 2023; Graska *et al*., 2023; Khator, 2023). NO reacts with glutathione to form GSNO, a more stable molecule capable of propagating NO signals over long distances *via* the xylem (Kolbert *et al*., 2024). The GSNO reductase enzyme (GSNOR) breaks down GSNO into glutathione disulfide and ammonia, thus modulating intracellular GSNO levels and NO signaling (Jahnová *et al*., 2019). GSNOR is an evolutionarily highly conserved enzyme in mammals, yeast, and plants (Liu *et al*., 2001). It has a cytosolic, homodimeric structure composed of alpha helices and beta sheets, with each subunit containing a structural function. GSNOR plays a crucial role in RNS metabolism by removing GSNO, maintaining the balance of intracellular NO levels, and regulating the transnitrosation equilibrium between *S*-nitrosylated proteins and GSNO (Lindermayr, 2018). It is rich in cysteine, with 13 out of 14-16 cysteines in plants being highly conserved. Cysteines play an important role in redox signaling by serving as targets for both reversible and irreversible redox modifications (Xu *et al*., 2013). The GSNO reduction carried out by GSNOR is an irreversible process, during which the products can no longer perform nitrosation on proteins (Staab *et al*., 2008). GSNOR activity is sensitive to *S*-nitrosation, but in a reducing environment, the function can be restored, suggesting that the catalytic inactivation is caused by *S*-nitrosation (Frungillo *et al*., 2014; Guerra *et al*., 2016).

The physiological processes of plants, both under normal and stress conditions, are regulated through the post-translational modifications (mainly nitration and nitrosation) of NO and its derivatives. Tyrosine nitration is the most common NO-associated amino acid modification in proteins, but tryptophan, phenylalanine, and histidine can also be affected. In plants, the central molecule in nitration is $ONOO^-$, which results from the rapid reaction between NO and superoxide anion ($O_2^{\bullet-}$) (León, 2022). This modification, involving the addition of a nitro group to tyrosine residues, may result in changes in protein functionality or interfere with tyrosine phosphorylation, thereby influencing signal transduction pathways (Galetskiy *et al*., 2011, Kolbert *et al*., 2017; Corpas *et al*., 2021; León, 2022).

Tyrosine nitration occurs in two steps, during which a nitro group is covalently attached to the ortho position of the aromatic ring of the tyrosine molecule (Souza *et al*., 2008). As a result of the formation of 3-nitrotyrosine, the structure, function, and activity of the nitrated protein are altered through changes in the physical and chemical properties of the amino acids that make up the protein (such as their redox potential, hydrophobic/hydrophilic properties, and acid dissociation constant) (Sabadashka *et al.*, 2021). In plants, nitration leads to the loss of protein function, suggesting that nitration plays a role mainly in protein degradation. In stress-free plants, a certain level of nitration can be detected in the proteome, indicating that plants possess a physiological nitroproteome (Kolbert *et al.*, 2017). In animals, tyrosine nitration is a reversible process catalyzed by the denitrase enzyme, and as a result, it can also play a role in signal transduction (Sabadashka *et al.*, 2021). However, this enzyme has not been identified in plants. Tyrosine nitration is considered a selective process, despite the absence of a consensus sequence in the target proteins that would ensure this specificity. Interestingly, only 1-2% of the total tyrosine pool is targeted for in vivo nitration (Bartesaghi *et al.*, 2007), suggesting that the process is highly selective. The low number of 3-nitrotyrosine in plant enzymes containing more tyrosine amino acids further supports this (Lozano-Juste *et al.*, 2011; Begara-Morales *et al.*, 2015).

The oxidative stress induced by NiO NPs extends to genetic material, resulting in genotoxic effects such as chromosomal abnormalities, disruptions in the cell cycle, and clastogenic activity in *Allium cepa* (Manna and Bandyopadhyay, 2017b; Manna *et al.*, 2022). Furthermore, NiO NP exposure can lead to mitochondrial dysfunction, apoptotic cell death, and DNA hypermethylation due to excessive ROS and NO generation, which further contribute to autophagy and necrotic cell death (Faisal *et al.*, 2013; Manna *et al.*, 2023). Additionally, RNS play a crucial role in regulating these processes through protein modifications and NO signaling pathways, further influencing NiO NP-induced toxicity.

The cumulative effects of NiO NPs at subcellular, cellular, and tissue levels result in visible organ-level stress responses, including reduced root and shoot growth. Inhibition of root elongation and biomass production induced by NiO NPs have been reported in several species, such as *Solanum lycopersicum*, *Raphanus sativus*, *Solanum melongena*, *Triticum aestivum*, *Lycium barbarum and Nigella arvensis*, with the severity of these effects depending on species and nanoparticle dosage (Faisal *et al.*, 2013; Abdel-Salam *et al.*, 2018; Baskar *et al.*, 2018; Saleh *et al.*, 2019; Pinto *et al.*, 2019; Chahardoli *et al.*, 2020). NiO NPs negatively impact photosynthetic efficiency by reducing chlorophyll and carotenoid content, and in *Lemna gibba*, they impair photosynthetic electron transport (Oukarroum *et al.*, 2015; Pinto *et al.*, 2019; Chung *et al.*, 2019; Saleh *et al.*, 2019).

3. 4. Serpentine soils and Ni hyperaccumulation

Ni is known to have toxic effects in elevated concentrations on most plants (see above); however, hyperaccumulators have developed unique metabolic mechanisms that enable them to survive and even flourish in Ni-rich serpentine soils without experiencing toxicity. These soils, which can contain grams of Ni per kilogram, pose significant challenges for plant growth due to their rocky texture, poor water retention, and unbalanced nutrient composition. Serpentine soils are typically low in phosphorus, nitrogen, and potassium while having elevated concentrations of heavy metals such as manganese, cobalt, chromium, and nickel (Kruckeberg, 2002; Hseu and Chen, 2019). These harsh conditions create strong selective pressures on plant life, making serpentine ecosystems distinct and unique, yet many aspects of these processes remain unclear (Delhaye *et al*., 2024).

Despite the challenges posed by serpentine soils, certain plant species exhibit specialized adaptations that allow them to persist in Ni-rich environments. Some plants adopt a resource-conservative strategy to cope with metal stress, aligning with the predictions of the leaf economics spectrum (Wright *et al*., 2004; Kazakou *et al*., 2008; Adamidis *et al*., 2014; Delhaye *et al*., 2024). In nickel-rich environments, *Plantago lagopus* tends to produce smaller leaves, while *Filago eriocephala* develops thicker leaves. Similarly, *Lolium rigidum* and *Aegilops biuncialis* exhibit higher leaf dry matter content, potentially as an adaptation to drought stress. However, not all plants follow this pattern. *Avena barbata*, for example, displays increased leaf area, which could be linked to reduced pathogen pressure in metal-rich soils (Boyd, 2007; Boyd *et al*., 1994).

Furthermore, proline accumulation, a key molecule for osmoregulation, has been found to be present in higher concentrations in plants growing on serpentine soils compared to those on non-serpentine soils (Verbruggen and Hermans, 2008; Karatassiou *et al*., 2021). The relationship between hyperaccumulation and drought resistance has been suggested for decades (Severne, 1974). Some researchers propose that excess nickel in plant cells may function as an osmotic agent, reducing water potential and allowing photosynthesis to continue under drought conditions (Baker and Walker, 1989; Fitter and Hay, 1981).

3. 5. Mechanisms of Ni hyperaccumulation in plants

Hyperaccumulator plants not only survive in environments with high Ni concentrations but also store more than 1000 mg/kg of Ni in their shoots (Reeves, 1992). These plants exhibit enhanced Ni uptake, efficient root to shoot translocation, and robust detoxification and sequestration mechanisms compared to non-accumulators (Rascio and Navari-Izzo, 2011; Hipfinger *et al*., 2022) (**Fig. 3**).

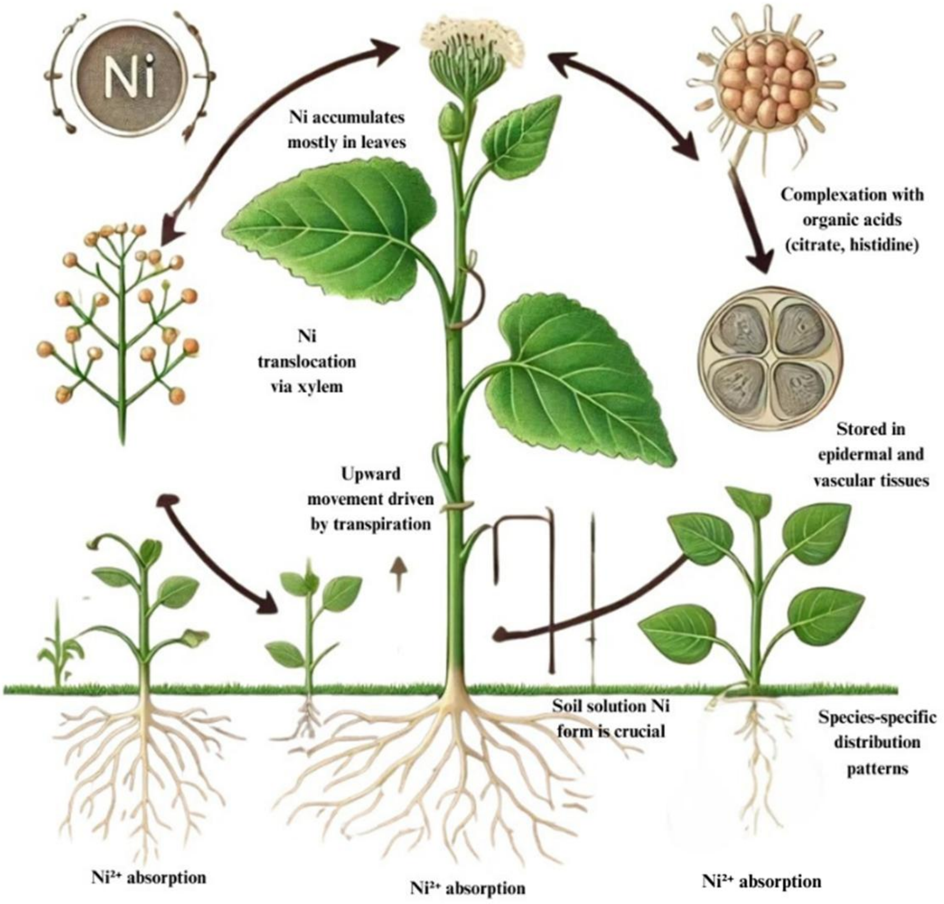

Fig. 3. Mechanisms of Ni hyperaccumulation including Ni uptake by roots, translocation *via* xylem, and storage in plant tissues. Prepared with Canva.com.

For instance, in *Odontarrhena lesbiaca* and other hyperaccumulator species within the genus *Odontarrhena*, selective chelation, primarily with histidine, has been shown to play a crucial role in the translocation of Ni from the root to the shoot and ultimately to the leaves through the xylem, although approximately 50% of the metal is estimated to remain in its free, hydrated Ni^{2+} form (Krämer *et al*., 1996). In the rhizosphere of hyperaccumulators, microbial populations that resist metals are vital for enhancing metal uptake, and strains with plant growth promoting activity can also be found in serpentine bacterial isolates (Rosatto *et al*., 2019; Lopez *et al*., 2019).

Ni transport from the roots to the shoots occurs through both passive diffusion and active transport, with active transport being more significant at low concentrations of Ni. Hyperaccumulator plants are particularly efficient in transporting Ni to the shoots *via* the xylem, with metal transporters in the root symplast playing a key role in this process (Maestri *et al*., 2010). Transpiration also aids in driving xylem flow, contributing to metal transport (Salt *et al*., 1995).

Organic acids, such as citric acid and nicotinamine (NA), are crucial for Ni hyperaccumulation. In certain hyperaccumulators, such as *Alyssum bertolonii*, citric acid enhances Ni uptake, while in others like *Datura innoxia*, higher citric acid concentrations lead to higher Ni concentrations in the stems (Jean *et al*., 2008). NA is important in facilitating the translocation of Ni by forming complexes with the metal, assisting its movement to the shoots (Maestri *et al*., 2010).

While a specific Ni transporter has yet to be identified, studies have shown that certain transport proteins are involved in Ni hyperaccumulation. Zinc-regulated transporter, iron-regulated transporter-like proteins (ZIP) and natural resistance-associated macrophage proteins (NRAMP) are important for metal homeostasis and play a role in Ni uptake and tolerance (Guerinot, 2000; Williams *et al*., 2000). Research on *Thlaspi japonicum* has demonstrated that ZIP and NRAMP transporters mediate Ni transport and tolerance (Mizuno *et al*., 2005). The Heavy Metal ATPase 4 (*HMA4*) transporter is particularly important in Ni hyperaccumulation, as it helps increase the expression of other metal transporter genes, further enhancing Ni translocation (Hanikenne *et al*., 2008).

The phloem transport, which was once overlooked, has more recently been observed in both woody tropical and herbaceous hyperaccumulating plant species (Deng *et al*., 2018). Although phloem transport has not been conclusively demonstrated in *Odontarrhena lesbiaca*, the exceptionally high Ni concentrations found in the flowers of this species (well above 1000 mg/kg; (Adamidis *et al*., 2017; Stefanatou *et al*., 2020) provide strong support for this mechanism, as flowers are the primary sink for phloem translocation (Deng *et al*., 2018). This hypothesis is further supported by the work of Bani et al. 2018, who proposed that *Orobanche nowackiana* (syn. *Phelipanche nowackiana*) likely derives nutrients exclusively from the phloem of *Alyssum murale*, as its low transpiration rate would not be sufficient to account for nutrient uptake through xylem flow diversion (Shen *et al*., 2006).

Understanding the spatial distribution and localization of metals like Ni within plant tissues is essential for comprehending hyperaccumulation and tolerance mechanisms. Generally, Ni is more concentrated in above-ground plant parts than in roots (Shallari *et al*., 1998; Broadhurst *et al*., 2004; Bani *et al*., 2007). In *Alyssum murale* grown on ultramafic soils near Pogradec, Albania, the highest Ni concentrations were found in seeds (11,400 mg/kg), followed by roots (1260 mg/kg) and stems (1170 mg/kg) (Barbaroux *et al*., 2009). Similarly, in *Senecio coronatus*, Ni is predominantly localized in the leaf epidermis (Mesjasz-Przybylowicz *et al*., 1994). A general pattern of Ni distribution is observed as leaves > stems > roots, though species-specific variations exist. For instance, *Berkheya coddii* accumulates higher Ni levels in the epidermis and vascular bundles of leaves and stems (Budka *et al*., 2005; Gramlicha *et al*., 2011).

Variations in Ni distribution reflect different tolerance mechanisms. In *Rubus ulmifolius*, Ni is primarily stored in roots (Marques *et al*., 2009), whereas in *Grevillea exul*, a serpentinic plant, Ni is concentrated more in roots than in stems and leaves (Rabier *et al*., 2007; 2008). Other species, such as *Quercus ilex*, store Ni in conducting tissues, while herbaceous plants tend to accumulate Ni in the leaf epidermis (Nabais *et al*., 1996; Broadhurst *et al*., 2004).

Plants can directly absorb Ni^{2+}, ion pairs (such as $Ni^{2+}(H_2O)_5\ SO_4^{2-}$), and simple complexes (*e.g*., $NiOH^+$) from the soil solution (Kabata-Pendias and Pendias, 1992; Tack, 2010). Typically, hyperaccumulators absorb Ni as Ni^{2+}, which is then transported to the shoots in complex forms with organic acids like citrate, malate, or histidine (Ingle *et al*., 2005). Nickel forms complexes with organic substances like organic acids, which helps in the desorption or dissolution of Ni in soils. Based on solubility and plant uptake, Ni in the soil is classified into available, potentially available, and unavailable pools. The available pool contains water-soluble and exchangeable forms of Ni, while the potentially available pool includes Ni that is specifically adsorbed, sparingly soluble minerals, and strongly bonded organic complexes. Forms that are occluded in oxides or insoluble compounds are considered unavailable to plants during the growing season (Robinson, 1997ab; Sheoran *et al*., 2009). Plants typically absorb Ni from the available pool, depending on various soil factors.

The availability of Ni is influenced by soil pH, redox potential, organic matter content, and temperature (Kabata-Pendias and Pendias, 1992; Fageria *et al*., 2002; Tack, 2010). Ni uptake is characterized by both passive and active processes, with a positive correlation between Ni concentrations in the soil solution and uptake. The study observed that metal cations like Zn^{2+}, Cu^{2+}, Ca^{2+}, and Mg^{2+} inhibited Ni^{2+} uptake in excised barley roots. Zn^{2+} and Cu^{2+} compete for Ni^{2+} uptake, while Ca^{2+} and Mg^{2+} do not exhibit competitive inhibition (Körner *et al*., 1986). Soil pH plays a significant role, with Ni uptake decreasing as pH increases from 4.5 to 6.5 (Kabata-Pendias and Pendias, 1992).

Dimitrakopoulos et al. (2021), in their study on the nickel hyperaccumulator plant *Odontarrhena lesbiaca*, examined the distribution of Ni in plant tissues and the impact of broomrape infection and site on this distribution. They focused on plants from three study sites: Loutra, Ampeliko, and Olympos. They found that healthy plants from Ampeliko consistently had higher leaf nickel concentrations compared to those from Olympos and Loutra, which aligned with the soil Ni concentrations in these areas. However, the Ni concentrations in infected plants from Loutra were notably different from those in the other two sites, suggesting that the infection altered the typical pattern of Ni accumulation in these plants.

3. 6. The study context: *Odontarrhena lesbiaca* and NiO NPs

Species of *Odontarrhena lesbiaca* (**Fig. 4**) are small shrubs or long-lived perennial herbs, characterized by a strong taproot and numerous sterile shoots emerging from the base. The aerial parts are usually covered with dense stellate hairs, which give the plants a distinctive silvery-grey appearance. The inflorescence is typically a branched compound corymb, though in some cases, it can be reduced to a simple raceme. The flowers consist of five ovate sepals and five bright yellow, cuneate-spathulate petals. The stamens are equipped with denticulate appendages, and the fruits are silicles, each containing two seeds. The genus *Odontarrhena* is distributed from Western Asia to the Western Mediterranean Basin, with certain regions, particularly the Middle East and the Balkan Peninsula, serving as significant centers of diversity. Despite its wide distribution, the taxonomy of several *Odontarrhena* species remains unresolved, with many taxa lacking clear definitions. (Cecchi *et al*., 2018; Cecchi *et al*., 2020; Bettarini *et al*., 2021).

Fig. 4. *Odontarrhena lesbiaca* (Brassicaceae) plant from Lesbos Island, Greece. Image sourced from Lesvos Birders.

One of the remarkable traits of *Odontarrhena* species is their ability to hyperaccumulate Ni. Among the 532 known Ni hyperaccumulators, 62 species belong to the genus *Odontarrhena* (formerly Alyssum, Brassicaceae), predominantly distributed in the serpentine soils of southeastern Europe and the Middle East (Reeves *et al*., 2017, 2021; Bani *et al*., 2021). One notable endemic species, *Odontarrhena lesbiaca* (formerly *Alyssum lesbiacum*), thrives on the serpentine soils of Lesbos, Greece, and grows up to 40 cm tall (Strid and Tan, 2002; Kazakou *et al*., 2010). Previous research has shown that populations of *Odontarrhena lesbiaca* from different locations exhibit varying Ni hyperaccumulation capacities, correlating with soil Ni content in their native habitats (Adamidis *et al*., 2014; Kazakou *et al*., 2010).

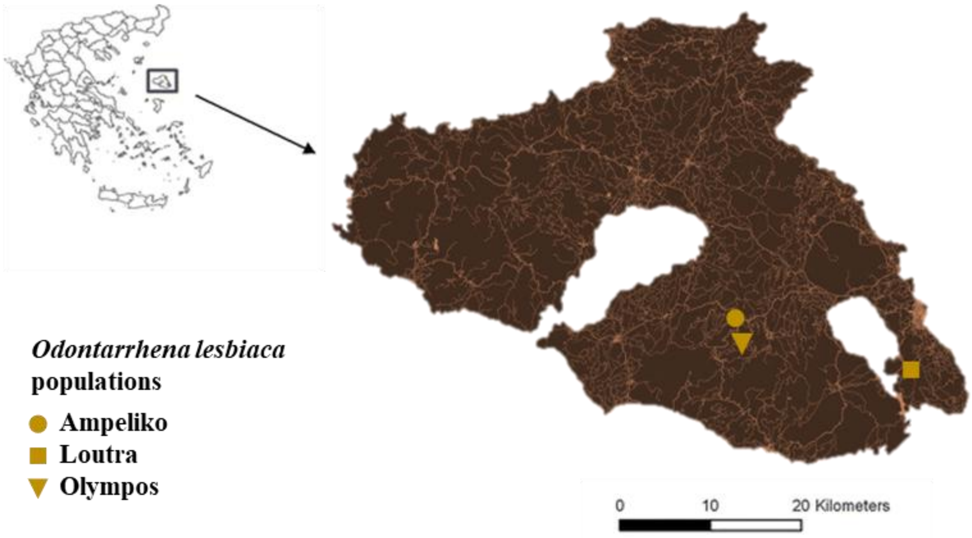

Fig. 5. Map of Lesbos Island (Greece) showing the Ampeliko (●), Loutra (■) and Olympos (▼) populations of *Odontarrhena lesbiaca* (modified from Adamidis, 2013).

As the nanoforms of Ni has become more prevalent in the environment, understanding their effects on hyperaccumulators like *Odontarrhena lesbiaca* is crucial. The present thesis focuses on three ecotypes of *Odontarrhena lesbiaca*—Ampeliko, Loutra, and Olympos (**Fig. 5**)—to investigate the effects of NiO NPs. It specifically examines Ni accumulation, microelement homeostasis, alterations in root structure, and nitro-oxidative processes, as these aspects have not been previously characterized in these hyperaccumulators. By shedding light on plant-nanoparticle dynamics, this thesis not only enhances our understanding of hyperaccumulators but also provides a foundation for sustainable nanoparticle applications in ecological restoration and phytoremediation.

4. Research Objectives

We aimed to examine the responses of the Ni hyperaccumulator *Odontarrhena lesbiaca* to NiO NPs. In order to be able to set up a simple, reproducible experimental system, we used seedling-stage plants grown and treated in Petri dishes. By comparing geographically distinct populations (Ampeliko, Loutra, and Olympos) growing on soils with different Ni contents, we aimed to find correlations between NiO NP effects and Ni accumulation/tolerance. Multiscale analyses of plant responses were performed at the cellular, tissue, organ, and molecular levels. Our hypothesis was that the ecotypes display unique cellular, structural, and molecular adaptations in response to NiO NP exposure, which are linked to their varying tolerance to Ni.

Therefore, we formulated the following key questions:

1) What is the extent of Ni uptake, root-to-shoot translocation and changes in element distribution of *Odontarrhena lesbiaca* seedlings in the presence of nano or bulk Ni form? Can NPs be detected in plant tissues? Can ecotype-dependent differences be identified?

2) Does the presence of NiO NPs induce modifications in root tissue structure and cell wall composition as root tissue-level protection mechanisms? Can ecotype-dependent differences be identified?

3) Do the nano and the bulk Ni form induce changes in biomass production of *Odontarrhena lesbiaca* root and shoot organs? Can ecotype-dependent differences be identified?

4) Among the molecular mechanisms of plant responses to Ni, can nitro-oxidative mechanisms be identified in *Odontarrhena lesbiaca* exposed to NiO NP? Can ecotype-dependent differences be identified?

5. Materials and Methods

5. 1. Characterization of NiO NPs

NiO NPs were sourced from Sigma-Aldrich (St. Louis, USA, catalog number: 637130). To analyze the particle size, chemical composition, and crystallinity of the synthesized nanoparticles, transmission electron microscopy (TEM) images and electron diffraction (ED) patterns were recorded using a FEI Tecnai G2 20 X-Twin instrument (FEI Corporate Headquarters, Hillsboro, OR, USA) at an acceleration voltage of 200 kV. Additionally, X-ray diffraction (XRD) analysis was conducted with Cu Kα radiation on a Rigaku MiniFlex II powder diffractometer (Rigaku Corporation, Tokyo, Japan) to confirm the crystallinity of the particles by comparing with the literature. The scan rate was set at $2°\text{min}^{-1}$ over a 2θ range of 5°–80°. Energy dispersive X-ray spectroscopy (EDS) was employed to determine the elemental composition of the sample. The EDS analysis was carried out using a Hitachi S-4700 scanning electron microscope, operating at an accelerating voltage of 30 kV, equipped with a Röntec energy dispersive X-ray spectrometer. The specific surface area of the samples was measured *via* the 5-point Brunauer-Emmett-Teller (BET) method from nitrogen (N_2) adsorption isotherms at 77.15 K, using a Quantachrome NOVA 3000e instrument (Quantachrome, FL, USA). Prior to measurement, the samples were degassed at 373.15 K for 1.5 hours.

5. 2. Preparation of NiO NP and bulk $NiCl_2$ solutions

For the preparation of the nano-sample, NiO NPs were suspended in distilled water, forming a heterogeneous mixture characterized by the presence of large NiO NP aggregates. This suspension was further treated using an ultrasound sonicator for two cycles of 30 minutes each. The pH of the suspension was modified to fall within the range of 5.7-5.8, with the final concentrations of NiO NPs adjusted to either 250 mg/L or 500 mg/L. In the case of the bulk sample, $NiCl_2 \times 6H_2O$ was dissolved in distilled water, with the pH similarly adjusted to 5.7-5.8. The volume of the solution was then modified to achieve final concentrations of either 250 mg/L or 500 mg/L $NiCl_2$.

5. 3. Conditions for plant growth

Seeds of *Odontarrhena lesbiaca* were provided by Prof. Dr. Panayiotis G. Dimitrakopoulos (Department of Environment of the University of the Aegean, Greece). They were collected from over 100 randomly selected individuals growing at three geographically distinct serpentine sites on Lesbos Island, Greece: Ampeliko, Loutra and Olympos (site details in Kazakou *et al*., 2010, **Fig. 5**). The collected seeds underwent surface sterilization with 70% (v/v) ethanol for 1 minute, followed by treatment with 5% (v/v) sodium hypochlorite for 15 minutes. Afterward, they were placed in Petri dishes containing filter paper that was moistened with either distilled water (as a control) or an equivalent volume of aqueous solutions of $NiCl_2$ or NiO NP suspension. The Petri dishes were maintained in a greenhouse for 5 days under controlled conditions, including a photon flux density of 150 μmol m^{-2} s^{-1}, a light/dark cycle of 12/12 hours, relative humidity of 45-55%, and a temperature of 25 ± 2 °C. All analyses were conducted using seedlings that were 5 days old.

5. 4. Ni concentration analysis by ICP-MS

The roots and shoots of the *Odontarrhena lesbiaca* ecotypes were harvested separately and subsequently dried at 70 °C for a duration of 24 hours. A quantity of 100 mg of the dried plant material was incubated with 6 ml of trace analytical quality nitric acid (65% w/v, Reanal, Hungary) for 2 hours. This was followed by the addition of 2 ml of hydrogen peroxide (30% w/v, VWR Chemicals, Hungary). The samples underwent microwave-assisted digestion at 200 °C and 1600 W for 2 hours within closed PTFE reaction vessels (MarsXpress CEM, Matthews, USA). The nickel content in the resulting solutions was analyzed using a quadrupole Agilent 7700X (Santa Clara, USA) inductively coupled plasma mass spectrometer (ICP-MS), which was equipped with the standard Agilent integrated sample introduction system. The instrumental parameters employed included a plasma forward power of 1550 W, a plasma gas flow rate of 15.0 L/min, a carrier gas flow rate of 1.05 L/min, a plasma sampling depth of 10.0 mm, an integration time of 1 s, and a sample uptake rate of 600 µL/min. Measurements were conducted by recording signals at the ^{60}Ni isotope, utilizing ^{45}Sc as an internal standard to correct for potential matrix effects, and implementing helium collision cell technology to mitigate polyatomic interferences (He cell gas flow rate: 5 ml/min, octopole bias: -18V, energy discrimination: 5 V). Instrumental tuning was carried out prior to all measurements with Agilent's tuning solutions (No. G1820-60410). Data evaluation was performed using the built-in Agilent Mass Hunter software.

5. 5. LIBS analysis and elemental mapping of plantlets

Before measurements were conducted, the plantlets were carefully extracted from the Petri dishes, and their roots were rinsed with trace analytical quality laboratory water to remove any remaining cultivation medium. The seedlings were then pressed, dried, and fixed onto glass microscope slides using a thin layer of epoxy regime (Epoxy-Embedding Kit, 45359, Sigma-Aldrich, Germany). LIBS spectra were obtained with a J-200 LA-LIBS tandem spectrometer (Applied Spectra Inc., USA) operating in LIBS mode under the following parameters: laser wavelength of 266 nm, laser pulse duration of 6 ns, laser pulse energy of 14 mJ, spot size of 60 μm, integration time of 1.05 ms, gate delay of 0.5 μs, and laser pulse repetition rate of 10 Hz. Scanning was performed across the entire plantlet area (approximately 15-20 × 50-60 mm) without overlapping measurement points, and single-shot LIBS spectra were collected from each position. Each recorded spectrum from a given spot contained over 12000 data points, representing the UV-Vis optical emission spectrum over a wavelength range of 190 to 1040 nm with an optical resolution of 0.07 nm. Multiple layers of the plant material were ablated, and the spectra from each location were vertically summed, providing sufficient spectral data for further analysis and elemental map generation. The hyperspectral data set was processed using Clarity software (Applied Spectra Inc., USA), while elemental maps were visualized with ImageLab software (Epina GmbH, Austria). Elemental maps for Nickel (Ni), Potassium (K), Sodium (Na), Magnesium (Mg), and Calcium (Ca) were based on net signal intensities measured at the Ni I 352.4 nm, K I 766.5 nm, Na I 588.9 nm, Mg I 518.3 nm, and Ca I 422.7 nm spectral lines, respectively.

5. 6. TEM examination of root and hypocotyl sections

Samples from the mature regions of the root and hypocotyl were fixed in 3% glutardialdehyde prepared in phosphate-buffered saline (PBS, pH 7.4). The samples were then embedded in Embed812 resin (EMS, Hatfield, PA, USA) and cut into ultrathin sections, approximately 70 nm thick, using a Leica Ultracut S ultramicrotome (Leica, Vienna, Austria). The sections were stained with uranyl acetate and lead citrate before being analyzed under a Jeol 1400 plus transmission electron microscope (Jeol, Tokyo, Japan), following the procedure outlined by Molnár et al. (2020).

5. 7. Microscopic observation of root anatomy and analysis of cell wall components (lignin, suberin, pectin)

Root anatomy was examined using a Zeiss Axiovert 200M microscope (Carl Zeiss, Jena, Germany). Cross sections of roots were prepared according to a method similar to Barroso et al. (2006). Mature root segments were first fixed in a 4% (w/v) paraformaldehyde solution and then washed with distilled water. The samples were embedded in 5% (w/v) bacterial agar, utilizing a slightly modified version of the procedure outlined by Zelko et al. (2012). Root cross sections, 100 µm in thickness, were cut using a vibratome (Zeiss-Microm, HM650V). To visualize lignin and suberin in the root cross sections, Auramine-O staining was applied. The sections were stained in a solution of 0.01% (w/v) Auramine-O in 10 mM Tris-HCl buffer (pH 7.4) for 10 minutes in the dark (Rahoui *et al*., 2017). For bright field microscopy, another set of root cross sections was stained with 0.02% (w/v) toluidine blue (TB) for 1 minute at room temperature under light exposure (Mitra and Loqué, 2014).

To highlight the pectin content in the root tips, Ruthenium Red (RR) staining was performed following the method of Durand et al. (2009). Roots were incubated in 0.05% (w/v) RR solution for 15 minutes, then washed with distilled water before being placed on slides for microscopic observation.

5. 8. Biomass production assessment

The lengths of both the primary root and the shoot were manually measured and recorded in centimeters (cm). The fresh weight (FW) of the root and shoot was determined using an analytical balance, and the dry weight (DW) was measured after drying the plant material at 70 °C for 24 hours. Both measurements were expressed in milligrams (mg).

5. 9. Translocation factor (TF) calculation

The translocation factor (TF) was determined to assess the efficiency of nickel (Ni^{2+}) translocation from roots to shoots. TF was calculated using the following formula:

$$\mathrm{TF} = \frac{[\mathrm{Ni}^{2+}]\ \text{in shoot}\ (\mu\text{g/g DW})}{[\mathrm{Ni}^{2+}]\ \text{in root}\ (\mu\text{g/g DW})}$$

A TF value greater than 1 suggests that Ni^{2+} is efficiently translocated from roots to shoots, indicating the plant's capability to transport and accumulate nickel in aerial parts. Conversely, a TF value less than 1 indicates that Ni^{2+} predominantly accumulates in the roots, with limited translocation to the shoots.

5. 10. Assessment of reactive nitrogen species (RNS) in roots

The levels of nitric oxide (NO) in the root tips were determined using the fluorescent dye 4-amino-5-methylamino 2′,7′-difluorofluorescein diacetate (DAF-FM DA). Root samples were stained for 30 minutes in a 10 µM fluorophore solution (prepared in 10 mM Tris-HCl buffer, pH 7.4), then washed twice with the buffer solution and mounted on slides for observation (Kolbert *et al.*, 2012).

To detect peroxynitrite ($ONOO^-$) levels, dihydrorhodamine 123 (DHR) was used, following the protocol described by Kolbert et al. (2012). The root samples were stained with a 10 µM DHR 123 solution (in 5 mM Tris-HCl buffer, pH 7.4), incubated for 15 minutes at room temperature, washed twice with the buffer, and then prepared for microscopic analysis.

5. 11. Fluorescence imaging and quantification

Fluorescence and light microscopy analyses were conducted using a Zeiss Axiovert 200M inverted fluorescence microscope (Carl Zeiss, Jena, Germany). Filter set 10 (excitation: 450-490 nm, emission: 515-565 nm) was employed for measurements involving DAF-FM, DHR, and Auramine-O staining. Pixel intensity was quantified within defined circular areas, with the radii adjusted to encompass the largest sample regions. The Axiovision Rel. 4.8 software (Carl Zeiss, Jena, Germany) was used to evaluate pixel intensity from digital images.

5. 12. Evaluation of GSNOR activity *via* UV-vis absorption spectroscopy

The plant samples (250 mg of shoot and root separately) were homogenized with double the volume of an extraction buffer composed of 50 mM Tris-HCl (pH 7.6-7.8), 0.1 mM EDTA, 0.1% Triton X-100, and 10% glycerol. GSNOR activity was assessed by monitoring NADH oxidation in the presence of GSNO at a wavelength of 340 nm, following the protocol established by Sakamoto et al. (2002). The homogenate was centrifuged at 9300 × g for 20 minutes at 4 °C. A 150 µL aliquot of the protein extract was then incubated in a 1 mL reaction buffer containing 20 mM Tris-HCl (pH 8.0), 0.5 mM EDTA, 0.2 mM NADH, and 0.4 mM GSNO. The results are reported as nanomoles of NADH consumed per minute per milligram of protein, with protein concentration determined using the Bradford (1976) protein assay. The activity was expressed as nmol NADH min^{-1} mg^{-1} protein. Measurements were carried out using a Kontron Uvikon double-beam UV-vis absorption spectrophotometer.

5. 13. Protein extraction and assessment of GSNOR protein levels and tyrosine nitration by western blot

The shoot and root tissues of *Odontarrhena lesbiaca* ecotypes were homogenized with a double volume of an extraction buffer, which contained 50 mM Tris-HCl (pH 7.6-7.8), 0.1 mM EDTA, 0.1% Triton X-100, and 10% glycerol. The homogenate was then centrifuged at 9300 × g for 20 minutes at 4 °C. The protein extract was treated with a 1% protease inhibitor cocktail and subsequently stored at -20 °C. Protein concentrations were determined using bovine serum albumin as a standard, following the Bradford method (1976).

After denaturation *via* SDS-PAGE (12%), 15 µg of the protein extract underwent wet blotting (25 mA for 16 hours). The membranes obtained were used for cross-reactivity assays with various antibodies. Loading controls were conducted using an anti-actin antibody (Agrisera, Cat. No. AS13 2640), with actin (bovine muscle, Sigma-Aldrich, Cat. No. A3653) serving as the protein standard. GSNOR immunoassays were performed using a polyclonal primary antibody from rabbit (anti-GSNOR, Agrisera, Cat. No. AS09 647) and an affinity-isolated goat anti-rabbit IgG–alkaline phosphatase secondary antibody (Sigma-Aldrich, Cat. No. A3687, diluted 1:10,000; further details available in Oláh *et al*., 2020). To detect protein tyrosine nitration, the primary antibody used was anti-3-nitrotyrosine (Sigma-Aldrich, Cat. No. N0409, diluted 1:2000). The secondary antibody remained the same as previously mentioned. Visualization of the bands was achieved through the NBT/BCIP (5-bromo-4-chloro-3-indolylphosphate) reaction. For the positive control, nitrated bovine serum albumin (NO_2-BSA) obtained from Sigma-Aldrich (Cat. No. A3653) was utilized. The quantification of protein bands was conducted using Gelquant software (biochemlabsolutions.com) and expressed as pixel densities. Western blot analyses were carried out on three independent protein extracts derived from separate plant generations, with each extract undergoing the process at least twice (Kolbert *et al*., 2018).

5. 14. Statistical analysis

The results are presented as mean values of raw data (± SE or ± SD). Student’s *t*-test or Duncan’s multiple range test (One-Way ANOVA, $P < 0.05$) was employed for statistical analysis using SigmaPlot 12. To verify ANOVA assumptions, Hartley’s Fmax test was conducted for homogeneity, and the Shapiro-Wilk test was utilized to assess normality.

6. Results

6. 1. Physicochemical characteristics of NiO NPs

NiO NPs were observed using TEM, which revealed that the particles exhibited rhombus and rod-shaped shapes (**Fig. 6, A**). Image analysis determined that the average particle size was 23.2±8.3 nm. The electron diffraction (ED) pattern (inset in **Fig. 6, A**) and XRD analysis (**Fig. 6**, **B**) confirmed both the crystallinity and chemical composition of the particles. The XRD peaks at 2θ values of 37.2°, 43.3°, 62.8°, 75.3°, and 79.3° correspond to the characteristic reflections of NiO with a cubic crystal structure. Additionally, EDS analysis (**Fig. 6, C**) was performed to assess the elemental composition, showing that the sample consisted solely of Ni and O, indicating a high purity material. The specific surface area of the NiO sample, calculated using the BET method, was 76.40 m^2/g.

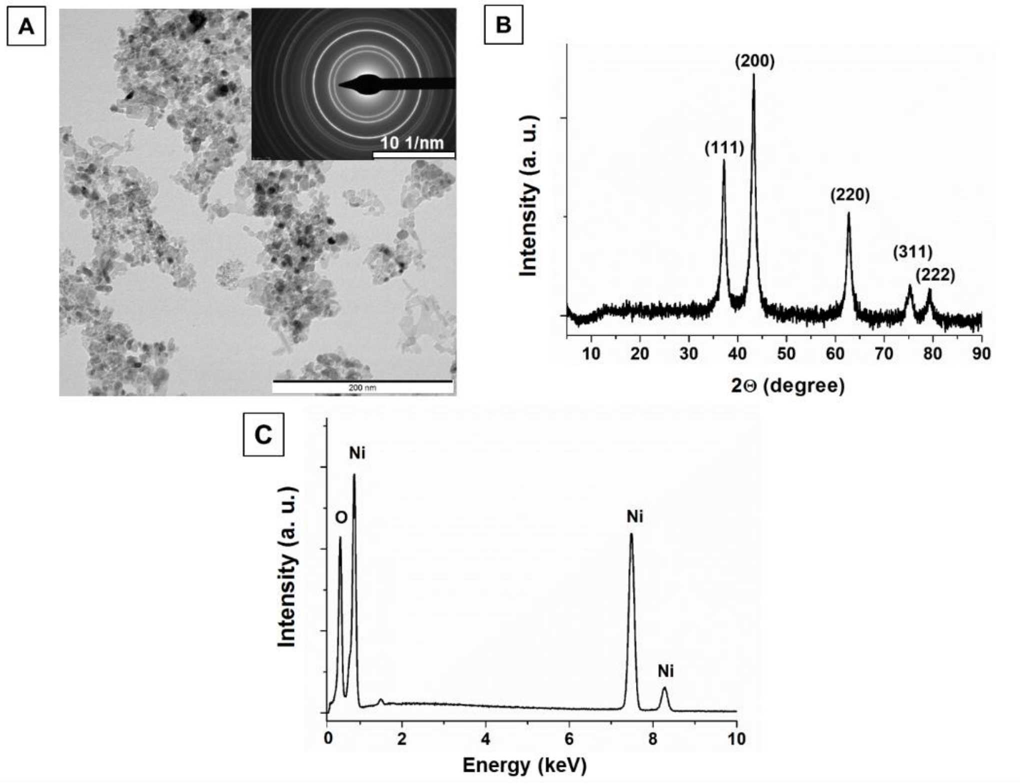

Fig. 6. Chemical characterization of nickel oxide nanoparticles. Transmission electron microscopic (TEM) image (A), with the corresponding electron diffraction (ED) pattern (A inset) and X-ray diffractogram (XRD) of the nanoparticles (B) and their EDS spectrum (C).

6. 2. Ni accumulation and translocation in *Odontarrhena lesbiaca* ecotypes following NiO NP and bulk Ni treatment

NiO NP treatment resulted in a concentration-dependent increase in Ni content in the roots of all ecotypes (**Table 1**). For the Ampeliko ecotype, Ni accumulation was 2.9 and 7.2 times higher than the control at 250 and 500 mg/L NiO NP treatments, respectively. A similar pattern was observed for the Loutra and Olympos ecotypes. Notably, exposure to 250 mg/L NiO NP led to only a 1.2-fold increase in Ni content in Olympos roots, compared to 2.8-fold and 2.7-fold increases in Ampeliko and Loutra, respectively. In contrast, treatment with 250 mg/L $NiCl_2$ led to higher Ni accumulation in the roots compared to NiO nanoparticles at the same concentration. This difference was especially pronounced in the Olympos ecotype, where the 250 mg/L $NiCl_2$ treatment caused a 4.64-fold higher Ni concentration in the roots compared to the NiO NP treatment (**Table 1**).

Table 1 Ni concentrations (µg/g dry weight, DW) in the roots and shoots of *Odontarrhena lesbiaca* ecotypes (Ampeliko, Loutra, Olympos) grown with 0, 250, or 500 mg/L of NiO NP or $NiCl_2 \times 6H_2O$. Data are presented as mean ± SD, n = 3. TFs were determined as described in the Materials and Methods section.

	Root	**Shoot**	
Ecotype/Treatment	**[Ni] µg/g DW**	**[Ni] µg/g DW**	**Translocation factor**
O. lesbiaca Ampeliko 0 mg/L NiO NP	1052.21 ± 0.05	5592.52 ± 0.39	5.31
O. lesbiaca Ampeliko 250 mg/L NiO NP	3038.12 ± 0.07	5674.29 ± 0.30	1.86
O. lesbiaca Ampeliko 500 mg/L NiO NP	7573.15 ± 0.15	6269.75 ± 0.46	0.82
O. lesbiaca Loutra 0 mg/L NiO NP	948.78 ± 0.04	4428.64 ± 0.14	4.66
O. lesbiaca Loutra 250 mg/L NiO NP	2581.25 ± 0.02	4994.95 ± 0.10	1.93
O. lesbiaca Loutra 500 mg/L NiO NP	9566.24 ± 0.07	5576.49 ± 0.86	0.58
O. lesbiaca Olympos 0 mg/L NiO NP	1186.85 ± 0.05	4538.57 ± 0.03	3.82
O. lesbiaca Olympos 250 mg/L NiO NP	1480.96 ± 0.05	5009.04 ± 0.61	3.38
O. lesbiaca Olympos 500 mg/L NiO NP	8813.02 ± 0.45	5388.61 ± 0.75	0.61
O. lesbiaca Ampeliko 0 mg/L $NiCl_2$	844.12 ± 0.01	6988.41 ± 0.16	8.27
O. lesbiaca Ampeliko 250 mg/L $NiCl_2$	5467.66 ± 0.03	8898.81 ± 0.33	1.62
O. lesbiaca Ampeliko 500 mg/L $NiCl_2$	9069.75 ± 0.09	11601.10 ± 0.11	1.27
O. lesbiaca Loutra 0 mg/L $NiCl_2$	975.36 ± 0.002	5308.93 ± 0.31	5.44
O. lesbiaca Loutra 250 mg/L $NiCl_2$	5185.62 ± 0.03	7093.00 ± 0.26	1.36
O. lesbiaca Loutra 500 mg/L $NiCl_2$	8991.49 ± 0.05	9616.90 ± 0.05	1.06
O. lesbiaca Olympos 0 mg/L $NiCl_2$	1193.24 ± 0.01	6801.26 ± 0.31	5.69
O. lesbiaca Olympos 250 mg/L $NiCl_2$	6923.81 ± 0.06	8432.92 ± 0.06	1.21
O. lesbiaca Olympos 500 mg/L $NiCl_2$	8309.98 ± 0.19	9975.73 ± 0.26	1.20

In the untreated *Odontarrhena lesbiaca* ecotypes, Ni concentrations in the shoot system were notably high (4000-6000 µg/g DW) (**Table 1**). Interestingly, Ni content in the shoots of all three ecotypes showed only a slight increase following NiO NP treatment, suggesting that most of the Ni either released from the nanoparticles or absorbed in nanoparticle form remains in the roots. The limited translocation of Ni from root to shoot is further supported by the decrease in translocation factors to values below 1 in the *Odontarrhena lesbiaca* ecotypes treated with NiO NP (**Table 1**). In contrast, Ni salt treatment resulted in an increase in shoot Ni content across all three ecotypes, with concentrations reaching 10,000-12,000 µg/g DW (**Table 1**). The translocation factors in $NiCl_2$-treated plants remained above 1 in every samples.

6. 3. Element distribution in *Odontarrhena lesbiaca* ecotypes: Focusing on Ni (ionic or nano-Ni)

The ICP-MS results were complemented by LIBS elemental mapping. Overall, the LIBS technique did not reveal significant Ni concentrations in the hypocotyls and roots of the *Odontarrhena lesbiaca* seedlings (**Fig. 7**). In the cotyledons of the Loutra and Olympos ecotypes, the Ni signal generated by $NiCl_2$ treatment was stronger than that induced by NiO NP. However, for the Ampeliko ecotype, the signals triggered by NiO NP and $NiCl_2$ were comparable in intensity, suggesting a variation in response between the ecotypes. Based on the signal scale, which correlates with concentration, it seems that Ampeliko treated with NiO NP contained higher levels of Ni than the other ecotypes. This observation is further supported by the larger Ni-containing areas in Ampeliko cotyledons, despite Olympos showing a similar signal level at around 15,000. Notably, similar Ni signal intensities were detected for both NiO NP and $NiCl_2$ treatments, implying that in this experimental setup, LIBS could not differentiate between concentrations, in contrast to ICP-MS.

Additionally, the LIBS analysis indicated an increase in signal intensity for other elements, including K, Na, Mg, and Ca, following Ni exposure. Minor changes were observed in their distribution, suggesting that nutrient homeostasis in Ampeliko, Loutra, and Olympos seedlings remains stable despite the elevated Ni exposure.

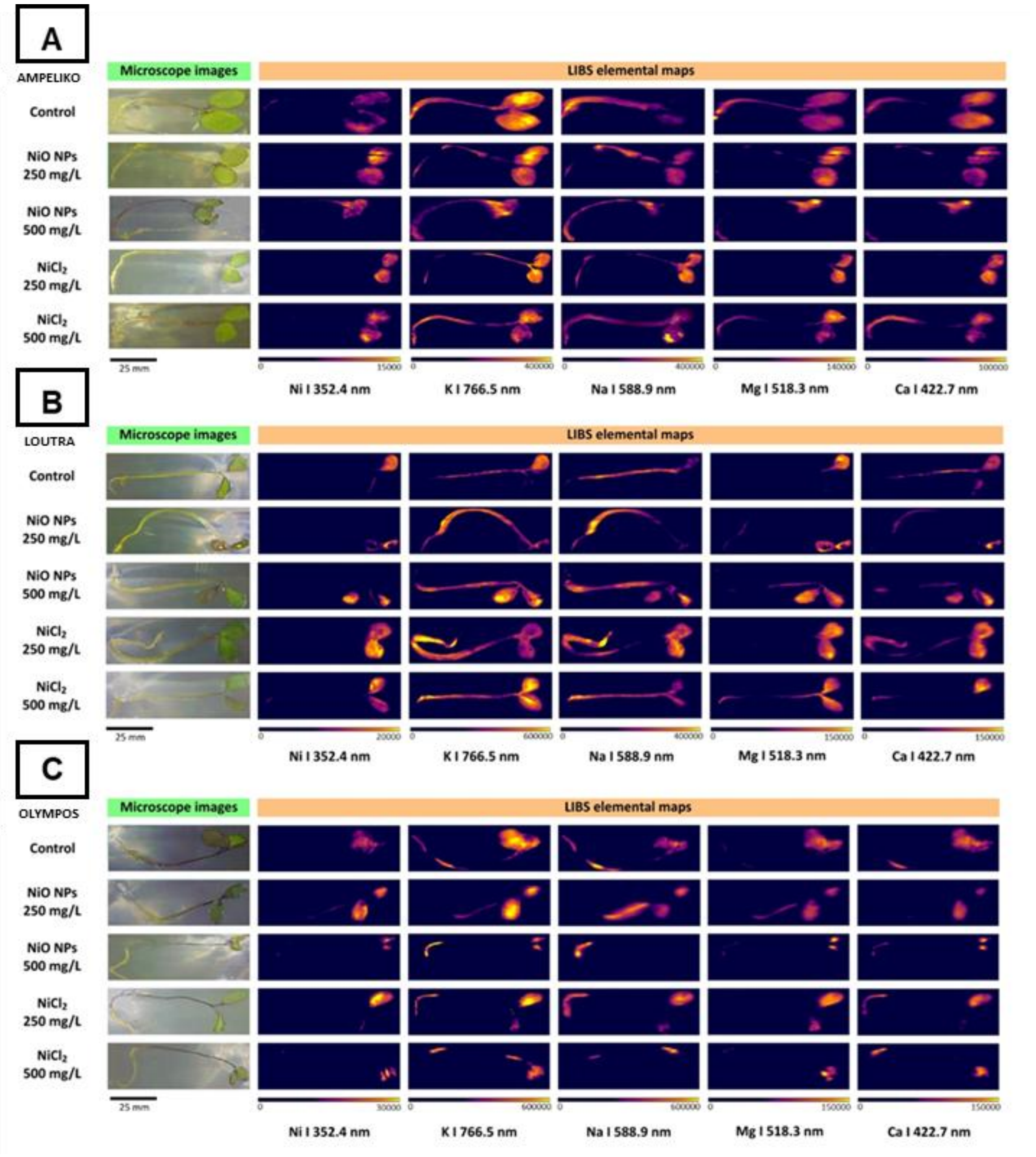

Fig. 7. Representative LIBS elemental maps demonstrating the *in planta* distribution of selected nutrients in the ecotypes of Ampeliko (A), Loutra (B) and Olympos (C) of *Odontarrhena lesbiaca* seedlings cultivated with 0 (Control, Cont), 250 mg/L or 500 mg/L NiO NP or $NiCl_2 \times 6H_2O$ for 5 days. The pixel color scale in the maps represents the net optical emission intensity of the specific spectral line of the element, which is directly proportional to its concentration (for instance, deep blue indicates a very low concentration, while light yellow signifies a high concentration). Scale bars= 25 mm.

6. 4. Interaction of NiO NPs with root cell walls and limited translocation to hypocotyl in *Odontarrhena lesbiaca* ecotypes

The data on Ni ion concentration and translocation factors suggested the possibility that NiO NPs might bind to the root cell wall. This hypothesis was investigated using TEM, and in NiO NP-treated ecotypes, a more pronounced electron-dense signal was observed in the root cell wall compared to the untreated control (**Fig. 8**). Within the root cells, no electron-dense signal indicative of NiO NPs was detected.

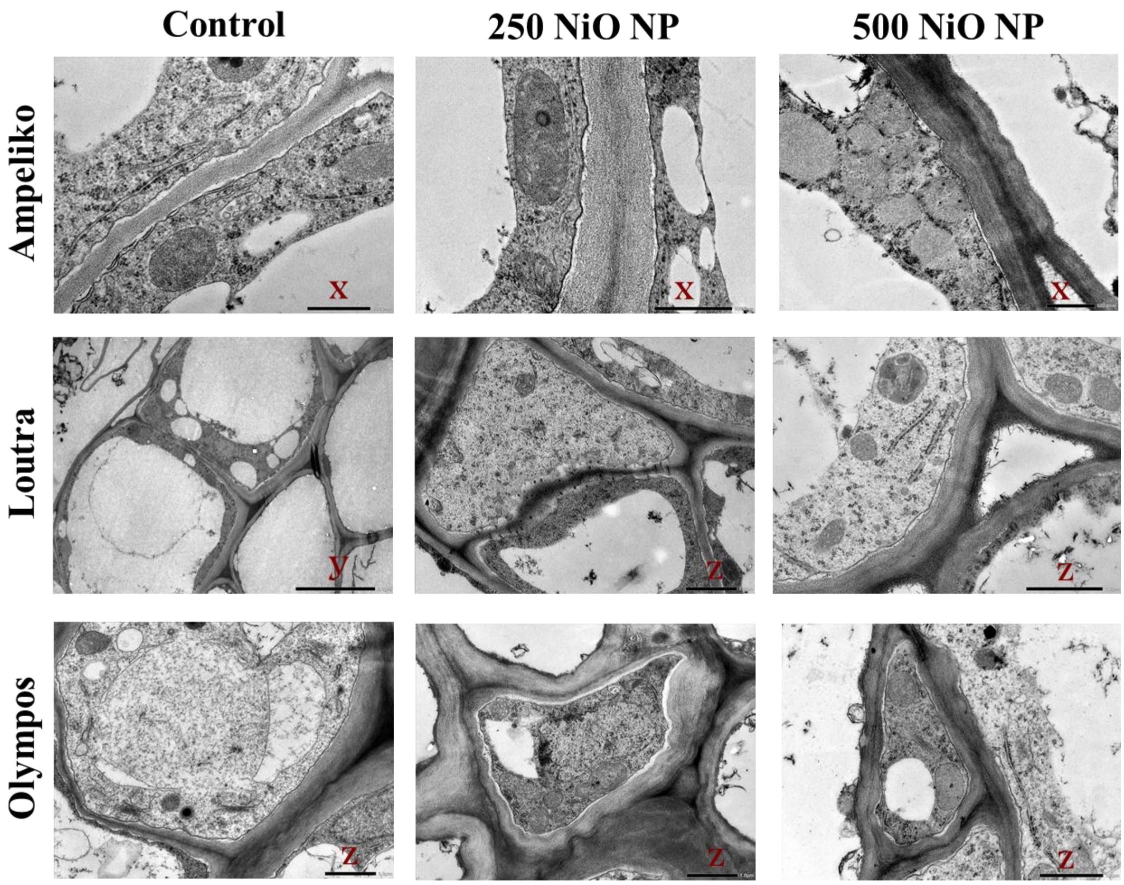

Fig. 8. TEM images showing root cells of the *Odontarrhena lesbiaca* ecotypes (Ampeliko, Loutra Olympos) treated with 0 mg/L (control), 250 mg/L and 500 mg/L NiO NP. Scale bars= x: 500 nm, y: 5 µm, z: 1 µm.

6. 5. Effects of NiO NPs on root tissue structure and cell wall composition of *Odontarrhena lesbiaca* seedlings

Initially, we examined the tissue structure of the root in *Odontarrhena lesbiaca*, using the untreated Ampeliko, Loutra and Olympos ecotypes as a model system. In cross-sections of the differentiation zone, several distinct tissues were identified: the rhizodermis, composed of trichoblast and atrichoblast cells; 2-3 layers of cortical cells; the endodermis, exhibiting U-shaped thickening of the cell walls (tertiary endodermis); the pericycle; and the stele, which contained two xylem bundles and two phloem bundles (diarch stele) (**Fig. 9**).

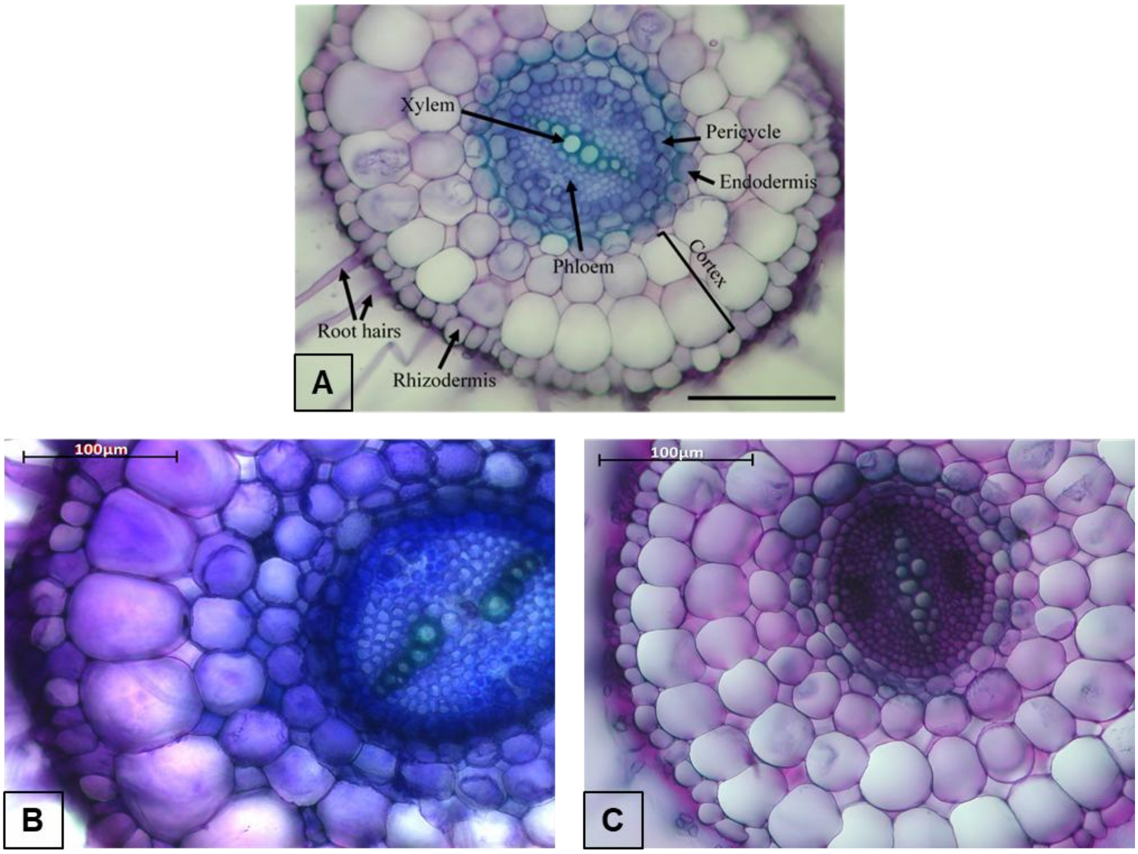

Fig. 9. Root cross-section of untreated *Odontarrhena lesbiaca* stained with toluidine blue. Ampeliko (A), Loutra (B), Olympos (C). Scale bar= 100 µm.

In the roots of the Olympos ecotype, all measured parameters—including root area, cortex, stele areas, and the stele-to-cortex ratio—were significantly decreased following NiO NP treatment, particularly at the 500 mg/L concentration (**Fig. 10 A, B, C, D**). In contrast, exposure to 250 mg/L NiO NP led to a significant increase in the stele-to-cortex ratio in the Loutra ecotype (**Fig. 10 A, C, D**).

In the Ampeliko roots, exposure to 500 mg/L of NiO NP caused an enlargement of both the stele and cortex areas (**Fig. 10 B**), which resulted in an overall increase in root area (**Fig. 10 A**). At 0 and 250 mg/L of NiO NP, the Ampeliko cortex consisted of two cell layers, while at 500 mg/L, three cell layers were observed (**Fig. 10 E**).

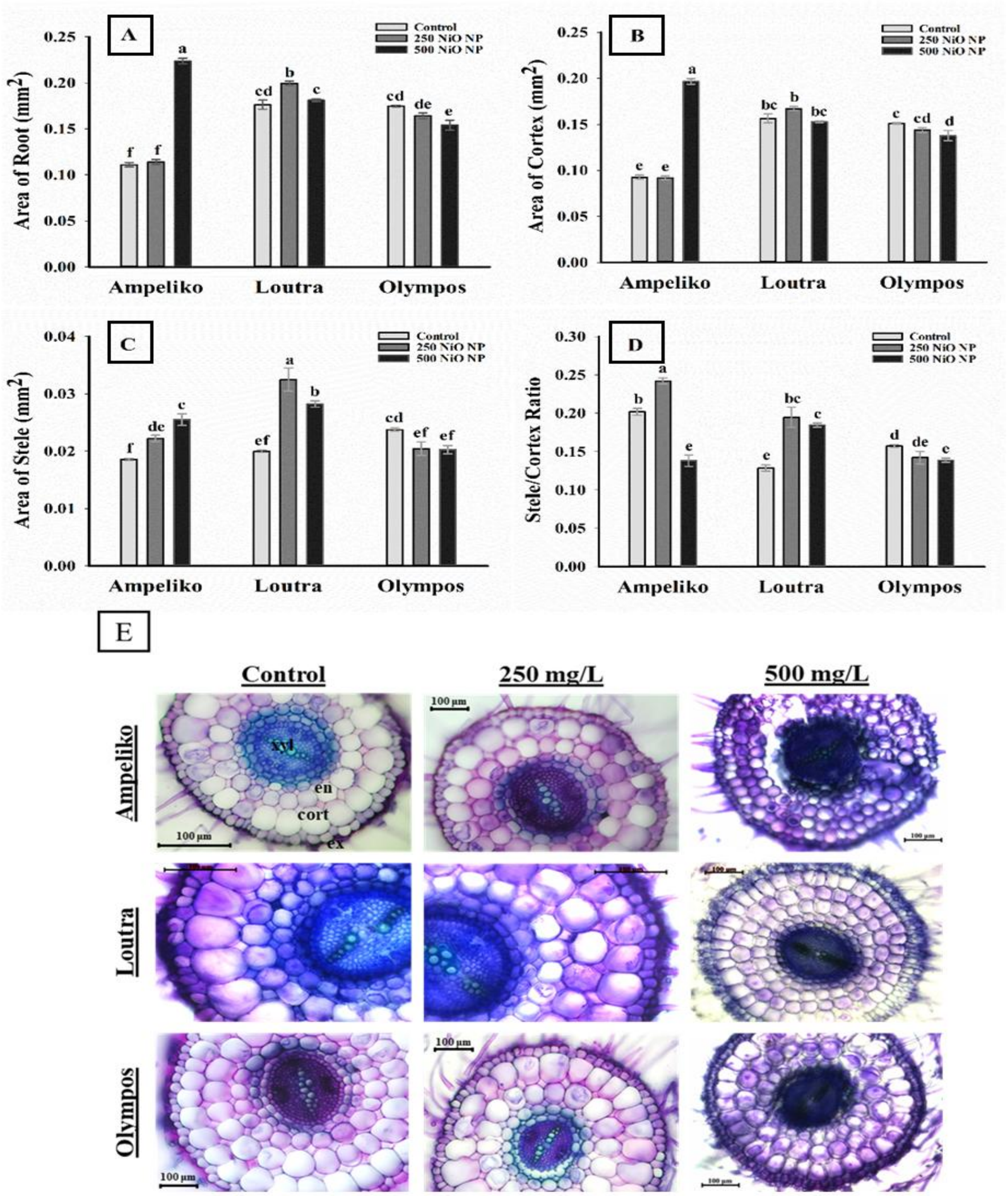

Fig. 10. Root area (A), cortex area (B), stele area (C) and stele/cortex ratio (D) measured in cross sections of primary roots of *Odontarrhena lesbiaca* (Ampeliko, Loutra and Olympos ecotypes) grown in the presence of 0, 250 or 500 mg/L NiO NP. Different letters indicate significant differences according to Duncan's test (n= 10, P< 0.05). (E) Representative cross sections of *Odontarrhena lesbiaca* roots stained with toluidine blue. Scale bars= 100 µm. Abbreviations: xyl=xylem, en=endodermis, cort= cortex.

Pectin levels in the root tissues of *Odontarrhena lesbiaca* ecotypes exhibited varying responses to NiO NP treatments. In the mature zone of Ampeliko roots, the pink color associated with pectin slightly diminished under the influence of NiO NPs (as indicated by arrows in **Fig. 11 A**). In contrast, the pectin levels in the Loutra and Olympos ecotypes increased—within the root cap and apical meristem in Loutra, and in the mature root zone of Olympos (arrows in **Fig. 11 A**).

In addition, lignin and suberin were observed in root cross sections using Auramine-O staining (**Fig. 11 B**). In the untreated Ampeliko roots, fluorescence was detected in both the outer and inner tangential cell walls of the epidermis/exodermis, indicating suberin presence and the development of an exodermis. In all three ecotypes, treatment with both doses of NiO NP resulted in enhanced fluorescence in the tangential and radial cell walls of exodermal cells compared to the untreated control (**Fig. 11 B**), suggesting the formation of an exodermal suberin layer.

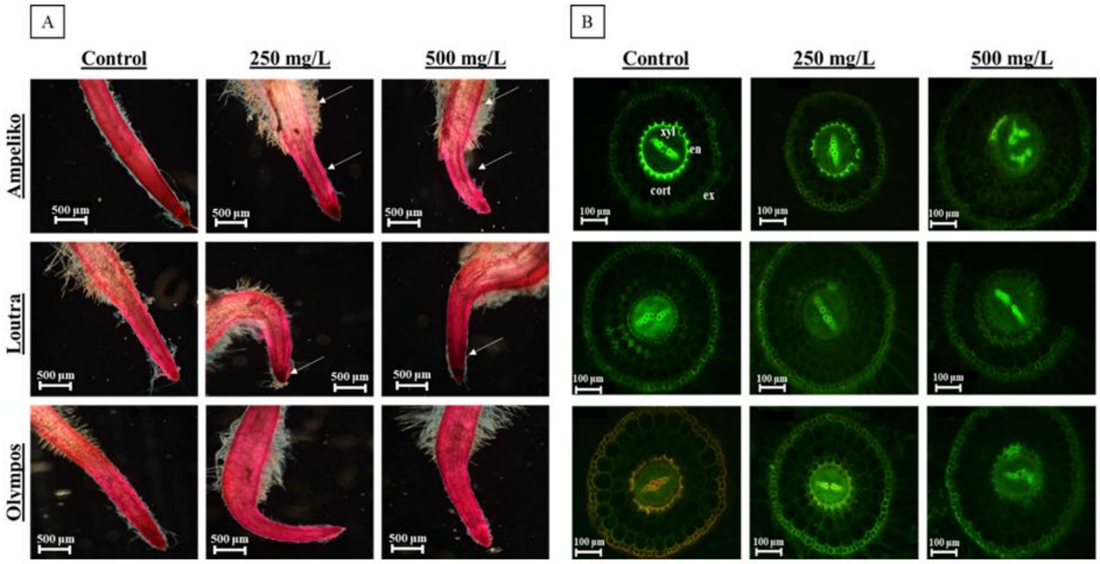

Fig. 11. (A) Pectin levels in the root tips of *Odontarrhena lesbiaca* ecotypes (Ampeliko, Loutra, and Olympos) exposed to 0 (control), 250, or 500 mg/L NiO NP for 5 days. Roots were stained with ruthenium red (see Materials and Methods for details). Arrows highlight regions where staining intensity increased or decreased relative to the control. Scale bars= 500 µm. (B) Lignin and suberin content in cross-sections of *O. lesbiaca* ecotypes. Root samples were stained with Auramine-O (see Materials and Methods for details). Scale bars= 100 µm. Abbreviations: xyl=xylem, en=endodermis, ex= exodermis, cort= cortex.

6. 6. Biomass production and growth responses to NiO NP treatment in different *Odontarrhena lesbiaca* ecotypes

The control plants of the Olympos seedlings exhibited significantly smaller sizes compared to those of Ampeliko and Loutra, as demonstrated by most of the biomass measurements (**Fig. 12**). In terms of the effects of NiO NP treatment, the primary root length, shoot length, root fresh weight, shoot fresh weight, and shoot dry weight of Loutra were not significantly affected by either 250 or 500 mg/L of NiO NP. For Ampeliko, most biomass parameters remained unchanged by the applied NiO NP doses, with the exception of root length and fresh weight, where the 250 mg/L NiO NP treatment caused a notable reduction compared to untreated plants (**Fig. 12 A, B**). In contrast, all biomass parameters of Olympos seedlings showed a dose-dependent increase in response to NiO NP treatment (**Fig. 12**). For instance, 250 mg/L NiO NP resulted in a 1.80-fold increase in root length, while 500 mg/L led to a 2.69-fold increase compared to the control group (**Fig. 12 A**).

Across all parameters, it was observed that the Olympos seedlings treated with NiO NP reached the size of the control plants of Ampeliko and Loutra (**Fig. 12 A, B, D, E**). The overall growth of representative individuals from the *Odontarrhena lesbiaca* ecotypes is shown in **Fig. 12 G.**

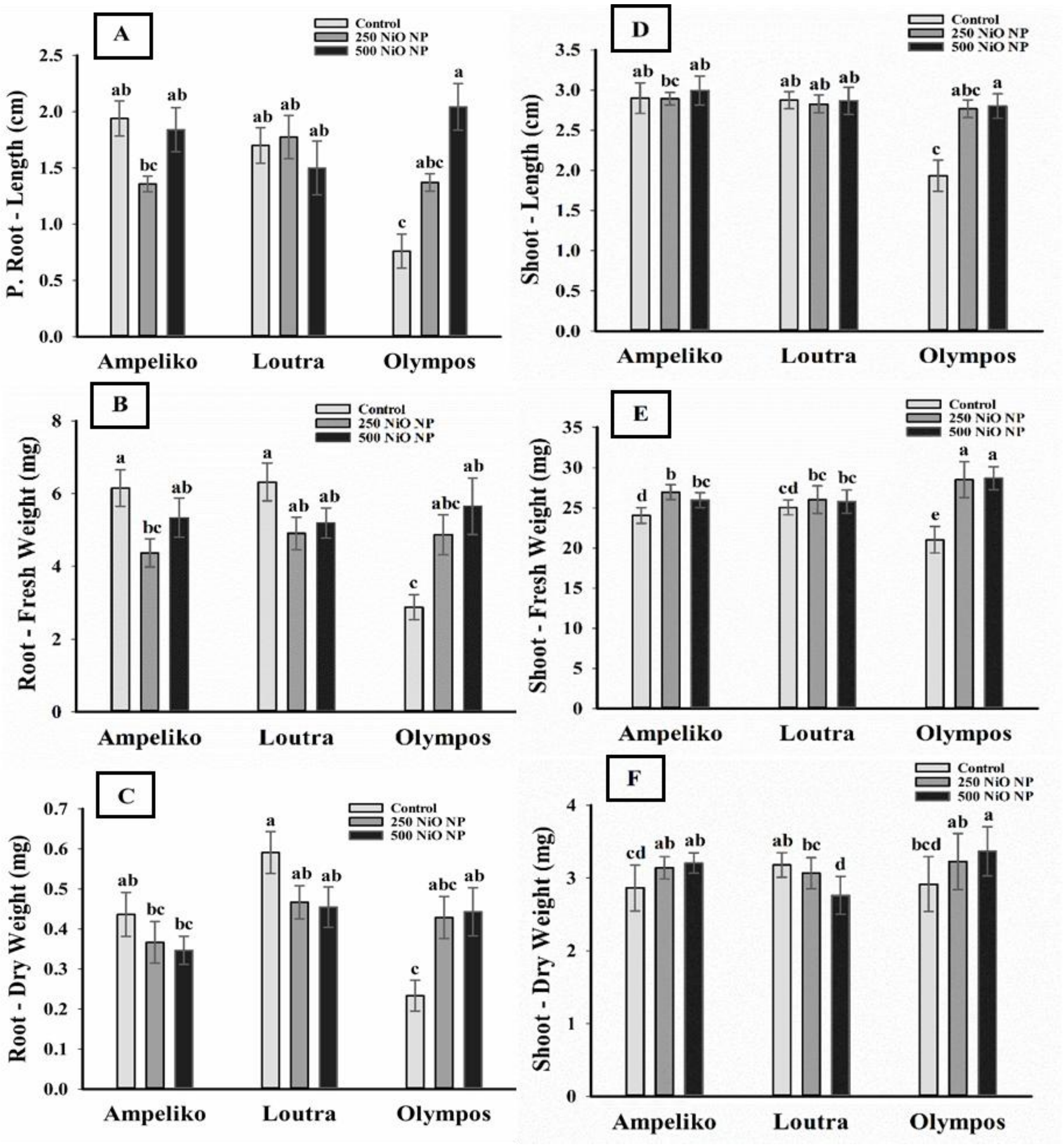
A
Control
250 NiO NP
500 NiO NP
P. Root - Length (cm)
0.0
0.5
1.0
1.5
2.0
2.5
ab
bc
ab
ab
ab
ab
c
abc
a
Ampeliko
Loutra
Olympos
D
Shoot - Length (cm)
0.0
0.5
1.0
1.5
2.0
2.5
3.0
3.5
ab
bc
ab
ab
ab
ab
c
abc
a
B
Root - Fresh Weight (mg)
0
2
4
6
8
a
bc
ab
a
ab
ab
c
abc
ab
E
Shoot - Fresh Weight (mg)
0
5
10
15
20
25
30
35
d
b
bc
cd
bc
bc
e
a
a
C
Root - Dry Weight (mg)
0.0
0.1
0.2
0.3
0.4
0.5
0.6
0.7
ab
bc
bc
a
ab
ab
c
abc
ab
F
Shoot - Dry Weight (mg)
0
1
2
3
4
cd
ab
ab
ab
bc
d
bcd
ab
a

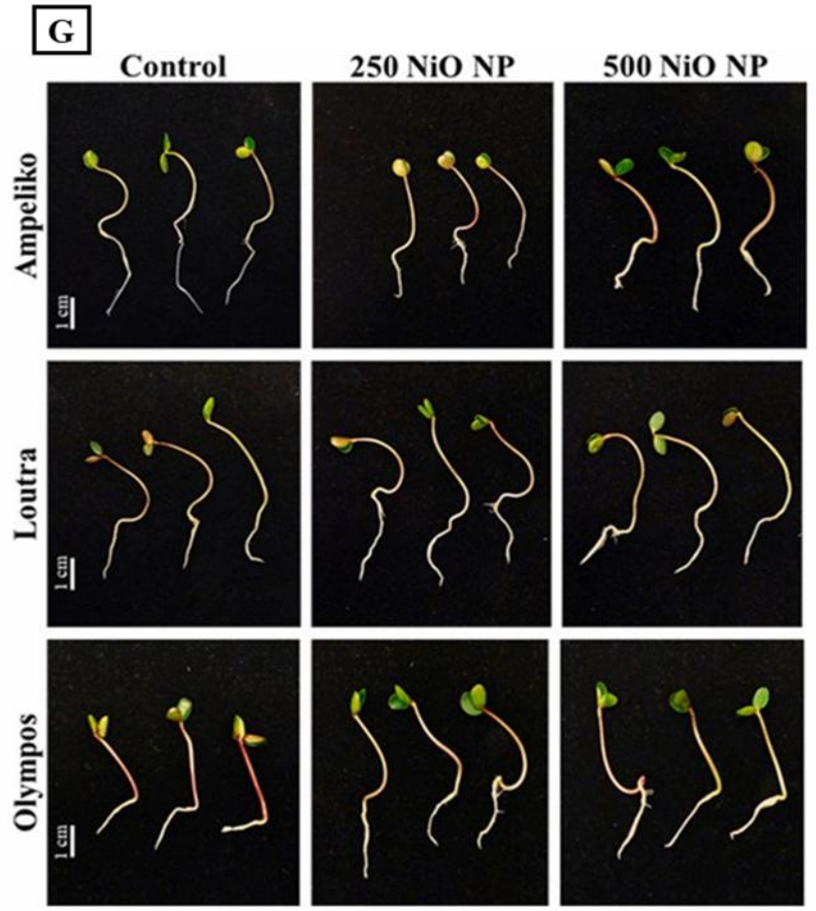

Fig. 12. Primary root length (A), root fresh weight (B), root dry weight (C), shoot length (D), shoot fresh weight (E) and shoot dry weight (F) of 5 days old *Odontarrhena lesbiaca* seedlings germinated in the presence of 0 mg/L (control), 250 mg/L or 500 mg/L NiO NP. Different letters indicate significant differences according to Duncan's test (n= 10, P< 0.05). (G) Growth status of the control and NiO NP-exposed *Odontarrhena lesbiaca* ecotypes (three representative seedlings/treatment). Scale bars= 1 cm.

Applying ionic Ni in the form of $NiCl_2$ at the same concentration and exposure time as the nanoparticle form led to a significant reduction in Ampeliko shoot length, while other parameters remained unaffected, with a slight increase observed in root dry weight at the 250 mg/L dose (**Fig. 13**). In contrast, for the Loutra ecotype, root length as well as both shoot fresh and dry weights decreased under both $NiCl_2$ concentrations (**Fig. 13 A, D, E**).

Interestingly, no notable changes in growth or biomass parameters were detected in Olympos in response to $NiCl_2$, unlike the growth-promoting effect observed at the same concentrations of NiO NP (**Fig. 12**).

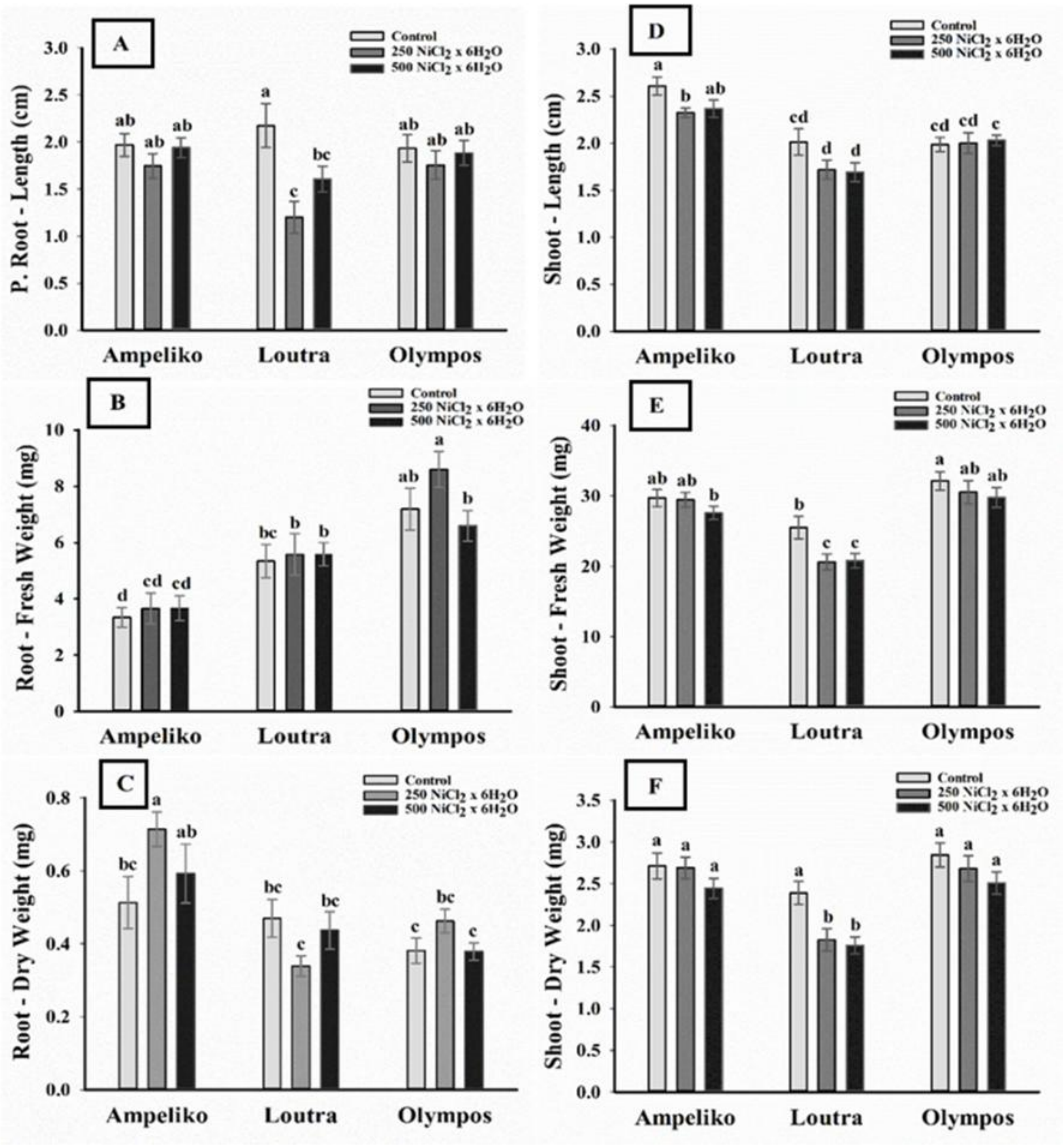

Fig. 13. Primary root length (A), root fresh weight (B), root dry weight (C), shoot length (D), shoot fresh weight (E) and shoot dry weight (F) of 5 days old *Odontarrhena lesbiaca* seedlings germinated in the presence of 0 mg/L (control), 250 mg/L or 500 mg/L $NiCl_2 \times 6H_2O$. Different letters indicate significant differences according to Duncan's test (n= 10, P< 0.05).

6. 7. Differential nitro-oxidative and protein nitration responses to NiO NP exposure across *Odontarrhena lesbiaca* ecotypes

The application of 250 mg/L NiO NP significantly increased NO production in the roots of the Ampeliko and Loutra ecotypes, while the NO levels in the roots of the Olympos ecotype remained unchanged (**Fig. 14 A**). Specifically, the 250 mg/L NiO NP treatment led to a 26% elevation in NO levels in Ampeliko and a 20% increment in Loutra compared to the control, whereas doubling the NiO NP dose resulted in NO levels similar to those of the control. In Olympos, neither of the NiO NP concentrations had a notable effect on NO production (**Fig. 14 A**).

Regarding $ONOO^-$, NiO NP treatment led to a concentration-dependent increase in its levels in the roots of Loutra and Olympos compared to the control (**Fig. 14 B**). For Olympos, $ONOO^-$ levels increased by 20.7% and 35.6% with 250 and 500 mg/L NiO NP treatments, respectively, while no alterations in $ONOO^-$ levels were observed in the roots of Ampeliko after NiO NP exposure (**Fig. 14 B**).

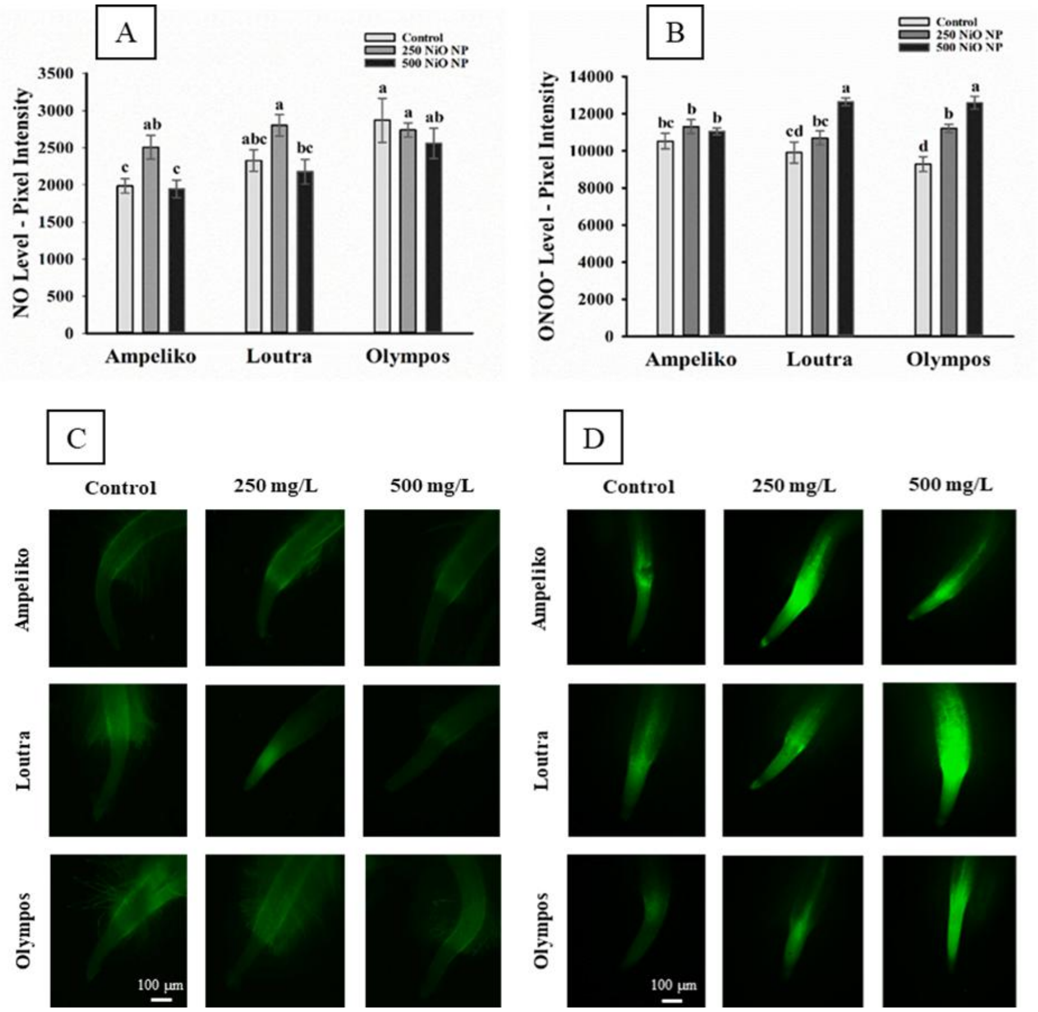

Fig. 14. The levels of nitric oxide (NO, A) and peroxynitrite ($ONOO^-$, B) (expressed as pixel intensities) in the root tips of the Ampeliko, Loutra, and Olympos ecotypes of *Odontarrhena lesbiaca* seedlings grown in the presence of 0, 250 mg/L or 500 mg/L NiO NP for 5 days. Different letters indicate significant differences according to Duncan's test (n= 10, P< 0.05). Representative images showing root tips labelled with DAF-FM DA (C) or DHR123 (D) probes. Scale bars= 100 µm.

NiO NP exposure led to a concentration-dependent reduction in GSNOR protein levels in the roots of the Ampeliko ecotype, whereas in Loutra, a significant decrease was observed only at the 500 mg/L NiO NP dose. In contrast, the GSNOR protein levels significantly increased in the Olympos ecotype following treatment with 500 mg/L NiO NP (**Fig. 15 A, Fig. 16 A**). Additionally, in the shoots of the Loutra ecotype, a clear increase in GSNOR protein levels was induced by NiO NPs, while in Ampeliko and Olympos, both NiO NP concentrations resulted in decreased GSNOR protein levels (**Fig. 15 B, Fig. 16 B**).

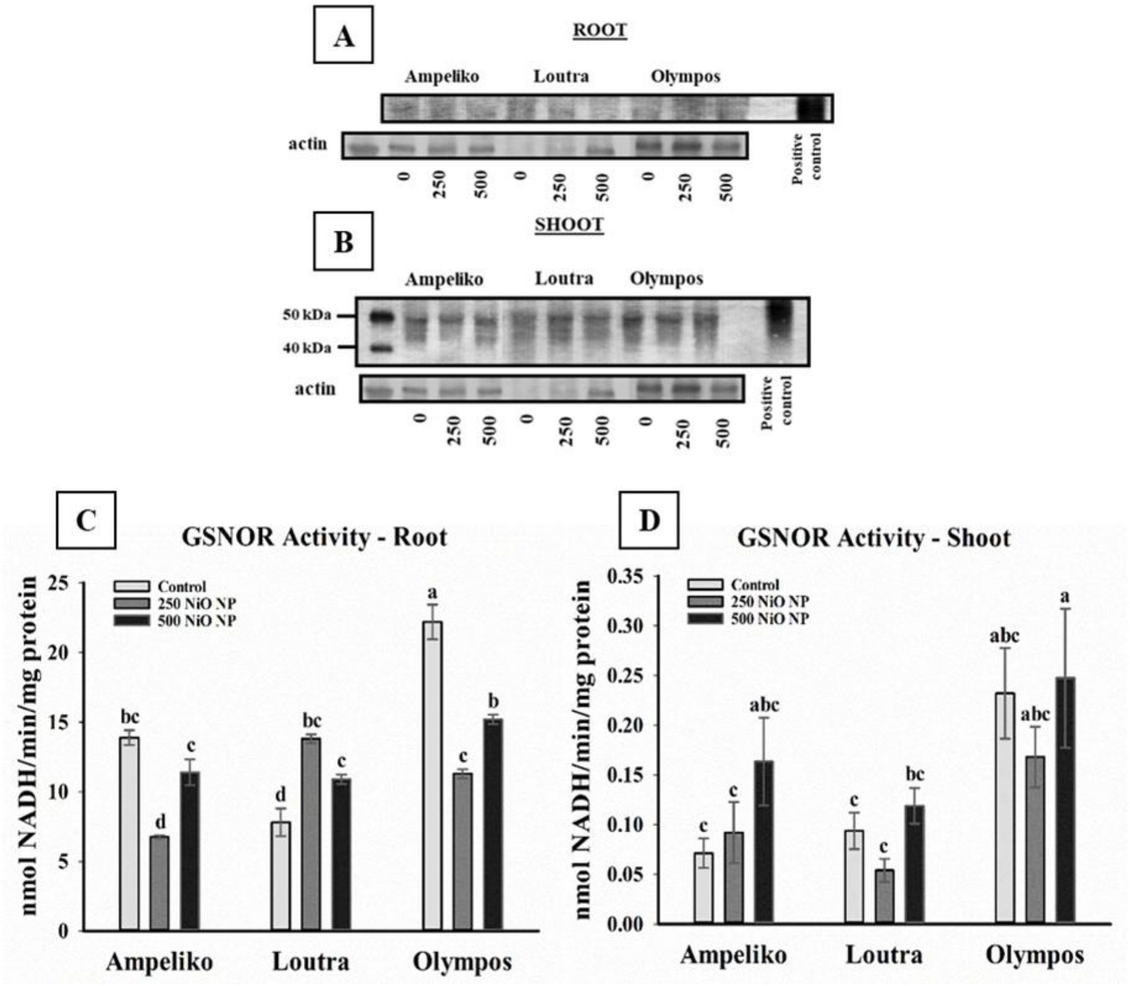

Fig. 15. Abundance of GSNOR protein in the root (A) and shoot (B) of *Odontarrhena lesbiaca* ecotypes (Ampeliko, Loutra, Olympos) exposed to 0, 250 or 500 mg/L of NiO NP for 5 days. Actin was used as internal control. Positive control= protein extract form GSNOR overproducing *Arabidopsis thaliana* seedlings (35S::FLAG-GSNOR1). Activity of GSNOR (expressed as nmol NADH/min/mg protein) in the root (C) and shoot (D) of NiO NP-treated *Odontarrhena lesbiaca* seedlings. Different letters indicate significant differences according to Duncan's test (n= 5, P< 0.05).

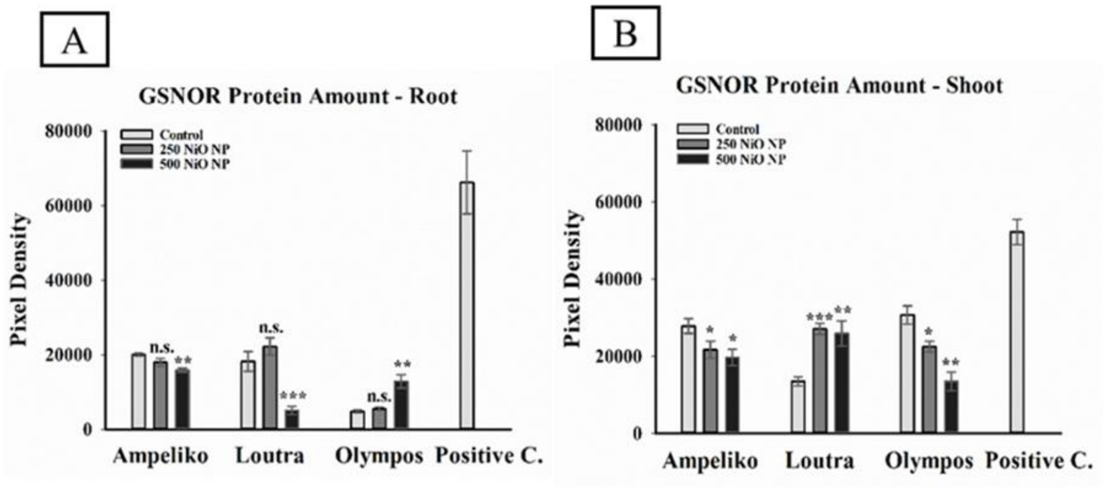

Fig. 16. Amount of GSNOR protein (expressed as pixel density) in the root (A) and shoot (B) of the *Odontarrhena lesbiaca* ecotypes (Ampeliko, Loutra, Olympos) exposed to 0, 250 or 500 mg/L NiO NP. Significant differences compared to controls were determined using the Student's t test (n= 3, * P< 0.05, ** P< 0.01, *** P< 0.001, ns= non-significant). Pixel desities were measured on representative western blot membranes using GelQuant (see Materials and Methods). Positive C= positive control, protein extract form GSNOR overproducing *Arabidopsis thaliana* seedlings (35S::FLAG-GSNOR1).

Although NiO NP treatments led to changes in protein levels, no significant differences in enzyme activity were detected in the shoots due to the large variability in the data (**Fig. 15 D**). In the roots, 250 mg/L NiO NP treatment led to a reduction in GSNOR activity in Ampeliko, and both NiO NP concentrations significantly decreased GSNOR activity in Olympos (by 49% at 250 mg/L and 31.5% at 500 mg/L, **Fig. 15 C**). In contrast, in Loutra, 250 mg/L of NiO NP caused a 77% increase in activity, while 500 mg/L treatment led to a 39.6% increase compared to the control.

All three ecotypes exhibit a basal pattern of protein tyrosine nitration in both roots and shoots, suggesting a pre-existing physiological pool of nitrated proteins. Upon exposure to NiO NPs, the roots of the Ampeliko ecotype showed a notable increase in protein nitration, with elevated nitration observed across at least seven distinct protein bands (indicated by arrows in **Fig. 17 A**). These bands, estimated to range approximately from 20 to 70 kDa, imply that NiO NP exposure may be influencing a broad spectrum of proteins with varying molecular functions. In Loutra roots, nitration increased across at least four bands, particularly in the approximate range of 35 to 60 kDa (indicated by arrows in **Fig. 17 A**), indicating a narrower yet targeted response in specific protein groups. In contrast, Olympos roots displayed an increase in tyrosine nitration intensity in one band around 35 kDa, while two other bands, approximately 25 and 45 kDa, exhibited a reduction (indicated by arrows in **Fig. 17 A**), suggesting a differential regulation in nitration levels depending on the protein size and function (**Fig. 17 A, Fig. 18**).

In the shoots, NiO NP treatment similarly led to increased nitration in specific protein bands, with Ampeliko displaying an elevation across at least four bands, likely between 15 and 55 kDa (indicated by arrows in **Fig. 17 B**), suggesting an upregulation of nitration in various proteins upon NiO NP exposure. Loutra shoots showed an increase across three bands, with estimated molecular masses in the 40 to 60 kDa range; however, a decrease in one protein band around 45 kDa was also observed (indicated by arrows in **Fig. 17 B**), possibly indicating a nuanced regulatory response. In the Olympos ecotype, nitration levels decreased in two bands estimated at 40 and 100 kDa, despite a slight increase in two others around 50 and 140 kDa (indicated by arrows in **Fig. 17 B**), suggesting selective nitrative modifications potentially linked to adaptive or protective mechanisms against Ni-induced stress in specific protein subsets (**Fig. 17 B, Fig. 18**).

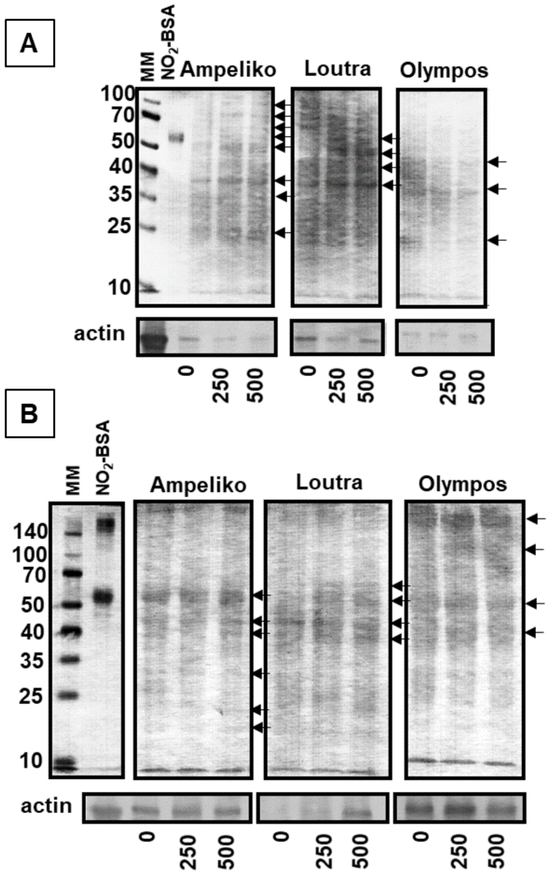

Fig. 17. Representative western blot membranes showing tyrosine protein nitration in root (A) and shoot (B) of the *Odontarrhena lesbiaca* ecotypes (Ampeliko, Loutra, Olympos) exposed to 0, 250 or 500 mg/L NiO NP. MM= molecule marker, NO$_2$-BSA= nitrated bovine serum albumin. Actin was used as an internal control. The black arrows indicate protein bands with altered signal intensity.

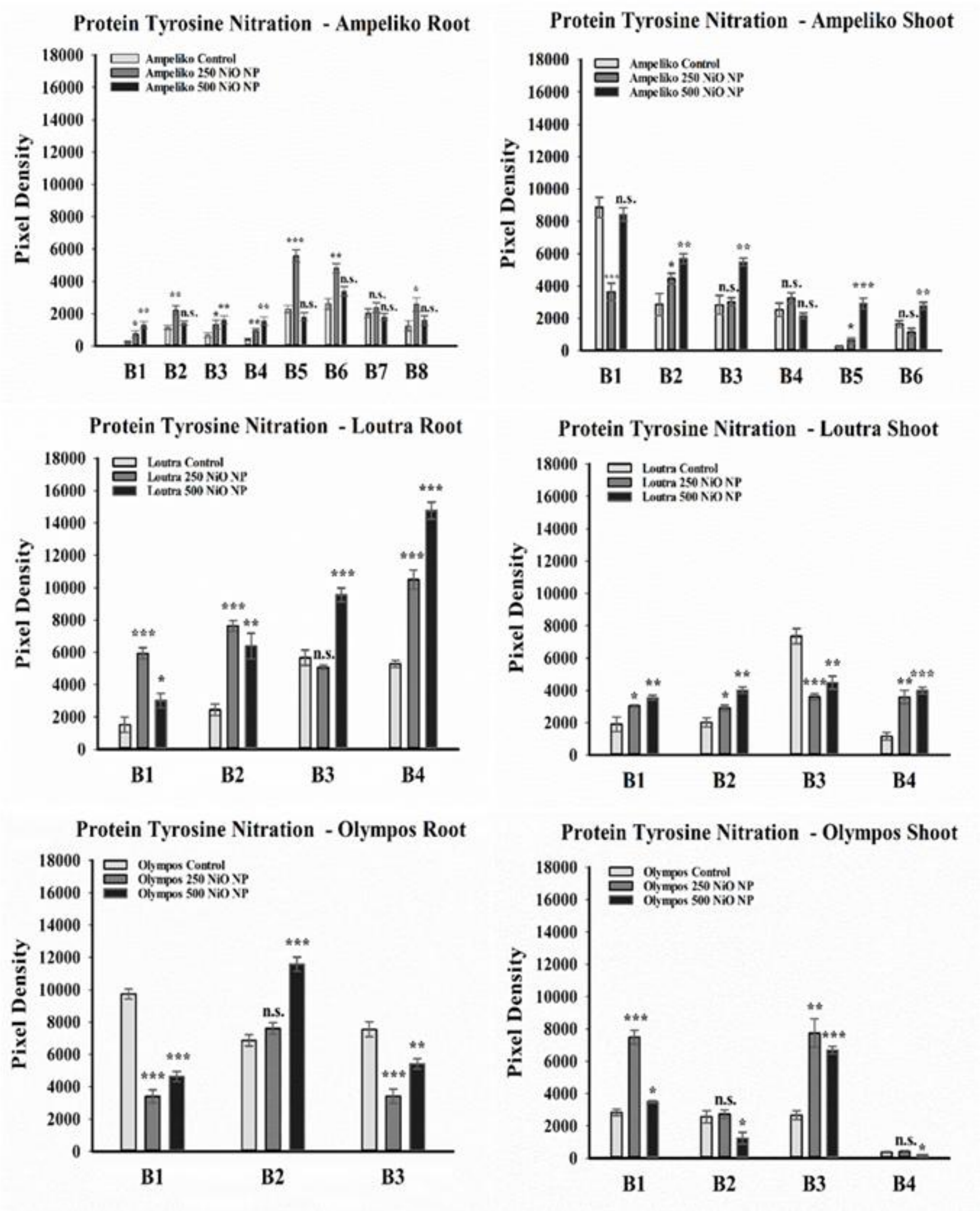

Fig. 18. Protein tyrosine nitration in the root and shoot of *Odontarrhena lesbiaca* ecotypes (Ampeliko, Loutra, Olympos) exposed to 0, 250 or 500 mg/L NiO NP. (B1, B2,....B8 represent different protein bands in the graph). Significant differences compared to controls were determined using the Student's t test (n= 3, * P< 0.05, ** P< 0.01, *** P< 0.001, ns= non-significant).

7. Discussion

In this section, the findings presented in the Results part were discussed and interpreted in the context of the existing literature. Patterns observed among different *Odontarrhena lesbiaca* ecotypes under NiO NP exposure were compared, with a focus on elucidating the underlying physiological and biochemical mechanisms. Particular attention was given to how variations in Ni accumulation, Ni NP uptake, root structure modification, biomass production, and protein tyrosine nitration align with the ecological and functional differences between ecotypes.

7. 1. Ni accumulation and translocation in *Odontarrhena lesbiaca* ecotypes following NiO NP and bulk Ni treatment

First of all, we focused to examine the effects of NiO NP exposure on Ni accumulation and translocation in different *Odontarrhena lesbiaca* ecotypes. In this part, we aimed to compare the behavior of nanoparticulate Ni with ionic Ni forms, particularly in terms of their impact on root-to-shoot translocation. The high Ni concentrations in untreated *Odontarrhena lesbiaca* ecotypes confirm this species' capability for hyperaccumulation (**Table 1**). NiO NP treatment resulted in a concentration-dependent increase in root Ni content, with varying degrees of accumulation among the ecotypes. Specifically, Olympos exhibited a much lower Ni accumulation in the roots at 250 mg/L NiO NP compared to Ampeliko and Loutra. Furthermore, NiO NP exposure leads to reduced root-to-shoot translocation, as indicated by translocation factors below 1, suggesting that most of the Ni remained localized in the roots, potentially bound to cell walls or retained within root cells. This contrasts with $NiCl_2$ treatments, where efficient Ni translocation to the shoots occurred, as reflected by higher translocation factors and elevated shoot Ni concentrations. These findings underscore the differing behaviors of nanoparticulate and ionic Ni forms in plant systems, which may have implications for their use in phytoremediation or agricultural practices.

7. 2. Element distribution in *Odontarrhena lesbiaca* ecotypes: Focusing on Ni (ionic or nano-Ni)

Next, we focused on examining the distribution of various elements, especially divalent cations, in *Odontarrhena lesbiaca* ecotypes exposed to either NiO NP or $NiCl_2$ treatment. This section compares how nanoparticulate and ionic Ni forms affect the uptake and distribution of other essential elements like K, Na, Mg, and Ca in these hyperaccumulator plants. Using the LIBS technique, we visualized the spatial distribution of these elements within the seedlings, which helped provide insights into nutrient homeostasis and the interactions of elements under Ni stress.

Rather than a Ni-specific transporter, it appears that poorly selective cation transporters facilitate Ni uptake in the roots (van der Pas and Ingle, 2019), indicating that increased Ni ion absorption may also influence the uptake of other divalent cations. Consequently, the distribution of other elements, especially divalent cations, was visualized in *Odontarrhena lesbiaca* seedlings treated with either NiO NP or $NiCl_2$. In particular, increases in signal intensity for elements such as K, Na, Mg, and Ca were observed, suggesting that their uptake may be enhanced in the presence of elevated Ni concentrations and minor changes observed in their distribution suggest that nutrient homeostasis in Ampeliko, Loutra, and Olympos seedlings remains stable despite elevated Ni exposure (**Fig. 7**). It is likely that the activation of the Ni ion transport system enhances the absorption of other (divalent) cations in these hyperaccumulating plants. However, cellular uptake cannot be ruled out entirely since this statement should be refined as there are indications that the NPs may increase the pore size of the cell wall (Kurczyńska *et al*., 2021; Oliveira *et al*., 2023).

In summary, the LIBS technique provides valuable spatial information regarding element distribution and supports the hypothesis that LIBS is effective in visualizing both macroelement and microelement distributions, primarily in the shoots of Ni hyperaccumulator *Odontarrhena lesbiaca* seedlings.

7. 3. Effects of NiO NPs on root tissue structure and composition of the cell wall of *Odontarrhena lesbiaca* seedlings

In this part, we focused on examining the effects of NiO NP exposure on root tissue structure and the composition of the root cell wall in *Odontarrhena lesbiaca* seedlings. The goal was to investigate how NiO NPs influence the anatomical changes in roots, particularly in relation to the accumulation of specific compounds like pectin and suberin, which are thought to help plants cope with Ni-induced stress and at the same time influence the cells' interaction with the NPs. By assessing the structural modifications in the root tissue, this section aims to provide a clearer understanding of how these plants adapt to elevated Ni levels.

Previous studies have suggested that approximately 80% of Ni accumulates in the vascular cylinder, potentially leading to a reduction in phloem and xylem diameters (Page *et al*., 2006; dos Reis *et al*., 2017). The observed decrease in root, cortex, and stele areas in the Olympos ecotype, particularly under 500 mg/L NiO NP exposure, aligns with this idea (**Fig. 10 A, B, C, D**). Additionally, the significant increase in the stele-to-cortex ratio in Loutra ecotype roots exposed to 250 mg/L NiO NP supports the hypothesis that Ni may affect the structural integrity of the vascular tissues. The thickening of the cortex observed in Ampeliko roots treated with 500 mg/L NiO NP (**Fig. 10 E**), resulted in an increase in both stele and cortex areas, which may contribute to Ni tolerance by restricting radial water flow and reducing heavy metal transport (Pandey *et al*., 2022). This thickening of cell layers and increase in root area are likely structural adaptations that enhance the plants' ability to cope with elevated Ni levels.

The accumulation of pectic compounds in the cell walls of Loutra and Olympos ecotypes following NiO NP exposure (**Fig. 11 A**), particularly in the root cap, apical meristem, and mature zones, suggests that pectin may play a role in the sequestration of Ni^{2+}. This could be due to the replacement of Ca^{2+} ions previously bound to the cell wall (Dronnet *et al*., 1996; Krzesłowska, 2011; Loix *et al*., 2017), effectively limiting Ni's entry into the cytoplasm.

The formation of an exodermal suberin layer, indicated by increased fluorescence in exodermal cell walls (**Fig. 11 B**), suggests that suberin plays a protective role by acting as an outer barrier potentially delaying the uptake of metal ions or nanoparticles. Studies have shown that increased lignin and suberin deposition in the exodermis occurs in response to heavy metal exposure (Cheng *et al*., 2010; 2012). and a positive correlation between exodermal suberin formation and metal tolerance has been observed in mangrove species (Cheng *et al*., 2014).

7. 4. Biomass production and growth responses to NiO NP treatment in different *Odontarrhena lesbiaca* ecotypes

This part of the discussion addresses the effects of NiO NP treatment on the biomass production and growth of *Odontarrhena lesbiaca* ecotypes. Specifically, we aimed to assess how different concentrations of NiO NPs influence the growth dynamics of these plants, with a particular focus on changes in root and shoot development. By comparing the responses of the ecotypes, this part explores the differential tolerance mechanisms to NiO NPs and seeks to understand the relationship between metal form, concentration, and plant growth.

The results suggest that NiO NP treatment affects the biomass production and growth of *Odontarrhena lesbiaca* ecotypes in a concentration-dependent manner, with notable variations among the ecotypes. The Olympos ecotype showed a pronounced growth response to NiO NP exposure, with significant increases in root length, shoot length, and biomass at both 250 mg/L and 500 mg/L concentrations (**Fig. 12**). This suggests that Olympos may possess unique mechanisms that allow it to thrive in the presence of NiO NPs, potentially through enhanced uptake or more efficient detoxification of Ni.

In contrast, the Ampeliko and Loutra ecotypes exhibited less pronounced growth responses to NiO NP treatment, showing limited or no significant changes in biomass parameters. Ampeliko displayed a decrease in root length and fresh weight at 250 mg/L (**Fig. 12 A, B**). These results suggest that these ecotypes may be less tolerant to NiO NP exposure, potentially due to their lower capacity to manage the influx of Ni ions or their limited ability to cope with nanoparticle-induced stress. These ecotype-specific differences highlight the need for further understanding of the underlying mechanisms governing the growth responses to NiO NPs.

The results indicate that the lower concentration of Ni ions released from NiO NPs promote growth in the Olympos ecotype (**Fig. 12**), while the higher ion concentrations from $NiCl_2$ did not induce further growth and led to a reduction in biomass in the Ampeliko and Loutra ecotypes (**Fig. 13**). These findings suggest that the ionic form of Ni, as a free salt, exerts more negative effects compared to the nanoparticle form, possibly due to the higher amount of Ni ions released (**Table 1**). Furthermore, the observed effects of NiO NP appear to be primarily driven by the release of Ni ions, with the nanoparticle form inducing a more balanced or growth-promoting response in certain ecotypes, such as Olympos.

Interestingly, while NiO NP treatment enhanced growth in Olympos (**Fig. 12**), $NiCl_2$ treatment did not induce the same positive effects. In fact, $NiCl_2$ exposure led to a reduction in biomass in both Ampeliko and Loutra, particularly in shoot length and fresh weight (**Fig. 13**). This implies the possibility that the ionic form of Ni, compared to the nanoparticle form, may have more detrimental effects on plant growth. The slower release of Ni ions from NiO NPs likely provides a more controlled exposure, allowing plants to better manage the metal, whereas the rapid release from $NiCl_2$ could overwhelm the plant's detoxification pathways, leading to growth inhibition.

The differential growth responses between the nanoparticle and ionic forms of Ni may also be related to how plants interact with these two forms at the cellular level. Nanoparticles could trigger milder oxidative stress and might be processed by the plant in a way that minimizes toxicity. In contrast, the ionic form may induce stronger stress responses, such as antioxidant production and activation, which could limit growth potential, even when Ni accumulation is similar or lower.

Overall, these findings highlight the complexity of plant responses to different metal forms, particularly in hyperaccumulator species like *Odontarrhena lesbiaca*. These insights are crucial for optimizing phytoremediation strategies, where both the form and concentration of metals need to be carefully managed to balance plant growth and metal uptake.

7. 5. Differential nitro-oxidative and protein nitration responses to NiO NP exposure across *Odontarrhena lesbiaca* ecotypes

In this part of the discussion, by investigating the levels of NO, $ONOO^-$, and the role of GSNOR in each ecotype, we aim to understand the unique stress management strategies employed by these plants when exposed to NiO NPs. The final aspect of our research focused on investigating the variations in protein tyrosine nitration patterns among different *Odontarrhena lesbiaca* varieties following exposure to NiO NPs. This part of the study aimed to understand how each ecotype modulates protein nitration as part of its defense mechanisms against oxidative stress. By analyzing these patterns, we sought to uncover how different varieties manage oxidative damage at the protein level and how these responses relate to their overall growth and stress tolerance.

This study demonstrates that NiO NP treatment induces varying effects on the levels of NO and $ONOO^-$ in different *Odontarrhena* ecotypes. Specifically, the increase in NO production in the roots of Ampeliko and Loutra ecotypes suggests these ecotypes may activate NO-associated signaling pathways more efficiently when exposed to NiO NPs (**Fig. 14 A**). NO plays a crucial role in plant stress responses and defense mechanisms, and its increased production in response to metal exposure might enhance the plants' ability to cope with metal toxicity. However, no significant change in NO levels was observed in the Olympos ecotype, which may indicate a higher tolerance to Ni, possibly due to a more regulated NO signaling process in this ecotype. NO has been shown to alleviate metal-induced oxidative stress in various systems. For example, NO's role in regulating redox balance and signaling pathways under various abiotic stresses, including heavy metal toxicity, has been highlighted in recent studies (Liu *et al.*, 2023; Khator *et al.*, 2023). Moreover, according to a recent study, in paddy field cyanobacteria, NO reduced ROS levels and enhanced enzymatic defense systems under Ni toxicity (Singh and Prasad, 2024).

In the previous research of our research group, it was found that $NiCl_2$ stimulate NO production in the Ampeliko ecotype grown in rhizotrons (Feigl *et al.*, 2020), and similar effects were observed in *Arabidopsis thaliana* plants (Kolbert *et al.*, 2020). Likewise, increasing doses of NiO NPs led to elevated NO levels in *Allium cepa* roots, where NiO NPs activated nitrate reductase and nitric oxide synthase-like (NOS-like) enzymes, indicating their role in the NP-induced increase in NO production (Manna *et al.*, 2021). However, it is important to note that the gene and protein for the NOS-like enzyme have not yet been identified in higher plants (Jeandroz *et al.*, 2016), suggesting the need for further research to clarify the underlying mechanisms.

Regarding $ONOO^-$, the results show a concentration-dependent increase in its levels in the roots of Loutra and Olympos ecotypes, suggesting that this reactive nitrogen species plays a role in the oxidative stress responses triggered by NiO NP exposure (**Fig. 14 B**). However, no increase in $ONOO^-$ was observed in Ampeliko, which may reflect a different oxidative stress response strategy or a more effective detoxification mechanism in this ecotype. Recent studies have indicated that GSNOR activity could be post-translationally regulated through NADPH oxidase/respiratory burst oxidase homolog-related calcium and redox signaling, potentially representing an additional regulatory mechanism in response to NiO NP exposure (Zhang *et al*., 2020; Chae *et al*., 2021; Li *et al*., 2021; Song *et al*., 2022).

Notably, the differential regulation of GSNOR across ecotypes suggests that this enzyme is a critical player in the response to NiO NP exposure. In Loutra, increased GSNOR protein levels in the roots suggest an adaptive mechanism to mitigate oxidative damage induced by NiO NPs (**Fig. 15 A**). Conversely, a reduction in GSNOR protein levels in the roots of Ampeliko and Olympos suggests that these ecotypes may employ different strategies for managing nitrosative stress, potentially balancing NO production and its downstream effects more efficiently (**Fig. 15 A**). Furthermore, the increased GSNOR levels in the shoots of Loutra further support the idea that this ecotype may regulate nitrosative stress across different tissues (**Fig. 15 B**), while the decrease in GSNOR protein levels in the shoots of Ampeliko and Olympos points to a more systemic response to NiO NP exposure (**Fig. 15 B**).

Overall, these findings underscore the ecotype-specific responses of *Odontarrhena lesbiaca* to NiO NP exposure, particularly in how they regulate reactive nitrogen species like NO and $ONOO^-$. While Ampeliko and Loutra exhibited enhanced NO production, potentially improving their metal stress tolerance, Olympos showed no significant changes, suggesting a higher resistance to Ni. The differential $ONOO^-$ accumulation also highlights varied oxidative stress management strategies across ecotypes. Furthermore, the distinct regulation of GSNOR across ecotypes points to a complex mechanism for coping with nitrosative stress, with Loutra possibly utilizing GSNOR to better manage oxidative damage. These insights are important for understanding the adaptability of different plant varieties to metal-induced stress, with potential applications in phytoremediation and agriculture.

The observed decrease in nitration signals suggests the activation of defense mechanisms, potentially involving the proteasomal degradation of nitrated proteins. Minor differences among ecotypes were noted, with Ampeliko showing the most intense nitration response, while Loutra exhibited a more targeted nitration pattern. In contrast, Olympos displayed fewer changes in nitration, indicating a more efficient response to NiO NP exposure (**Fig. 17 A, B**).

These variations in protein nitration levels correspond with the biomass production of the ecotypes, suggesting that Ampeliko is the most sensitive, Loutra exhibits moderate sensitivity, and Olympos shows the highest tolerance to NiO NP exposure (reviewed in Feigl *et al*., 2020). The higher nitration in Ampeliko likely reflects more significant oxidative stress, which correlates with its reduced growth under NiO NP exposure. Conversely, the lower nitration levels in Olympos suggest that this ecotype may efficiently mitigate oxidative damage, supporting higher biomass production despite NiO NP exposure.

In summary, the differential protein nitration responses across ecotypes underline the varying stress responses to NiO NP exposure. Olympos appears to manage Ni-induced stress more efficiently, while Ampeliko and Loutra show varying degrees of sensitivity, which may influence their suitability for phytoremediation strategies.

This discussion emphasized the effects of NiO NP exposure on the tolerance and sensitivity of *Odontarrhena lesbiaca* ecotypes, exploring the potential applications of these findings in phytoremediation strategies. Furthermore, important insights were assessed by linking these results to previous studies on the role of oxidative stress and protein regulation in plant adaptation.

8. Summary

This study explores the unique Ni hyperaccumulation mechanisms in *Odontarrhena lesbiaca* ecotypes (Ampeliko, Loutra, and Olympos) when exposed to Ni in NiO NP and $NiCl_2$ forms, highlighting their structural, physiological, and molecular adaptations. All three ecotypes demonstrated hyperaccumulator characteristics, evidenced by high basal Ni content, efficient root-to-shoot Ni translocation, and significant Ni concentrations in shoot tissues. Additionally, the distinction between ionic and nanoparticulate Ni forms revealed crucial insights into how these plants differentially handle metal stress at cellular and tissue levels. Notably, $NiCl_2$ exposure led to greater Ni movement to shoots, whereas NiO NPs largely remained in root cell walls, indicating that nanoparticle form limited translocation, likely due to NP binding to cell wall components.

In-depth analysis using TEM revealed electron-dense areas in root cell walls upon NiO NP treatment, which supports the hypothesis that NPs are largely immobilized within the roots. This limitation on NP internalization corresponds with ICP-MS results, underscoring a minimal translocation of NPs from roots to shoots. Pectin accumulation in root cell walls was particularly pronounced in NiO NP-treated plants, likely facilitating Ni^{2+} binding and retention in roots. These mechanisms vary among ecotypes, with each showing distinct structural and biochemical strategies for Ni handling and sequestration. Such mechanisms reflect adaptive responses that enhance the plants' capacity to cope with and stabilize high levels of heavy metals.

Ecotype-specific responses included variations in root anatomy. Ampeliko roots displayed cortex thickening under high NiO NP levels, which may restrict radial water flow and thereby limit Ni transport—a structural adaptation potentially enhancing metal tolerance. The increase in root area observed in both the Ampeliko and Loutra ecotypes suggests that cell wall thickening may occur in response to NiO NP exposure. The Olympos ecotype, by contrast, maintained growth under NiO NP exposure, while Loutra showed modifications in the stele-to-cortex ratio, indicating distinct vascular adaptations that support Ni handling. These anatomical responses may help each ecotype cope with Ni stress differently, with root tissue modifications acting as a first line of defense against excessive Ni uptake. Such differences highlight the role of ecotype-specific traits in optimizing metal tolerance and accumulation, which may guide the selection of suitable plant varieties for environmental applications.

Further, molecular analysis demonstrated that NiO NP exposure increased NO and $ONOO^-$ levels, which regulate nitrosative signaling processes involved in stress tolerance. These findings suggest that NiO NP exposure leads to organ-specific variations in GSNOR protein levels between roots and shoots. In Loutra, reduced GSNOR levels were associated with increased enzyme activity, suggesting post-translational regulation. In contrast, Olympos roots showed increased protein levels, but with reduced activity, indicating potential post-translational inhibition. The observed decrease in nitration signals suggests the activation of defense mechanisms, potentially involving the proteasomal degradation of nitrated proteins. The overall modest enhancement of physiological protein nitration in response to NiO NPs across all ecotypes aligns with the hyperaccumulator and tolerant characteristics of this species. These molecular findings underline the importance of redox signaling in regulating Ni stress responses and highlight its potential role in supporting phytoremediation efficiency.

The study's findings not only enhance our understanding of the differential responses of *Odontarrhena lesbiaca* ecotypes to nanoparticulate and ionic forms of Ni but also offer insights into potential applications in phytoremediation. The ability of these plants to tolerate and retain Ni, particularly in nanoparticulate form, could be leveraged in soil remediation strategies, where controlled Ni sequestration is desirable. Moreover, the distinct molecular and structural adaptations identified in each ecotype provide a framework for optimizing the use of hyperaccumulators in environmental detoxification and sustainable metal recovery applications. The observed adaptations at cellular, tissue, and molecular levels underscore the utility of *Odontarrhena lesbiaca* as a model for heavy metal tolerance and suggest its broader application in environmental detoxification and metal recovery.

Overall, this research contributes new knowledge on the selective and complex Ni handling mechanisms in hyperaccumulator plants, illustrating the distinct ways in which nanoparticulate and ionic forms of metals interact with plant systems. These insights could guide future studies on plant-based remediation technologies and foster development in sustainable approaches to managing metal-contaminated environments.

9. Összegzés

Ez a tanulmány az *Odontarrhena lesbiaca* ökotípusok (Ampeliko, Loutra és Olympos) egyedi nikkel-hiperaccumulációs mechanizmusait vizsgálja, amikor a növények NiO NPs és $NiCl_2$ formájában nikkelnek vannak kitéve, kiemelve azok szerkezeti, fiziológiai és molekuláris alkalmazkodási mechanizmusait. Mindhárom ökotípus hiperakkumuláló tulajdonságokat mutatott, amit a magas alap Ni tartalom, a hatékony gyökér-és hajtás közötti Ni transzport és a hajtás szövetek jelentős Ni koncentrációi bizonyítanak. Ezen kívül az ionikus és nanorészecske formájú Ni közötti különbség fontos információkat adott arra vonatkozóan, hogy e növények miként kezelik különböző módon a fémstresszt a sejt- és szöveti szinten. A $NiCl_2$ kitettség nagyobb Ni transzlokációt eredményezett a hajtások felé, míg a NiO NPs nagyrészt a gyökérsejtfalakban kötődtek meg, ami arra utal, hogy a nanorészecske formája korlátozta a transzportot, valószínűleg a NP-k sejtfal komponensekhez való kötődése miatt.

A TEM segítségével végzett részletes elemzés elektrondenz területeket mutatott ki a gyökérsejtfalakban NiO NP kezelés után, ami alátámasztja azt a feltételezést, hogy a nanorészecskék nagyrészt immobilizálódtak a gyökereken. A NP-k gyökérbe való bejutásának a korlátozása összhangban van az ICP-MS eredményekkel, amelyek alátámasztják a NP-k gyökérből a hajtásokba történő kismértékű transzportját. A pektin felhalmozódása a gyökérsejtfalakban igen jelentős volt a NiO NP kezelt növényekben, valószínűleg elősegítve a Ni^{2+} megkötését a gyökerekben. Ezek a mechanizmusok ökotípusonként változnak, mindegyik különböző struktúrális és biokémiai stratégiákat alkalmaz a Ni kezelésére és elkülönítására. Ezek a mechanizmusok adaptív válaszokat tükröznek, amelyek javítják a növények túlélését a nehézfémek jelenlétében .

Az ökotípus-specifikus válaszok a gyökér anatómiájában is változást mutattak. Az Ampeliko gyökerei megvastagodtak a nagy NiO NP szintek mellett, ami valószínűleg korlátozta a radiális vízáramlást és így a Ni szállítását; ezegy szerkezeti adaptáció, amely potenciálisan javítja a fém toleranciát. Az Ampeliko és Loutra ökotípusoknál megfigyelt gyökérterület-növekedés azt sugallja, hogy sejtfal vastagodás következett be NiO NP kitettség hatására. Ezzel szemben az Olympos ökotípus fenntartotta növekedését NiO NP kezelés alatt, míg a Loutra a sztéle és kortex arányában mutatott változásokat, amelyek egyedi vaszkuláris adaptációs mechanizmusra utanak. Ezek az anatómiai válaszok segíthetnek abban, hogy az egyes ökotípusok más-más módon birkózzanak meg a Ni stresszel, a gyökérszöveti módosítások pedig első védelmi vonalként működnek a túlzott Ni felvétel ellen. Ezek a különbségek rámutatnak az ökotípus-specifikus jellemzők szerepére a fém tolerancia és felhalmozódás optimalizálásában.

A további molekuláris elemzés azt mutatta, hogy a NiO NP kezelés megemelkedett NO és $ONOO^-$ szintet eredményezett a gyökerekben, amelyek a nitrozatív jelátviteli folyamatokat szabályozzák és szerepet játszanak a stressztűrésben. Eredményeink azt sugallják, hogy a NiO NP kitettség szervspecifikus változásokat eredményezett a GSNOR fehérje szintjében a gyökerekben és hajtásokban.

A Loutra esetében a csökkent GSNOR szintek fokozott enzimaktivitással társultak, ami poszt-transzlációs szabályozásra utal. Ezzel szemben az Olympos gyökerei megnövekedett fehérje szinteket mutattak, de csökkent aktivitással, ami potenciálisan poszt-transzlációs gátlást jelez. A nitrációs jelek csökkenése aktív védelmi mechanizmusok működésére utalhat, amelyek a nitrált fehérjék proteaszómális degradációját foglalják magukban. Az összes ökotípus esetében a NiO NP-kre adott fiziológiás fehérje nitráció kismértékű növekedése összhangban áll a hiperakkumuláló és toleráns jellemzőkkel, amelyeket ez a faj képvisel. Ezek a molekuláris eredmények hangsúlyozzák a redox jelátvitel fontosságát a Ni stressz válaszok szabályozásában, és kiemelik annak potenciális szerepét a fitoremediáció hatékonyságának támogatásában.

A tanulmány eredményei nemcsak az *Odontarrhena lesbiaca* ökotípusok különböző válaszait segítenek jobban megérteni a nanorészecske és ionos Ni hatásaira, hanem betekintést nyújtanak a fitoremediációban való potenciális alkalmazásokba is. E növények képessége, hogy tolerálják és felhalmozzák a Ni-t, különösen nanorészecske formában, felhasználható a talaj rehabilitációs stratégiák során, ahol a kontrollált Ni elkülönítés kívánatos. Ezen kívül az ökotípusokban azonosított különböző molekuláris és struktúrális alkalmazkodási mechanizmusok keretet adnak a hiperakkumulálók optimális használatához környezeti detoxikációs és fenntartható fémkivonási alkalmazásokban. A megfigyeltsejt-, szövet- és molekuláris szintű alkalmazkodási mechanizmusok alátámasztják az *Odontarrhena lesbiaca* hasznosságát a nehézfémek toleranciájának modelljeként, és szélesebb alkalmazását sugallják környezeti detoxikációs és fémkivonási technológiákban.

Összességében a kutatás új ismereteket ad a hiperakkumuláló növények összetett és egyedi Ni tűrési mechanizmusairól, bemutatva a nanopartikulum és ionos formájú fémek kölcsönhatásait a növényi rendszerekkel. Ezek az ismeretek segíthetik a jövőbeli kutatásokat a növényalapú remediációs technológiák terén, és előmozdíthatják a fenntartható megközelítéseket a fémekkel szennyezett környezetek kezelésében.

10. Acknowledgement

The journey of preparing and compiling my Ph.D. dissertation has been one of endurance, learning, and reflection. Along the way, I had the privilege of receiving guidance and support from esteemed individuals whose contributions were invaluable to my research. The completion of this thesis would not have been possible without their unwavering dedication, insightful contributions, and constant encouragement. Their wisdom and support were crucial in shaping this work, and for that, I am deeply grateful. The collaborative efforts and thoughtful insights I received have been fundamental to reaching this fulfilling milestone.

First and foremost, I would like to express my deepest gratitude to my esteemed supervisor, **Dr. Zsuzsanna Ördögné Kolbert**. Her unwavering guidance, support, and expertise have been invaluable throughout my Ph.D. journey. Her advice and constant motivation have shaped not only my research but also my growth as a scholar. I am profoundly grateful for the opportunity to work under her mentorship. Her dedication and passion for science have been a continuous source of inspiration. Being her Ph.D. student has been both an honor and a privilege that I will always cherish. I sincerely thank her from the bottom of my heart.

I would like to extend my heartfelt appreciation to **Prof. Dr. Attila Fehér**, the esteemed Head of the Department, for providing me with the opportunity to conduct my experiments at the Department of Plant Biology.

I would also like to thank **Prof. Dr. László Erdei** for his encouraging words, helpfulness, and for sharing his knowledge.

I would like to extend gratitude to **Dr. Fodor Ferenc** for his kind help in the correction of thesis.

I especially thank to **Prof. Dr. Panayiotis G. Dimitrakopoulos** for providing *Odontarrhena lesbiaca* seeds and his useful advice.

I would also like to thank **Dr. Árpád Molnár** for teaching me many techniques and for his help throughout my academic career. Among the current members, I would like to thank **Dr. Réka Szőllősi Véseiné** for her support and kindness, which have accompanied me throughout this journey.

I am deeply grateful to **Éva Kapásné Török** for her invaluable support and all the other tasks she has undertaken. She has been like a mother to me here, always offering care and guidance. It fills me with joy that we have become not only colleagues but also confidants, friends, and like family to each other. One could not wish for a better laboratory assistant than her.

Similarly, I would like to give special credit to technical assistants **Attiláné Bécs**, **Erika Dóri**, and **Erzsébet Porkoláb** for their unmatchable and tireless help in lab work. And many thanks to **Erika Pál** for her valuable assistance in administrative matters.

I also extend my gratitude to all faculty members and colleagues in the Department of Plant Biology for their valuable assistance and cooperation.

I am also thankful to my colleagues and friends; **Dr. Zalán Czékus**, **Dr. Riyazuddin Riyazuddin**, **Dr. Nadeem Iqbal**, **András Kukri**, **Oluwatosin Peace Adedokun**, **Gábor Herman**, **Dr. Szabolcs Lentner**, **Dr. Onur Kabadayı**, **Serap Şişik Pozsár**, **Res. Asst. Fatmagül Bag**ı, **Tayfun Kondak**, **Fizuli Israfilov** and all other well-wishers for supporting me all the time.

I would like to thank the **Ministry of National Education** (Türkiye) for selecting and providing me with this golden opportunity to seek scientific knowledge abroad.

I especially thank **Tempus Public Foundation** for providing the **Stipendium Hungaricum Scholarship** Programme, Hungary.

I would like to express my heartfelt gratitude to my family in Hungary, to my beloved wife's wonderful mother **Éva Oláhné Gyemengyi** and father **Imre Oláh**, and to all our neighbors in Csorvás for making me feel at home, and for their warmth and unwavering support.

Finally, I am indescribably grateful to my wife, **Dr. Dóra Kondak**, and my **Parents**, whose unwavering support, endless encouragement, and constant faith in me have been my greatest strength throughout this journey. Through every challenge and moment of doubt, they stood by my side, reminding me of what I am capable of. Their love, sacrifices, and guidance have been the foundation upon which I built this work, and for that, I will always be thankful.

11. References

Abdel-Salam, E. M., Qahtan, A. A., Faisal, M., Saquib, Q., Alatar, A. A., & Al-Khedhairy, A. A. (2018). Phytotoxic Assessment of nickel oxide (NiO) nanoparticles in radish. Phytotoxicity of nanoparticles, 269-284. https://doi.org/10.1007/978-3-319-76708-6_11.

Adamidis, G.C. (2013). Serpentine Ecology: ecosystem processes, plant functional traits and investigation of the function of metal hyperaccumulation in *Alyssum lesbiacum*, a serpentine endemic species from Lesbos Island (Greece).

Adamidis, G.C., Aloupi, M., Kazakou, E., Dimitrakopoulos, P.G. (2014). Intra-specific variation in Ni tolerance, accumulation and translocation patterns in the Ni-hyperaccumulator *Alyssum lesbiacum*. Chemosphere 95, 496–502. https://doi.org/10.1016/j.chemosphere.2013.09.106.

Adamidis, G. C., Aloupi, M., Mastoras, P., Papadaki, M. I., & Dimitrakopoulos, P. G. (2017). Is annual or perennial harvesting more efficient in Ni phytoextraction?. Plant and Soil, 418, 205-218. https://doi.org/10.1007/s11104-017-3287-9.

Adamidis, G. C., Kazakou, E., Fyllas, N. M., & Dimitrakopoulos, P. G. (2014). Species adaptive strategies and leaf economic relationships across serpentine and non-serpentine habitats on Lesbos, eastern Mediterranean. PLoS One, 9(5), e96034. https://doi.org/10.1371/journal.pone.0096034.

Ahmad, M. S. A., & Ashraf, M. (2011). Essential roles and hazardous effects of nickel in plants. Reviews of environmental contamination and toxicology, 125-167. https://doi.org/10.1007/978-1-4614-0668-6_6.

Ahmad, W., Bhatt, S. C., Verma, M., Kumar, V., & Kim, H. (2022). A review on current trends in the green synthesis of nickel oxide nanoparticles, characterizations, and their applications. Environ. Nanotechnol. Monit. Manag., 18, 100674, https://doi.org/10.1016/j.enmm.2022.100674.

Ahmed, A. I., Yadav, D. R., & Lee, Y. S. (2016). Applications of nickel nanoparticles for control of Fusarium wilt on lettuce and tomato. Int. J. Innov. Res. Sci. Eng. Technol, 5(5), 7378-7385. https://doi.org/10.15680/IJIRSET.2016.0505132.

Baker, A. J. M., & Walker, P. L. (1989). Ecophysiology of metal uptake by tolerant plants. In A. J. Shaw (Ed.), Heavy metal tolerance in plants: Evolutionary aspects (pp. 155–177). CRC Press. https://doi.org/10.1201/9781003574903.

Bani, A., Echevarria, G., Sulçe, S., Morel, J. L., & Mullai, A. (2007). In-situ phytoextraction of Ni by a native population of *Alyssum murale* on an ultramafic site (Albania). Plant and Soil, 293, 79-89. https://doi.org/10.1007/s11104-007-9245-1.

Bani, A., Pavlova, D., Benizri, E., Shallari, S., Miho, L., Meco, M., ... & Echevarria, G. (2018). Relationship between the Ni hyperaccumulator *Alyssum murale* and the parasitic plant *Orobanche nowackiana* from serpentines in Albania. Ecological Research, 33, 549-559. https://doi.org/10.1007/s11284-018-1593-1.

Bani, A., Pavlova, D., Garrido-Rodríguez, B., Kidd, P. S., Konstantinou, M., Kyrkas, D., ... & Echevarria, G. (2021). Element case studies in the temperate/mediterranean regions of Europe: Nickel. Agromining: Farming for metals: Extracting unconventional resources using plants, 341-363. https://doi.org/10.1007/978-3-030-58904-2_16.

Barbaroux, R., Meunier, N., Mercier, G., Taillard, V., Morel, J. L., Simonnot, M. O., & Blais, J. F. (2009). Chemical leaching of nickel from the seeds of the metal hyperaccumulator plant *Alyssum murale*. Hydrometallurgy, 100(1-2), 10-14. https://doi.org/10.1016/j.hydromet.2009.09.005.

Barroso, J.B., Corpas, F.J., Carreras, A., Rodríguez-Serrano, M., Esteban, F.J., Fernandez- Ocana, A. (2006). Localization of *S*-nitrosoglutathione and expression of *S*-nitrosoglutathione reductase in pea plants under cadmium stress. J. Exp. Bot. 57, 1785–1793. https://doi.org/10.1093/jxb/erj175.

Bartesaghi, S., Ferrer-Sueta, G., Peluffo, G., Valez, V., Zhang, H., Kalyanaraman, B., & Radi, R. (2007). Protein tyrosine nitration in hydrophilic and hydrophobic environments. Amino acids, 32, 501-515. https://doi.org/10.1007/s00726-006-0425-8.

Baskar, V., Nayeem, S., Kuppuraj, S. P., Muthu, T., & Ramalingam, S. (2018). Assessment of the effects of metal oxide nanoparticles on the growth, physiology and metabolic responses in in vitro grown eggplant (*Solanum melongena*). 3 Biotech, 8(8), 362. https://doi.org/10.1007/s13205-018-1386-9.

Begara-Morales, J. C., Sánchez-Calvo, B., Chaki, M., Mata-Pérez, C., Valderrama, R., Padilla, M. N., ... & Barroso, J. B. (2015). Differential molecular response of monodehydroascorbate reductase and glutathione reductase by nitration and *S*-nitrosylation. Journal of experimental botany, 66(19), 5983-5996. https://doi.org/10.1093/jxb/erv306.

Beig, B., Niazi, M. B. K., Jahan, Z., Zia, M., Shah, G. A., & Iqbal, Z. (2023). Biodegradable polymer encapsulated nickel nanoparticles for slow release urea promotes Rhode grass yield and nitrogen recovery. Journal of Polymers and the Environment, 31(5), 1866-1883. https://doi.org/10.1007/s10924-022-02729-2.

Besharat, H., Khavari-Nejad, R. A., Mahmoodzadeh, H., & Abadi, K. N. S. (2021). Effect of Nano and Bulk Nickel Oxide on Biomass and Antioxidant Enzymes Production of Fennel. Agritech, 41(1), 71-84. https://doi.org/10.22146/agritech.55643.

Bettarini, I. (2021). The nickel hyperaccumulating plants of genus *Odontarrhena* (Brassicaceae): novel insights from molecular, physiological and biochemical analyses. https://dx.doi.org/10.25434/bettarini-isabella_phd2021.

Bhat, J.A., Basit, F., Alyemeni, M.N., Mansoor, S., Kaya, C., Ahmad, P. (2023). Gibberellic acid mitigates nickel stress in soybean by cell wall fixation and regulating oxidative stress metabolism and glyoxalase system. Plant Physiology and Biochemistry 198, 107678. https://doi.org/10.1016/j.plaphy.2023.107678.

Bhoye, M., Pansambal, S., Basnet, P., Lin, K.-Y. A., Gutierrez-Mercado, K. Y., Pérez-Larios, A., Chauhan, A., Oza, R., & Ghotekar, S. (2023). Eco-Friendly Synthesis of Ni/NiO Nanoparticles Using *Gymnema sylvestre* Leaves Extract for Antifungal Activity. Journal of Composites Science, 7(3), 105. https://doi.org/10.3390/jcs7030105.

Boyd, R. S. (2007). The defense hypothesis of elemental hyperaccumulation: status, challenges and new directions. Plant and Soil, 293, 153-176. https://doi.org/10.1007/s11104-007-9240-6.

Boyd, R. S., Shaw, J. J., & Martens, S. N. (1994). Nickel hyperaccumulation defends *Streptanthus polygaloides* (Brassicaceae) against pathogens. American Journal of Botany, 81(3), 294-300. https://doi.org/10.1002/j.1537-2197.1994.tb15446.x.

Bradford, M.M. (1976). A rapid and sensitive method for the quantitation of microgram quantities of protein utilizing the principle of protein-dye binding. Anal Biochem. 72, 248-254. https://doi.org/10.1016/0003-2697(76)90527-3.

Broadhurst, C. L., Chaney, R. L., Angle, J. S., Erbe, E. F., & Maugel, T. K. (2004). Nickel localization and response to increasing Ni soil levels in leaves of the Ni hyperaccumulator *Alyssum murale*. Plant and Soil, 265, 225-242. https://doi.org/10.1007/s11104-005-0974-8.

Budka, D., Mesjasz-Przybyłowicz, J., Tylko, G., & Przybyłowicz, W. J. (2005). Freeze-substitution methods for Ni localization and quantitative analysis in *Berkheya coddii* leaves by means of PIXE. Nuclear Instruments and Methods in Physics Research Section B: Beam Interactions with Materials and Atoms, 231(1-4), 338-344. https://doi.org/10.1016/j.nimb.2005.01.080.

Caffall, K. H., & Mohnen, D. (2009). The structure, function, and biosynthesis of plant cell wall pectic polysaccharides. Carbohydrate research, 344(14), 1879-1900. https://doi.org/10.1016/j.carres.2009.05.021.

Carocci, A.; Catalano, A.; Lauria, G.; Sinicropi, M.S.; Genchi, G. (2016). A review on mercury toxicity in foods. In Food Toxicology; CRC Press: Boca Raton, FL, USA; Volume 16, pp. 315–326.

Cecchi, L., Bettarini, I., Colzi, I., Coppi, A., Echevarria, G., Pazzagli, L., ... & Selvi, F. (2018). The genus *Odontarrhena* (Brassicaceae) in Albania: taxonomy and nickel accumulation in a critical group of metallophytes from a major serpentine hot-spot. Phytotaxa, 351(1), 1-28. https://doi.org/10.11646/phytotaxa.351.1.1.

Cecchi, L., Španiel, S., Bianchi, E., Coppi, A., Gonnelli, C., & Selvi, F. (2020). *Odontarrhena stridii* (Brassicaceae), a new Nickel-hyperaccumulating species from mainland Greece. Plant Systematics and Evolution, 306, 1-14. https://doi.org/10.1007/s00606-020-01687-3.

Chae, H.B., Kim, M.G., Kang, C.H., Park, J.H., Lee, E.S., Lee, S.U., ... & Lee, S.Y. (2021). Redox sensor QSOX1 regulates plant immunity by targeting GSNOR to modulate ROS generation. Mol. Plant 14 (8), 1312-1327. https://doi.org/10.1016/j.molp.2021.05.004.

Chahardoli, A., Karimi, N., Ma, X., & Qalekhani, F. (2020). Effects of engineered aluminum and nickel oxide nanoparticles on the growth and antioxidant defense systems of *Nigella arvensis* L. Scientific Reports, 10(1), 3847. https://doi.org/10.1038/s41598-020-60841-6.

Chen, D. H., & Wu, S. H. (2000). Synthesis of nickel nanoparticles in water-in-oil microemulsions. Chemistry of Materials, 12(5), 1354-1360. https://doi.org/10.1021/cm991167y.

Cheng, H., Jiang, Z.Y., Liu, Y., Ye, Z.H., Wu, M.L., Sun, C.C., ... & Wang, Y.S. (2014). Metal (Pb, Zn and Cu) uptake and tolerance by mangroves in relation to root anatomy and lignification/suberization. Tree Physiol. 34 (6), 646-656. https://doi.org/10.1093/treephys/tpu042.

Cheng, H., Liu, Y., Tam, N.F.Y., Wang, X., Li, S.Y., Chen, G.Z., & Ye, Z.H. (2010). The role of radial oxygen loss and root anatomy on zinc uptake and tolerance in mangrove seedlings. Environ. Pollut. 158 (5), 1189-1196. https://doi.org/10.1016/j.envpol.2010.01.025.

Cheng, H., Tam, N.F.Y., Wang, Y., Li, S., Chen, G., & Ye, Z. (2012). Effects of copper on growth, radial oxygen loss and root permeability of seedlings of the mangroves *Bruguiera gymnorrhiza* and *Rhizophora stylosa*. Plant and Soil 359, 255-266. https://doi.org/10.1007/s11104-012-1171-1.

Chouhan, D., Dutta, A., Kumar, A., Mandal, P., & Choudhuri, C. (2022). Application of nickel chitosan nanoconjugate as an antifungal agent for combating *Fusarium* rot of wheat. Scientific Reports, 12(1), 14518. https://doi.org/10.1038/s41598-022-18670-2.

Chung, I. M., Venkidasamy, B., & Thiruvengadam, M. (2019). Nickel oxide nanoparticles cause substantial physiological, phytochemical, and molecular-level changes in Chinese cabbage seedlings. Plant Physiology and Biochemistry, 139, 92-101. https://doi.org/10.1016/j.plaphy.2019.03.010.

Corpas, F.J., González-Gordo, S., & Palma, J.M. (2021). Protein nitration: a connecting bridge between nitric oxide (NO) and plant stress. Plant Stress 2, 100026. https://doi.org/10.1016/j.stress.2021.100026.

Corpas, F. J., González-Gordo, S., Rodríguez-Ruiz, M., Munoz-Vargas, M. A., & Palma Martínez, J. M. (2022). Nitric oxide and hydrogen sulfide share regulatory functions in higher plant events. https://doi.org/10.32604/biocell.2021.017300.

Danjumma, S. G., Abubakar, Y., & Suleiman, S. (2019). Nickel oxide (NiO) devices and applications: a review. J. Eng. Res. Technol, 8, 12-21. http://doi.org/10.17577/IJERTV8IS040281.

de Oliveira, J. B., Marques, J. P. R., Rodak, B. W., Galindo, F. S., Carr, N. F., Almeida, E., ... & Lavres, J. (2022). Fate of nickel in soybean seeds dressed with different forms of nickel. Rhizosphere, 21, 100464. https://doi.org/10.1016/j.rhisph.2020.100275.

De Souza-Torres, A., Govea-Alcaide, E., Gomez-Padilla, E., Masunaga, S. H., Effenberger, F. B., Rossi, L. M., ... & Jardim, R. F. (2021). Fe_3O_4 nanoparticles and *Rhizobium* inoculation enhance nodulation, nitrogen fixation and growth of common bean plants grown in soil. Rhizosphere, 17, 100275. https://doi.org/10.1016/j.rhisph.2020.100275.

Delhaye, G., Dimitrakopoulos, P. G., & Adamidis, G. C. (2024). Interspecific trait differences drive plant community responses on serpentine soils. Journal of Ecology, 112(12), 2887-2900. https://doi.org/10.1111/1365-2745.14429.

Deng, T. H. B., van Der Ent, A., Tang, Y. T., Sterckeman, T., Echevarria, G., Morel, J. L., & Qiu, R. L. (2018). Nickel hyperaccumulation mechanisms: a review on the current state of knowledge. Plant and Soil, 423, 1-11. https://doi.org/10.1007/s11104-017-3539-8.

Denkhaus, E., & Salnikow, K. (2002). Nickel essentiality, toxicity, and carcinogenicity. Critical reviews in oncology/hematology, 42(1), 35-56. https://doi.org/10.1016/S1040-8428(01)00214-1.

Dietz, K. J., & Herth, S. (2011). Plant nanotoxicology. Trends in plant science, 16(11), 582-589. https://doi.org/10.1016/j.tplants.2011.08.003.

Dimitrakopoulos, P. G., Aloupi, M., Tetradis, G., & Adamidis, G. C. (2021). Broomrape species parasitizing *Odontarrhena lesbiaca* (Brassicaceae) individuals act as nickel hyperaccumulators. Plants, 10(4), 816. https://doi.org/10.3390/plants10040816.

dos Reis, A.R., de Queiroz Barcelos, J.P., de Souza Osório, C.R.W., Santos, E.F., Lisboa, L.A.M., Santini, J.M.K., ... & Gratao, P.L. (2017). A glimpse into the physiological, biochemical and nutritional status of soybean plants under Ni-stress conditions. Environ. Exp. Bot. 144, 76-87. https://doi.org/10.1016/j.envexpbot.2017.10.006.

Dronnet, V.M., Renard, C.M.G.C., Axelos, M.A.V., Thibault, J.F. (1996). Heavy metals binding by pectins: selectivity, quantification and characterization. Biotechnol. Prog. 14, 535-540. https://doi.org/10.1016/S0921-0423(96)80283-8.

Durand, C., Vicré-Gibouin, M., Follet-Gueye, M.L., Duponchel, L., Moreau, M., Lerouge. P., & Driouich, A. (2009). The organization pattern of root border-like cells of Arabidopsis is dependent on cell wall homogalacturonan. Plant Physiol. 150 (3), 1411-1421. https://doi.org/10.1104/pp.109.136382.

Fabiano, C. C., Tezotto, T., Favarin, J. L., Polacco, J. C., & Mazzafera, P. (2015). Essentiality of nickel in plants: a role in plant stresses. Front. Plant Sci., 6, 754, https://doi.org/10.3389/fpls.2015.00754.

Fageria, N. K., Baligar, V. C., & Clark, R. B. (2002). Micronutrients in crop production. Advances in agronomy, 77, 185-268. https://doi.org/10.1016/S0065-2113(02)77015-6.

Faisal, M., Saquib, Q., Alatar, A. A., Al-Khedhairy, A. A., Hegazy, A. K., & Musarrat, J. (2013). Phytotoxic hazards of NiO-nanoparticles in tomato: a study on mechanism of cell death. Journal of hazardous materials, 250, 318-332. https://doi.org/10.1016/j.jhazmat.2013.01.063.

Feigl, G., Varga, V., Molnár, Á., Dimitrakopoulos, P.G., & Kolbert, Z. (2020). Different nitro-oxidative response of *Odontarrhena lesbiaca* plants from geographically separated habitats to excess nickel. Antioxidants 9 (9), 837. https://doi.org/10.3390/antiox9090837.

Fitter, A. H., & Hay, R. K. M. (1981). Environmental physiology of plants. Academic Press.

Frungillo, L., Skelly, M. J., Loake, G. J., Spoel, S. H., & Salgado, I. (2014). *S*-nitrosothiols regulate nitric oxide production and storage in plants through the nitrogen assimilation pathway. Nature Communications, 5(1), 5401. https://doi.org/10.1038/ncomms6401.

Gajewska, E., Skłodowska, M., Słaba, M., & Mazur, J. (2006). Effect of nickel on antioxidative enzyme activities, proline and chlorophyll contents in wheat shoots. Biol. Plant. 50, 653-659. https://doi.org/10.1007/s10535-006-0102-5.

Galetskiy, D., Lohscheider, J., Kononikhin, A., Popov, I., Nikolaev, E., Adamska, I. (2011). Phosphorylation and nitration levels of photosynthetic proteins are conversely regulated by light stress. Plant Mol. Biol. 77, 461–473. https://doi.org/10.1007/s11103-011-9824-7.

Gebretinsae, H. G., Tsegay, M. G., & Nuru, Z. Y. (2021). Biosynthesis of nickel oxide (NiO) nanoparticles from cactus plant extract. Materials Today: Proceedings, 36, 566-570. https://doi.org/10.1016/j.matpr.2020.05.331.

Genchi, G., Carocci, A., Lauria, G., Sinicropi, M. S., & Catalano, A. (2020). Nickel: Human health and environmental toxicology. Int. J. Environ. Res. Public Health, 17(3), 679, https://doi.org/10.3390/ijerph17030679.

Gnach, A., Lipinski, T., Bednarkiewicz, A., Rybka, J., & Capobianco, J. A. (2015). Upconverting nanoparticles: assessing the toxicity. Chem. Soc. Rev., 44(6), 1561-1584, http://dx.doi.org/10.1039/c4cs00177j.

Gramlich, A., Moradi, A. B., Robinson, B. H., Kaestner, A., & Schulin, R. (2011). Dimethylglyoxime (DMG) staining for semi-quantitative mapping of Ni in plant tissue. Environmental and Experimental Botany, 71(2), 232-240. https://doi.org/10.1016/j.envexpbot.2010.12.008.

Graska, J., Fidler, J., Gietler, M., Prabucka, B., Nykiel, M., & Labudda, M. (2023). Nitric oxide in plant functioning: metabolism, signaling, and responses to infestation with Ecdysozoa parasites. Biology, 12(7), 927. https://doi.org/10.3390/biology12070927.

Guerinot, M. L. (2000). The ZIP family of metal transporters. Biochimica et Biophysica Acta (BBA)-Biomembranes, 1465(1-2), 190-198. https://doi.org/10.1016/S0005-2736(00)00138-3.

Guerra, D., Ballard, K., Truebridge, I., & Vierling, E. (2016). S-nitrosation of conserved cysteines modulates activity and stability of *S*-nitrosoglutathione reductase (GSNOR). Biochemistry, 55(17), 2452-2464. https://doi.org/10.1021/acs.biochem.5b01373.

Halliwell, B., & Gutteridge, J. (1984). Oxygen toxicity, oxygen radicals, transition metals and disease. Biochemical journal, 219(1), 1. https://doi.org/10.1042/bj2190001.

Hamdan, A.M., Sardi, A., Reksamunanda,r R.P., Maulida, Z., Arsa, D.A., Lubis, S.S., Nisah, K. (2024) Green synthesis of NiO nanoparticles using a Cd hyperaccumulator (*Lactuca sativa* L.) and its application as a Pb(II) and Cu(II) adsorbent. Environ. Nanotechnol. Monitor. Manag., 21: 100910, https://doi.org/10.1016/j.enmm.2023.100910.

Hanikenne, M., Talke, I. N., Haydon, M. J., Lanz, C., Nolte, A., Motte, P., ... & Krämer, U. (2008). Evolution of metal hyperaccumulation required cis-regulatory changes and triplication of *HMA4*. Nature, 453(7193), 391-395. https://doi.org/10.1038/nature06877.

Hipfinger, C., Laux, M., & Puschenreiter, M. (2022). Comparison of four nickel hyperaccumulator species in the temperate climate zone of Central Europe. Journal of Geochemical Exploration, 234, 106933. https://doi.org/10.1016/j.gexplo.2021.106933.

Hossain, Z., Mustafa, G., & Komatsu, S. (2015). Plant responses to nanoparticle stress. International journal of molecular sciences, 16(11), 26644-26653. https://doi.org/10.3390/ijms161125980.

Hseu, Z.Y., and Chen, Z.S. (2019). Nickel in Serpentine Soils. Nickel in Soils and Plants. CRC Press Chapter 8, eBook ISBN 9781315154664. https://doi.org/10.1201/9781315154664.

Ingle, R. A., Mugford, S. T., Rees, J. D., Campbell, M. M., & Smith, J. A. C. (2005). Constitutively high expression of the histidine biosynthetic pathway contributes to nickel tolerance in hyperaccumulator plants. The Plant Cell, 17(7), 2089-2106. https://doi.org/10.1105/tpc.104.030577.

Jahnová, J., Luhová, L., & Petřivalský, M. (2019). S-nitrosoglutathione reductase—the master regulator of protein S-nitrosation in plant NO signaling. Plants 8 (2), 48. https://doi.org/10.3390/plants8020048.

Järup, L. (2003). Hazards of heavy metal contamination. British medical bulletin, 68(1), 167-182. https://doi.org/10.1093/bmb/ldg032.

Jean, L., Bordas, F., Gautier-Moussard, C., Vernay, P., Hitmi, A., & Bollinger, J. C. (2008). Effect of citric acid and EDTA on chromium and nickel uptake and translocation by Datura innoxia. Environmental Pollution, 153(3), 555-563. https://doi.org/10.1016/j.envpol.2007.09.013.

Jeandroz, S., Wipf, D., Stuehr, D.J., Lamattina, L., Melkonian, M., Tian, Z., ... & Wendehenne, D. (2016). Occurrence, structure, and evolution of nitric oxide synthase–like proteins in the plant kingdom. Sci. Signal. 9 (417), re2-re2. https://doi.org/10.1126/scisignal.aad4403.

Kabata-Pendias, A., and Pendias, H. (1992). Trace Elements in Soil and Plants (2nd ed.). Boca Raton, FL: CRC Press.

Karatassiou, M., Giannakoula, A., Tsitos, D., & Stefanou, S. (2021). Response of three Greek populations of *Aegilops Triuncialis* (Crop Wild Relative) to serpentine soil. Plants, 10(3), 516. https://doi.org/10.3390/plants10030516.

Kazakou, E., Adamidis, G.C., Baker, A.J.M., Reeves, R.D., Godino, M., Dimitrakopoulos, P.G. (2010). Species adaptation in serpentine soils in Lesbos Island (Greece): metal hyperaccumulation and tolerance. Plant and Soil 332, 369–385. https://doi.org/10.1007/s11104-010-0302-9.

Kazakou, E., Dimitrakopoulos, P. G., Baker, A. J. M., Reeves, R. D., & Troumbis, A. Y. (2008). Hypotheses, mechanisms and trade-offs of tolerance and adaptation to serpentine soils: from species to ecosystem level. Biological Reviews, 83(4), 495-508. https://doi.org/10.1111/j.1469-185X.2008.00051.x.

Khair, K. U., Farid, M., Ashraf, U., Zubair, M., Rizwan, M., Farid, S., ... & Ali, S. (2020). Citric acid enhanced phytoextraction of nickel (Ni) and alleviate *Mentha piperita* (L.) from Ni-induced physiological and biochemical damages. Environmental Science and Pollution Research, 27, 27010-27022. https://doi.org/10.1007/s11356-020-08978-9.

Khaliq, A., Ali, S., Hameed, A., Farooq, M.A., Farid, M., Shakoor, M.B., ... & Rizwan, M. (2015). Silicon alleviates nickel toxicity in cotton seedlings through enhancing growth, photosynthesis, and suppressing Ni uptake and oxidative stress. Arch. Agron. Soil Sci. 62 (5), 633-647. https://doi.org/10.1080/03650340.2015.1073263.

Khan, M., Ali, S., Al Azzawi, T. N. I., & Yun, B. W. (2023). Nitric oxide acts as a key signaling molecule in plant development under stressful conditions. International journal of molecular sciences, 24(5), 4782. https://doi.org/10.3390/ijms24054782.

Khan, S. A., Shahid, S., Ayaz, A., Alkahtani, J., Elshikh, M. S., & Riaz, T. (2021). Phytomolecules-coated NiO nanoparticles synthesis using abutilon indicum leaf extract: antioxidant, antibacterial, and anticancer activities. International Journal of Nanomedicine, 1757-1773. https://doi.org/10.2147/IJN.S294012.

Khator, K., Parihar, S., Jasik, J., & Shekhawat, G. S. (2024). Nitric oxide in plants: An insight on redox activity and responses toward abiotic stress signaling. Plant Signaling & Behavior, 19(1), 2298053. https://doi.org/10.1080/15592324.2023.2298053.

Kolbert, Z., Andrea, P., Nóra, L., Feigl, G., Ördög, A., Erdei, L. (2012). *In vivo* and *in vitro* studies on fluorophore-specificity. Acta Biologica Szegediensis 56 (1), 37-41

Kolbert, Z., Barroso, J. B., Boscari, A., Corpas, F. J., Gupta, K. J., Hancock, J. T., ... & Loake, G. J. (2024). Interorgan, intraorgan and interplant communication mediated by nitric oxide and related species. New Phytologist, 244(3), 786-797. https://doi.org/10.1111/nph.20085.

Kolbert, Z., Feigl, G., Bordé, Á., Molnár, Á., & Erdei L. (2017). Protein tyrosine nitration in plants: Present knowledge, computational prediction and future perspectives. Plant Physiol. Biochem. 113, 56-63. https://doi.org/10.1016/j.plaphy.2017.01.028.

Kolbert, Z., Molnár, Á., Szőllősi, R., Feigl, G., Erdei, L., & Ördög, A. (2018). Nitro-oxidative stress correlates with Se tolerance of *Astragalus* species. Plant Cell Physiol. 59 (9), 1827-1843. https://doi.org/10.1093/pcp/pcy099.

Kolbert, Z., Oláh, D., Molnár, Á., Szőllősi, R., Erdei, L., & Ördög, A. (2020). Distinct redox signalling and nickel tolerance in *Brassica juncea* and *Arabidopsis thaliana*. Ecotoxicology and Environmental Safety, 189, 109989. https://doi.org/10.1016/j.ecoenv.2019.109989.

Kolbert, Z., Szőllősi, R., Rónavári, A., & Molnár, Á. (2022). Nanoforms of essential metals: from hormetic phytoeffects to agricultural potential. Journal of experimental botany, 73(6), 1825-1840. https://doi.org/10.1093/jxb/erab547.

Körner, L. E., Møller, I. M., & Jensén, P. (1986). Free space uptake and influx of Ni^{2+} in excised barley roots. Physiologia Plantarum, 68(4), 583-588. https://doi.org/10.1111/j.1399-3054.1986.tb03400.x.

Krämer, U., Cotter-Howells, J. D., Charnock, J. M., Baker, A. J., & Smith, J. A. C. (1996). Free histidine as a metal chelator in plants that accumulate nickel. Nature, 379(6566), 635-638. https://doi.org/10.1038/379635a0.

Krämer, U., Pickering, I. J., Prince, R. C., Raskin, I., & Salt, D. E. (2000). Subcellular localization and speciation of nickel in hyperaccumulator and non-accumulator *Thlaspi* species. Plant physiology, 122(4), 1343-1354. https://doi.org/10.1104/pp.122.4.1343.

Kruckeberg, A. R. (2002). The Influences of Lithology on Plant Life. In Geology and Plant Life: The Effects of Landforms and Rock Type on Plants; University of Washington Press: Seattle, WA, USA, pp. 160–181.

Krzesłowska, M. (2011). The cell wall in plant cell response to trace metals: polysaccharide remodeling and its role in defense strategy. Acta Physiol. Plant. 33, 35–51. https://doi.org/10.1007/s11738-010-0581-z.

Kumar, S., Wang, M., Liu, Y., Fahad, S., Qayyum, A., Jadoon, S.A., ... & Zhu, G. (2022). Nickel toxicity alters growth patterns and induces oxidative stress response in sweetpotato. Front. Plant Sci. 13. https://doi.org/10.3389/fpls.2022.1054924.

Kurczyńska, E., Godel-Jędrychowska, K., Sala, K., & Milewska-Hendel, A. (2021). Nanoparticles—plant interaction: what we know, where we are?. Appl. Sci. 11 (12), 5473. https://doi.org/10.3390/app11125473.

Lavinia, B., Florina, R., & Augustin, C. (2018). Is it possible a nickel-free diet?. Acta Medica Marisiensis, 64, 5.

León, J. (2022). Protein tyrosine nitration in plant nitric oxide signaling. Frontiers in plant science, 13, 859374. https://doi.org/10.3389/fpls.2022.859374.

Lešková, A., Zvarík, M., Araya, T., & Giehl, R. F. (2020). Nickel toxicity targets cell wall-related processes and PIN2-mediated auxin transport to inhibit root elongation and gravitropic responses in Arabidopsis. Plant and Cell Physiology, 61(3), 519-535. https://doi.org/10.1093/pcp/pcz217.

Li, B., Sun, C., Lin, X., & Busch, W. (2021). The emerging role of GSNOR in oxidative stress regulation. Trends in Plant Sci. 26 (2), 156-168. https://doi.org/10.1016/j.tplants.2020.09.004.

Liao, W., Igamberdiev, A. U., & Palma, J. M. (2023). Advances in nitric oxide signalling and metabolism in plants. International Journal of Molecular Sciences, 24(7), 6397. https://doi.org/10.3390/ijms24076397.

Lindermayr, C. (2018). Crosstalk between reactive oxygen species and nitric oxide in plants: key role of *S*-nitrosoglutathione reductase. Free Radical Biology and Medicine, 122, 110-115. https://doi.org/10.1016/j.freeradbiomed.2017.11.027.

Liu, J., Zhang, W., Long, S., & Zhao, C. (2021). Maintenance of cell wall integrity under high salinity. International Journal of Molecular Sciences, 22(6), 3260. https://doi.org/10.3390/ijms22063260.

Liu, L., Hausladen, A., Zeng, M., Que, L., Heitman, J., & Stamler, J. S. (2001). A metabolic enzyme for *S*-nitrosothiol conserved from bacteria to humans. Nature, 410(6827), 490-494. https://doi.org/10.1038/35068596.

Liu, X., Gong, D., Ke, Q., Yin, L., Wang, S., & Gao, T. (2023). Meta-analysis of the effect of nitric oxide application on heavy metal stress tolerance in plants. Plants, 12(7), 1494. https://doi.org/10.3390/plants12071494.

Loix, C., Huybrechts, M., Vangronsveld, J., Gielen, M., Keunen, E., Cuypers, A. (2017). Reciprocal interactions between cadmium-induced cell wall responses and oxidative stress in plants. Front. Plant Sci. 8, 1867. https://doi.org/10.3389/fpls.2017.01867.

Lopez, S., Goux, X., Echevarria, G., Calusinska, M., Morel, J. L., & Benizri, E. (2019). Community diversity and potential functions of rhizosphere-associated bacteria of nickel hyperaccumulators found in Albania. Science of the Total Environment, 654, 237-249. https://doi.org/10.1016/j.scitotenv.2018.11.056.

Lozano-Juste, J., Colom-Moreno, R., & Leon, J. (2011). *In vivo* protein tyrosine nitration in *Arabidopsis thaliana*. Journal of Experimental Botany, 62(10), 3501-3517. https://doi.org/10.1093/jxb/err042.

Maestri, E., Marmiroli, M., Visioli, G., & Marmiroli, N. (2010). Metal tolerance and hyperaccumulation: costs and trade-offs between traits and environment. Environmental and Experimental Botany, 68(1), 1-13. https://doi.org/10.1016/j.envexpbot.2009.10.011.

Mageswari, A., Srinivasan, R., Subramanian, P., Ramesh, N., & Gothandam, K. M. (2016). Nanomaterials: classification, biological synthesis and characterization. Nanoscience in Food and Agriculture 3, 31-71. https://doi.org/10.1007/978-3-319-48009-1_2.

Malatesta, M. (2021). Transmission electron microscopy as a powerful tool to investigate the interaction of nanoparticles with subcellular structures. International journal of molecular sciences, 22(23), 12789. https://doi.org/10.3390/ijms222312789.

Manna, I., & Bandyopadhyay, M. (2017a). Engineered nickel oxide nanoparticle causes substantial physicochemical perturbation in plants. Frontiers in chemistry, 5, 92. https://doi.org/10.3389/fchem.2017.00092.

Manna, I., & Bandyopadhyay, M. (2017b). Engineered nickel oxide nanoparticles affect genome stability in *Allium cepa* (L.). Plant physiology and biochemistry, 121, 206-215. https://doi.org/10.1016/j.plaphy.2017.11.003.

Manna, I., & Bandyopadhyay, M. (2023). The impact of engineered nickel oxide nanoparticles on ascorbate glutathione cycle in *Allium cepa* L. Physiology and Molecular Biology of Plants, 29(5), 663-678. https://doi.org/10.1007/s12298-023-01314-8.

Manna, I., Sahoo, S., & Bandyopadhyay, M. (2023). Dynamic changes in global methylation and plant cell death mechanism in response to NiO nanoparticles. Planta, 257(5), 93. https://doi.org/10.1007/s00425-023-04127-x.

Manna, I., Sahoo, S., & Bandyopadhyay, M. (2021). Effect of Engineered Nickel Oxide Nanoparticle on Reactive Oxygen Species–Nitric Oxide Interplay in the Roots of *Allium cepa* L. Front. Plant Sci., 12, 586509, https://doi.org/10.3389/fpls.2021.586509.

Marques, A. P., Moreira, H., Rangel, A. O., & Castro, P. M. (2009). Arsenic, lead and nickel accumulation in *Rubus ulmifolius* growing in contaminated soil in Portugal. Journal of Hazardous Materials, 165(1-3), 174-179. https://doi.org/10.1016/j.jhazmat.2008.09.102.

Mekuye, B., & Abera, B. (2023). Nanomaterials: An overview of synthesis, classification, characterization, and applications. Nano Select, https://doi.org/10.1002/nano.202300038.

Mesjasz-Przybyłowicz, J., Balkwill, K., Przybyłowicz, W. J., & Annegarn, H. J. (1994). Proton microprobe and X-ray fluorescence investigations of nickel distribution in serpentine flora from South Africa. Nuclear Instruments and Methods in Physics Research Section B: Beam Interactions with Materials and Atoms, 89(1-4), 208-212. https://doi.org/10.1016/0168-583X(94)95174-8.

Meychik, N., Nikolaeva, Y., Kushunina, M., & Yermakov, I. (2014). Are the carboxyl groups of pectin polymers the only metal-binding sites in plant cell walls?. Plant and Soil, 381, 25-34. https://doi.org/10.1007/s11104-014-2111-z.

Mitra, P.P., & Loqué, D. (2014). Histochemical staining of *Arabidopsis thaliana* secondary cell wall elements. JoVE (J. Vis. Exp.) 87, e51381. https://dx.doi.org/10.3791/51381.

Mizuno, T., Usui, K., Horie, K., Nosaka, S., Mizuno, N., & Obata, H. (2005). Cloning of three ZIP/Nramp transporter genes from a Ni hyperaccumulator plant *Thlaspi japonicum* and their Ni^{2+}-transport abilities. Plant physiology and biochemistry, 43(8), 793-801. https://doi.org/10.1016/j.plaphy.2005.07.006.

Molas, J. (1998). Changes in morphological and anatomical structure of cabbage (*Brassica oleracea* L.) outer leaves and in ultrastructure of their chloroplasts caused by an in vitro excess of nickel. Photosynthetica, 34, 513-522. https://doi.org/10.1023/A:1006805327340.

Molnár, Á., Rónavári, A., Bélteky, P., Szőllősi, R., Valyon, E., Oláh, D., ... & Kolbert, Z. (2020). ZnO nanoparticles induce cell wall remodeling and modify ROS/RNS signalling in roots of *Brassica* seedlings. Ecotoxicol. Environ. Saf. 206, 111158. https://doi.org/10.1016/j.ecoenv.2020.111158.

Mustafa, G., & Komatsu, S. (2016). Toxicity of heavy metals and metal-containing nanoparticles on plants. Biochimica et Biophysica Acta (BBA)-Proteins and Proteomics, 1864(8), 932-944. https://doi.org/10.1016/j.bbapap.2016.02.020.

Mustafa, A., Zulfiqar, U., Mumtaz, M. Z., Radziemska, M., Haider, F. U., Holatko, J., ... & Brtnicky, M. (2023). Nickel (Ni) phytotoxicity and detoxification mechanisms: A review. Chemosphere, 138574, https://doi.org/10.1016/j.chemosphere.2023.138574.

Nabais, C., Freitas, H., Hagemeyer, J., & Breckle, S. W. (1996). Radial distribution of Ni in stemwood of *Quercus ilex* L. trees grown on serpentine and sandy loam (umbric leptosol) soils of NE-Portugal. Plant and soil, 183, 181-185. https://doi.org/10.1007/BF00011433.

Nasrollahzadeh, M., & Sajadi, S. M. (2015). Preparation of Au nanoparticles by *Anthemis xylopoda* flowers aqueous extract and their application for alkyne/aldehyde/amine A^3-type coupling reactions. Rsc Advances, 5(57), 46240-46246. https://doi.org/10.1039/C5RA08927A.

Oláh, D., Feigl, G., Molnár, Á., Ördög, A., & Kolbert, Z. (2020). Strigolactones interact with nitric oxide in regulating root system architecture of *Arabidopsis thaliana*. Front. Plant Sci. 11, 1019. https://doi.org/10.3389/fpls.2020.01019.

Oliveira, H.C., Seabra, A.B., Kondak, S., Adedokun, O.P., & Kolbert, Z. (2023). Multilevel approach to plant–nanomaterial relationships: from cells to living ecosystems. J. Exp. Bot. 74 (12), 3406–3424. https://doi.org/10.1093/jxb/erad107.

Oukarroum, A., Barhoumi, L., Samadani, M., & Dewez, D. (2015). Toxic effects of nickel oxide bulk and nanoparticles on the aquatic plant *Lemna gibba* L. BioMed research international, 2015(1), 501326. https://doi.org/10.1155/2015/501326.

Page, V., Weisskopf, L., & Feller, U. (2006). Heavy metals in white lupin: uptake, root-to-shoot transfer and redistribution within the plant. New Phytologist 171 (2), 329-341. https://doi.org/10.1111/j.1469-8137.2006.01756.x.

Pakzad, K., Alinezhad, H., & Nasrollahzadeh, M. (2019). Green synthesis of Ni@Fe_3O_4 and CuO nanoparticles using *Euphorbia maculata* extract as photocatalysts for the degradation of organic pollutants under UV-irradiation. Ceram. Int., 45(14), 17173-17182, https://doi.org/10.1016/j.ceramint.2019.05.272.

Pandey, A.K., Zorić, L., Sun, T., Karanović, D., Fang, P., Borišev, M., ... & Xu, P. (2022). The Anatomical Basis of Heavy Metal Responses in Legumes and Their Impact on Plant–Rhizosphere Interactions. Plants 11 (19), 2554. https://doi.org/10.3390/plants11192554.

Parsons, J. G., Lopez, M. L., Gonzalez, C. M., Peralta-Videa, J. R., & Gardea-Torresdey, J. L. (2010). Toxicity and biotransformation of uncoated and coated nickel hydroxide nanoparticles on mesquite plants. Environmental Toxicology and Chemistry, 29(5), 1146-1154. https://doi.org/10.1002/etc.146.

Parthasarathy, R., Jayabaskaran, C., Manikandan, A., & Anusuya, S. (2023). Synthesis of nickel-chitosan nanoparticles for controlling blast diseases in Asian rice. Applied Biochemistry and Biotechnology, 195(3), 2134-2148. https://doi.org/10.1007/s12010-022-04198-8.

Pérez-de-Luque, A. (2017). Interaction of nanomaterials with plants: what do we need for real applications in agriculture?. Frontiers in Environmental Science, 5, 12. https://doi.org/10.3389/fenvs.2017.00012.

Pinto, M., Soares, C., Pinto, A. S., & Fidalgo, F. (2019). Phytotoxic effects of bulk and nano-sized Ni on *Lycium barbarum* L. grown *in vitro*–Oxidative damage and antioxidant response. Chemosphere, 218, 507-516. https://doi.org/10.1016/j.chemosphere.2018.11.127.

Rabier, J., Laffont-Schwob, I., Bouraïma-Madjèbi, S., Léon, V., Prudent, P., Viano, J., ... & Pilon-Smits, E. A. (2007). Characterization of metal tolerance and accumulation in *Grevillea exul* var *exul*. International Journal of Phytoremediation, 9(5), 419-435. https://doi.org/10.1080/15226510701606315.

Rabier, J., Laffont-Schwob, I., Notonier, R., Fogliani, B., & Bouraïma-Madjèbi, S. (2008). Anatomical element localization by EDXS in *Grevillea exul* var. *exul* under nickel stress. Environmental Pollution, 156(3), 1156-1163. https://doi.org/10.1016/j.envpol.2008.04.001.

Rahoui, S., Martinez, Y., Sakouhi, L., Ben, C., Rickauer, M., Rickauer, M., Ferjani, E.E., Gentzbittel, L., Chaoui, A. (2017). Cadmium-induced changes in antioxidative systems and differentiation in roots of contrasted *Medicago truncatula* lines. Protoplasma 254, 473–489. https://doi.org/10.1007/s00709-016-0968-9.

Rascio, N., Navari-Izzo, F., 2011. Heavy metal hyperaccumulating plants: How and why do they do it? And what makes them so interesting?. Plant Sci 180 (2), 169–181. https://doi.org/10.1016/j.plantsci.2010.08.016.

Redjala, T., Sterckeman, T., Skiker, S., & Echevarria, G. (2010). Contribution of apoplast and symplast to short term nickel uptake by maize and *Leptoplax emarginata* roots. Environmental and Experimental Botany, 68(1), 99-106. https://doi.org/10.1016/j.envexpbot.2009.10.010.

Reeves, R.D., 1992. The hyperaccumulation of nickel by serpentine plants. In: Baker AJM, Proctor J, Reeves RD (eds) The vegetation of ultramafic (serpentine) soils. (Intercept Ltd: Andover, UK), pp 253–277.

Reeves, R.D., Baker, A.J., Jaffré, T., Erskine, P.D., Echevarria, G., & van Der Ent, A. (2017). A global database for plants that hyperaccumulate metal and metalloid trace elements. New Phytologist 218 (2), 407-411. https://doi.org/10.1111/nph.14907.

Reeves, R.D., van der Ent, A., Echevarria, G., Isnard, S., Baker, A.J.M. (2021). Global distribution and ecology of hyperaccumulator plants. In van der Ent, A., Baker, A.J.M., Echevarria, G., Simonnot, M.O., Morel, J.L., (Eds) Agromining: Farming for Metals; Mineral Resource Reviews; Springer: Cham, Switzerland, pp. 133–154. https://doi.org/10.1007/978-3-030-58904-2_7.

Robinson, B. H., Brooks, R. R., Howes, A. W., Kirkman, J. H., & Gregg, P. E. H. (1997a). The potential of the high-biomass nickel hyperaccumulator *Berkheya coddii* for phytoremediation and phytomining. Journal of Geochemical Exploration, 60(2), 115-126. https://doi.org/10.1016/S0375-6742(97)00036-8.

Robinson, B. H., Chiarucci, A., Brooks, R. R., Petit, D., Kirkman, J. H., Gregg, P. E. H., & De Dominicis, V. (1997b). The nickel hyperaccumulator plant *Alyssum bertolonii* as a potential agent for phytoremediation and phytomining of nickel. Journal of Geochemical Exploration, 59(2), 75-86. https://doi.org/10.1016/S0375-6742(97)00010-1.

Rosatto, S., Roccotiello, E., Di Piazza, S., Cecchi, G., Greco, G., Zotti, M., ... & Mariotti, M. (2019). Rhizosphere response to nickel in a facultative hyperaccumulator. Chemosphere, 232, 243-253. https://doi.org/10.1016/j.chemosphere.2019.05.193.

Saad, R., Kobaissi, A., Robin, C., Echevarria, G., & Benizri, E. (2016). Nitrogen fixation and growth of *Lens culinaris* as affected by nickel availability: a pre-requisite for optimization of agromining. Environmental and Experimental Botany, 131, 1-9. https://doi.org/10.1016/j.envexpbot.2016.06.010.

Sabadashka, M., Nagalievska, M., & Sybirna, N. (2021). Tyrosine nitration as a key event of signal transduction that regulates functional state of the cell. Cell Biology International, 45(3), 481-497. https://doi.org/10.1002/cbin.11301.

Sakamoto, A., Ueda, M., & Morikawa, H. (2002). *Arabidopsis* glutathione-dependent formaldehyde dehydrogenase is an *S*-nitrosoglutathione reductase. FEBS Letters 515 (1-3), 20-24. https://doi.org/10.1016/S0014-5793(02)02414-6.

Salata, O. V. (2004). Applications of nanoparticles in biology and medicine. J. Nanobiotechnol., 2(1), 1-6, https://doi.org/10.1186/1477-3155-2-3.

Saleh, A. M., Hassan, Y. M., Selim, S., & AbdElgawad, H. (2019). NiO-nanoparticles induce reduced phytotoxic hazards in wheat (*Triticum aestivum* L.) grown under future climate CO_2. Chemosphere, 220, 1047-1057. https://doi.org/10.1016/j.chemosphere.2019.01.023.

Salt, D. E., Prince, R. C., Pickering, I. J., & Raskin, I. (1995). Mechanisms of cadmium mobility and accumulation in Indian mustard. Plant physiology, 109(4), 1427-1433. https://doi.org/10.1104/pp.109.4.1427.

Schaumlöffel, D. (2012). Nickel species: analysis and toxic effects. Journal of trace elements in medicine and biology, 26(1), 1-6. https://doi.org/10.1016/j.jtemb.2012.01.002.

Scherer, M. D., Sposito, J. C., Falco, W. F., Grisolia, A. B., Andrade, L. H., Lima, S. M., ... & Caires, A. R. (2019). Cytotoxic and genotoxic effects of silver nanoparticles on meristematic cells of *Allium cepa* roots: A close analysis of particle size dependence. Science of the Total Environment, 660, 459-467. https://doi.org/10.1016/j.scitotenv.2018.12.444.

Severne, B. C. (1974). Nickel accumulation by *Hybanthus floribundus*. Nature. 248(5451):807-8. https://doi.org/10.1038/248807a0.

Shahzad, B., Tanveer, M., Rehman, A., Cheema, S. A., Fahad, S., Rehman, S., & Sharma, A. (2018). Nickel; whether toxic or essential for plants and environment-A review. Plant physiology and biochemistry, 132, 641-651. https://doi.org/10.1016/j.plaphy.2018.10.014.

Shallari, S., Schwartz, C., Hasko, A., & Morel, J. L. (1998). Heavy metals in soils and plants of serpentine and industrial sites of Albania. Science of the total environment, 209(2-3), 133-142. https://doi.org/10.1016/S0048-9697(98)80104-6.

Sharma, P., Sharma, A., Sharma, M., Bhalla, N., Estrela, P., Jain, A., ... & Thakur, A. (2017). Nanomaterial fungicides: in vitro and in vivo antimycotic activity of cobalt and nickel nanoferrites on phytopathogenic fungi. Global Challenges, 1(9), 1700041. https://doi.org/10.1002/gch2.201700041.

Shen, H. W. Y. L., Ye, W., Hong, L., Huang, H., Wang, Z., Deng, X., ... & Xu, Z. (2006). Progress in parasitic plant biology: host selection and nutrient transfer. Plant Biology, 8(02), 175-185. https://doi.org/10.1055/s-2006-923796.

Sheoran, V., Sheoran, A. S., & Poonia, P. (2009). Phytomining: a review. Minerals Engineering, 22(12), 1007-1019. https://doi.org/10.1016/j.mineng.2009.04.001.

Shi, G., & Cai, Q. (2009). Leaf plasticity in peanut (*Arachis hypogaea* L.) in response to heavy metal stress. Environmental and Experimental Botany, 67(1), 112-117. https://doi.org/10.1016/j.envexpbot.2009.02.009.

Singh, G., & Prasad, S. M. (2024). Interplay mechanism of exogenous hydrogen sulfide and nitric oxide in modulating ascorbate–glutathione cycle under nickel-induced oxidative stress in two paddy field cyanobacteria. Journal of Plant Biochemistry and Biotechnology, 1-18. https://doi.org/10.1007/s13562-024-00929-6.

Singh, V. P., Singh, S., Tripathi, D. K., Prasad, S. M., & Chauhan, D. K. (2021). Plant responses to nanomaterials. Springer International Publishing. https://doi.org/10.1007/978-3-030-36740-4.

Soares, C., Branco-Neves, S., de Sousa, A., Azenha, M., Cunha, A., Pereira, R., & Fidalgo, F. (2018). SiO_2 nanomaterial as a tool to improve *Hordeum vulgare* L. tolerance to nano-NiO stress. Science of the Total Environment, 622, 517-525. https://doi.org/10.1016/j.scitotenv.2017.12.002.

Song, X., Kenston, S. S. F., Kong, L., & Zhao, J. (2017). Molecular mechanisms of nickel induced neurotoxicity and chemoprevention. Toxicology, 392, 47-54. https://doi.org/10.1016/j.tox.2017.10.006.

Song, X., Liu, J., Geng, N., Shan, Y., Zhang, B., Zhao, B., ... & Zhang, Y. (2022). Multi-omics analysis to reveal disorders of cell metabolism and integrin signaling pathways induced by $PM_{2.5}$. J. Hazard. Mater. 424 (Part C), 127573. https://doi.org/10.1016/j.jhazmat.2021.127573.

Souza, J. M., Peluffo, G., & Radi, R. (2008). Protein tyrosine nitration—functional alteration or just a biomarker?. Free Radical Biology and Medicine, 45(4), 357-366. https://doi.org/10.1016/j.freeradbiomed.2008.04.010.

Sreekanth, T. V. M., Nagajyothi, P. C., Lee, K. D., & Prasad, T. N. V. K. V. (2013). Occurrence, physiological responses and toxicity of nickel in plants. International Journal of Environmental Science and Technology, 10, 1129-1140. https://doi.org/10.1007/s13762-013-0245-9.

Staab, C. A., Hellgren, M., & Höög, J. O. (2008). Medium-and short-chain dehydrogenase/reductase gene and protein families: Dual functions of alcohol dehydrogenase 3: implications with focus on formaldehyde dehydrogenase and S-nitrosoglutathione reductase activities. Cellular and Molecular Life Sciences, 65, 3950-3960. https://doi.org/10.1007/s00018-008-8592-2.

Stefanatou, A., Dimitrakopoulos, P. G., Aloupi, M., Adamidis, G. C., Nakas, G., & Petanidou, T. (2020). From bioaccumulation to biodecumulation: Nickel movement from *Odontarrhena lesbiaca* (Brassicaceae) individuals into consumers. Science of the Total Environment, 747, 141197. https://doi.org/10.1016/j.scitotenv.2020.141197.

Strid, A., and Tan, K. (2002). Flora Hellenica; A.R.G. Gantner Verlag K.G.: Ruggell, Liechtenstein, Volume 2.

Szőllősi, R., Molnár, Á., Kondak, S., & Kolbert, Z. (2020). Dual effect of nanomaterials on germination and seedling growth: Stimulation vs. phytotoxicity. Plants, 9(12), 1745. https://doi.org/10.3390/plants9121745.

Tack, F. M. (2010). Trace elements: general soil chemistry, principles and processes. Trace elements in soils, 9-37. Sussex, UK: Blackwell Publishing Ltd, John Wiley and Sons Publishing. http://doi.org/10.1002/9781444319477.

Tailor, G., Chaudhary, J., Jandu, S., Mehta, C., Yadav, M., & Verma, D. (2023). A Review on Plant Extract Based Route for Synthesis of Nickel Nanoparticles: Biological and Photo-catalytic Applications. Results Chem., 101195, https://doi.org/10.1016/j.rechem.2023.101195.

Taş, R., Köroğlu, E., & Celebioglu, H. U. (2021). Green synthesis of nickel nanoparticles using *Peumus Boldus* Koch. Extract and antibacterial activity. International Journal of Innovative Engineering Applications, 5(2), 152-155. https://doi.org/10.46460/ijiea.929625.

Tombuloglu, H., Slimani, Y., Tombuloglu, G., Almessiere, M., Baykal, A., Ercan, I., & Sozeri, H. (2019). Tracking of $NiFe_2O_4$ nanoparticles in barley (*Hordeum vulgare* L.) and their impact on plant growth, biomass, pigmentation, catalase activity, and mineral uptake. Environmental Nanotechnology, Monitoring & Management, 11, 100223. https://doi.org/10.1016/j.enmm.2019.100223.

Uddin, S., Safdar, L. B., Iqbal, J., Yaseen, T., Laila, S., Anwar, S., ... & Quraishi, U. M. (2021). Green synthesis of nickel oxide nanoparticles using leaf extract of *Berberis balochistanica*: Characterization, and diverse biological applications. Microscopy Research and Technique, 84(9), 2004-2016. https://doi.org/10.1002/jemt.23756.

Van der Pas, L., & Ingle, R.A. (2019). Towards an understanding of the molecular basis of nickel hyperaccumulation in plants. Plants 8 (1), 11. https://doi.org/10.3390/plants8010011.

Vasiluk, L., Sowa, J., Sanborn, P., Ford, F., Dutton, M. D., & Hale, B. (2019). Bioaccessibility estimates by gastric SBRC method to determine relationships to bioavailability of nickel in ultramafic soils. Science of the Total Environment, 673, 685-693. https://doi.org/10.1016/j.scitotenv.2019.04.059.

Verbruggen, N., & Hermans, C. (2008). Proline accumulation in plants: a review. Amino acids, 35, 753-759. https://doi.org/10.1007/s00726-008-0061-6.

Voxeur, A., & Höfte, H. (2016). Cell wall integrity signaling in plants: “To grow or not to grow that's the question”. Glycobiology, 26(9), 950-960. https://doi.org/10.1093/glycob/cww029.

Williams, L. E., Pittman, J. K., & Hall, J. L. (2000). Emerging mechanisms for heavy metal transport in plants. Biochimica et Biophysica Acta (BBA)-Biomembranes, 1465(1-2), 104-126. https://doi.org/10.1016/S0005-2736(00)00133-4.

Wright, I. J., Reich, P. B., Westoby, M., Ackerly, D. D., Baruch, Z., Bongers, F., ... & Villar, R. (2004). The worldwide leaf economics spectrum. Nature, 428(6985), 821-827. https://doi.org/10.1038/nature02403.

Xu, S., Guerra, D., Lee, U., & Vierling, E. (2013). *S*-nitrosoglutathione reductases are low-copy number, cysteine-rich proteins in plants that control multiple developmental and defense responses in Arabidopsis. Frontiers in plant science, 4, 430. https://doi.org/10.3389/fpls.2013.00430.

Yan, A., & Chen, Z. (2019). Impacts of silver nanoparticles on plants: a focus on the phytotoxicity and underlying mechanism. International journal of molecular sciences, 20(5), 1003. https://doi.org/10.3390/ijms20051003.

Yadav, V., Arif, N., Kováč, J., Singh, V. P., Tripathi, D. K., Chauhan, D. K., & Vaculík, M. (2021). Structural modifications of plant organs and tissues by metals and metalloids in the environment: A review. Plant Physiology and Biochemistry, 159, 100-112. https://doi.org/10.1016/j.plaphy.2020.11.047.

Yin, L., Cheng, Y., Espinasse, B., Colman, B. P., Auffan, M., Wiesner, M., ... & Bernhardt, E. S. (2011). More than the ions: the effects of silver nanoparticles on *Lolium multiflorum*. Environmental science & technology, 45(6), 2360-2367. https://doi.org/10.1021/es103995x.

Zelko, I., Lux, A., Sterckeman, T., Martinka, M., Kollárová, K., Lišková, D. (2012). An easy method for cutting and fluorescent staining of thin roots. Ann. Bot. 110 (2), 475–478. https://doi.org/10.1093/aob/mcs046.

Zhang, X., Wang, W., Kang, X., & Zhao, L. (2020). Arabidopsis CaM3 inhibits nitric oxide accumulation and improves thermotolerance by promoting *S*-nitrosoglutathione reductase *via* direct binding. Plant Growth Regul. 90, 41-50. https://doi.org/10.1007/s10725-019-00552-9.

Zhou, P., Jiang, Y., Adeel, M., Shakoor, N., Zhao, W., Liu, Y., ... & Zhang, P. (2023). Nickel oxide nanoparticles improve soybean yield and enhance nitrogen assimilation. Environmental Science & Technology, 57(19), 7547-7558. https://doi.org/10.1021/acs.est.3c00959.

Zulfiqar, F., Navarro, M., Ashraf, M., Akram, N. A., & Munné-Bosch, S. (2019). Nanofertilizer use for sustainable agriculture: Advantages and limitations. Plant science, 289, 110270. https://doi.org/10.1016/j.plantsci.2019.110270.

12. List of Publications

MTMT Identifier: 10090424

12. 1. Publications used in this dissertation

Kondak, S., Janovszky, P., Szőllősi, R., Molnár, Á., Oláh, D., Adedokun, O. P., Dimitrakopoulos, P. G., Rónavári, A., Kónya, Z., Erdei, L., Galbács, G., & Kolbert, Z. (2024). Nickel oxide nanoparticles induce cell wall modifications, root anatomical changes, and nitrosative signaling in ecotypes of Ni hyperaccumulator *Odontarrhena lesbiaca*. Environmental Pollution, 341, 122874. https://doi.org/10.1016/j.envpol.2023.122874.

IF: 7.6

Kondak, S., Kondak, D., Kabadayi, O., Erdei, L., Rónavári, A., Kónya, Z., Galbács, G., & Kolbert, Z. (2024). Current insights into the green synthesis, in planta characterization and phytoeffects of nickel nanoparticles and their agricultural implications. Environmental Research, 119665. https://doi.org/10.1016/j.envres.2024.119665.

IF: 7.7

Oliveira, H. C., Seabra, A. B., **Kondak, S.,** Adedokun, O. P., & Kolbert, Z. (2023). Multilevel approach of plant-nanomaterial relationship: from cells to living ecosystems. Journal of Experimental Botany, erad107. http://dx.doi.org/10.1093/jxb/erad107.

IF: 5.8

Szőllősi, R., Molnár, Á., **Kondak, S.,** & Kolbert, Z. (2020). Dual effect of nanomaterials on germination and seedling growth: Stimulation vs. phytotoxicity. Plants, 9(12), 1745. https://doi.org/10.3390/plants9121745.

IF: 4.658

12. 2. Other publications

Kondak, S., Molnár, Á., Dóra, Oláh., & Kolbert, Z. (2022). The role of nitric oxide (NO) in plant responses to disturbed zinc homeostasis. Plant Stress, 100068. https://doi.org/10.1016/j.stress.2022.100068.

IF: 6.8

Oláh, D., **Kondak, S.,** Molnár, Á., Adedokun, O. P., Czékus, Z., Gémes, K., ... & Kolbert, Z. (2023). Suboptimal zinc supply affects the *S*-nitrosoglutathione reductase enzyme and nitric oxide signaling in Arabidopsis. Plant Stress, 10, 100250. https://doi.org/10.1016/j.stress.2023.100250.

IF: 6.8

Molnár, A., **Kondak, S.,** Benkő, P., Janovszky, P., Kovács, K., Szőllősi, R., Gondor, O. K., Oláh, D., Gémes, K., Galbács, G., Janda, T., & Kolbert, Z. (2022). Limited Zn supply affects nutrient distribution, carbon metabolism and causes nitro-oxidative stress in sensitive *Brassica napus*. Environmental and Experimental Botany, 202, 105032. https://doi.org/10.1016/j.envexpbot.2022.105032.

IF: 4.5

Fejes, G., Bodor, T., Szőllősi, R., **Kondak, S.,** Kutasi, K., Fotopoulos, V., & Kolbert, Z. (2025). Nitric oxide as integral element in priming-induced tolerance and plant stress memory. Journal of Experimental Botany, eraf033. https://doi.org/10.1093/jxb/eraf033.

IF: 5.8

Naneli, İ., Bagı, F., **Kondak, S.,** & Özgen, Y. (2020). Response of some rice varieties (*Oryza sativa* L.) to salinity. Journal of Agricultural Biotechnology, 1(1), 1-5.

IF: -

Cumulative IF: 49.658

12. 3. Book chapters

Szőllősi, R., Molnár, Á., Oláh, D., **Kondak, S.,** & Kolbert, Z. (2022). Uptake and Metabolism of Selenium in Plants: Recent Progress and Future Perspectives. Selenium and Nano-Selenium in Environmental Stress Management and Crop Quality Improvement, 79-90. https://doi.org/10.1007/978-3-031-07063-1_5.

Szőllősi, R., Molnár, Á., Oláh, D., **Kondak, S.,** & Kolbert, Z. (2022). Selenium Toxicity and Tolerance in Plants: Recent Progress and Future Perspectives. Selenium and Nano-Selenium in Environmental Stress Management and Crop Quality Improvement, 311-324. https://doi.org/10.1007/978-3-031-07063-1_15.

Bodor, T., Fejes, G., Kondak, D., **Kondak, S.,** Szőllősi, R., & Kolbert, Z. (2025). Karrikin-Related Effects on Plant Development, Stress Tolerance, and Beyond. Strigolactones: Emerging Plant Hormones, 211-234. https://doi.org/10.1002/9781394302826.ch10.

Kondak, S., Kondak, D., Iqbal, N., Adedokun, O.P., Bagi, F., Kabadayi, O. (2025). Rice: A Crop Adapted to Flood. In: Riyazuddin, R., Gupta, R., Ramteke, P.W., Sayyed, R. (eds) Plant Flooding. Plant in Challenging Environments, vol 6. Springer, Cham. https://doi.org/10.1007/978-3-031-83068-6_15.

Iqbal, N., Nauman, M., Jamil, H.M.A., **Kondak, S.,** Singh, K., Riyazuddin, R. (2025). Effects of Flooding Stress on Plant Developmental Stages and Antioxidant Defense System and Its Alleviation Through Agronomic Measures. In: Riyazuddin, R., Gupta, R., Ramteke, P.W., Sayyed, R. (eds) Plant Flooding. Plant in Challenging Environments, vol 6. Springer, Cham. https://doi.org/10.1007/978-3-031-83068-6_3.

12. 4. Conference proceedings

Selahattin Kondak, Patrick Janovszky, Réka Szőllősi, Árpád Molnár, Dóra Oláh, Oluwatosin Peace Adedokun, Panayiotis G. Dimitrakopoulos, Andrea Rónavári, Zoltán Kónya, László Erdei, Gábor Galbács, Zsuzsanna Kolbert. (2024). Ecotype-Dependent Responses to Nickel Oxide Nanoparticles in Ni Hyperaccumulator *Odontarrhena lesbiaca*: Unraveling the Impact Across Cellular, Tissue, Organ, and Molecular Level. In

9th Plant Nitric oxide International Meeting (PNO9), National Institute of Plant Genome Research (NIPGR), New Delhi, India, 110067 (p.52).

Selahattin Kondak, Patrick Janovszky, Réka Szőllősi, Árpád Molnár, Dóra Oláh, Oluwatosin Peace Adedokun, Panayiotis G. Dimitrakopoulos, Andrea Rónavári, Zoltán Kónya, László Erdei, Gábor Galbács, Zsuzsanna Kolbert. (2024). Multi-Level Tolerance Mechanisms of *Odontarrhena lesbiaca* Ecotypes to Nickel Oxide Nanoparticles: Insights from Cellular Defense to Molecular Nitrosative Signaling. In Hungarian Society for Plant Biology, Society's Lecture Series for Young Plant Biologists (FIANÖVELŐ2024), University of Debrecen, Hungary.

Dóra Kondak, **Selahattin Kondak**, Oluwatosin Peace Adedokun, Tamás Bodor, Andrea Rónavári, Ágota Imre-Deák, Zsuzsanna Kolbert. (2024). Nanotechnological Interventions: Exploring the Impact of Nano-Nitric Oxide Donors in *Brassica napus*. In 9th Plant Nitric oxide International Meeting (PNO9), National Institute of Plant Genome Research (NIPGR), New Delhi, India, 110067 (p.14).

Tamás Bodor, Gábor Fejes, **Selahattin Kondak**, Réka Szőllősi, Kinga Kutasi, Zsuzsanna Kolbert. (2024). The effect of seed priming with plasma activated water on germination and RONS content of *Arabidopsis thaliana* L. In 9th Plant Nitric oxide International Meeting (PNO9), National Institute of Plant Genome Research (NIPGR), New Delhi, India, 110067 (p.57).

Gábor Fejes, Tamás Bodor, **Selahattin Kondak**, Réka Szőllősi, Kinga Kutasi, Zsuzsanna Kolbert. (2024). The effect of plasma-activated water on wheat seedling development and the levels of in planta reactive oxygen and nitrogen species. In 9th Plant Nitric oxide International Meeting (PNO9), National Institute of Plant Genome Research (NIPGR), New Delhi, India, 110067 (p.51).

Fernando A. Casian Plaza, Patrick M. Janovszky, Dávid J. Palásti, **Selahattin Kondak**, Zsuzsanna Kolbert, Gábor Galbács. (2024). Advanced laser-induced breakdown spectroscopy-based qualitative analytical methodologies for food and plant-related applications. In: Alapi, Tünde; Berkecz, Róbert; Ilisz, István (eds.) Proceedings of the 30th International Symposium on Analytical and Environmental Problems. Szeged, Hungary: Szegedi Tudományegyetem, 387 p. pp. 241-245., 5 p.

Kondak, Selahattin., Oláh, Dóra., Molnár, Árpád., Janovszky, Patrick., Dimitrakopoulos, Panayiotis G., Galbács, Gábor., & Kolbert, Zsuzsanna. (2022). Uptake and Effect of Nickel Oxide Nanoparticles on Biomass Production and Reactive Molecule Levels in Nickel-Hyperaccumulator *Odontarrhena lesbiaca* Ecotypes. In FIBOK2022 5th National Conference of Young Biotechnologists (p. 87).

Oláh, Dóra., Molnár, Árpád., **Kondak, Selahattin.,** & Kolbert, Zsuzsanna. (2022). Nitric oxide signalling in plant responses of *Arabidopsis thaliana* to limited zinc supply. In FIBOK2022 5th National Conference of Young Biotechnologists (p. 27).

Kondak, Selahattin., Oláh, Dóra., Molnár, Árpád., Dimitrakopoulos, Panayiotis G., & Kolbert, Zsuzsanna. (2021). Nickel oxide (NiO) nanoparticles uptake and effect on biomass production and reactive nitrogen species levels in Ni-hyperaccumulator *Odontarrhena lesbiaca* ecotypes. In XIII Magyar Növénybiológiai Kongresszus (p. 74).

Oláh, Dóra., Molnár, Árpád., **Kondak, Selahattin.,** & Kolbert, Zsuzsanna. (2021). A cinkhiány hatásainak vizsgálata *S*-nitrozoglutation reduktáz mutáns *Arabidopsis thaliana* gyökérrendszerében. In XIII Magyar Növénybiológiai Kongresszus (p. 80).

Kondak, Selahattin., Oláh, Dóra., Molnár, Árpád., & Kolbert, Zsuzsanna. (2021). Zinc Deficiency in *Pisum sativum*: Focusing on Reactive Oxygen, Nitrogen and Sulphur Species. In PNO2021 8th Plant Nitric Oxide International Meeting (NO82020) (p.72).

Oláh, Dóra., **Kondak, Selahattin.,** Molnár, Árpád., & Kolbert, Zsuzsanna. (2021). Zinc deficiency effect of nitric oxide (NO) signaling in *Arabidopsis thaliana*. In PNO2021 8th Plant Nitric Oxide International Meeting (NO82020) (p.76).

Kondak, Selahattin., Kumlay, Ahmet Metin, Bagı, Fatmagül., Yıldırım, Bünyamin., & Alma, Mehmet Hakkı. (2018). Biotechnological Methods for Improvement of Stevia Plant. In I. International Agricultural Science Congress, Van, Türkiye, (p.36).

Kondak, Selahattin., Rezaeieh, Kiarash Afshar Pour., Yıldırım, Bünyamin., & Gürbüz, Bilal. (2016). Ornamental Reproduction Potentials of Stevia (*Stevia rebaudiana*). (*Turkish*: Stevia (*Stevia rebaudiana* Bert.)`nın Süs Bitkisi Olma ve Üretim Potansiyeli) In VI. Ornamental Plants Congress, Antalya, Türkiye, (p. 279-282).

Kondak, Selahattin., Rezaeieh, Kiarash Afshar Pour., Yıldırım, Bünyamin., & Farshi, Sadabadi, Roya. (2016). Coneflowers (*Echinacea* spp.) capability as ornamental crops

(*Turkish*: Ekinezya (*Echinacea* spp.) Süs Bitkisi Olarak Kapasitesi). In VI. Ornamental Plants Congress, Antalya, Türkiye, (p.145).

Kondak, Selahattin., Rezaeieh, Kiarash Afshar Pour., & Yıldırım, Bünyamin. (2016). Worldwide Breeding Studies On Ornamental Plants: From Past To Present (*Turkish*: Dünyada Süs Bitkileri Üzerinde Geçmişten Günümüze Islah Çalışmaları). In VI. Ornamental Plants Congress, Antalya, Türkiye, (p.125).

Kondak, Selahattin., Rezaeieh, Kiarash Afshar Pour., Yıldırım, Bünyamin., & Kumlay, Ahmet Metin. (2016). Floriculture and Ornamental Crops: An Overview to Biotechnological Advances (*Turkish*: Çiçekçilik ve Süs Bitkileri: Biyoteknolojik Gelişmelere Genel Bir Bakış). In VI. Ornamental Plants Congress, Antalya, Türkiye, (p.124).

Rezaeieh, Kiarash Afshar Pour., **Kondak, Selahattin**., Farshi, Sadabadi, Roya., & Gürbüz, Bilal. (2016). Ornamental-Medicinal Plants: Commercially Important Crops (*Turkish*: Süs - Tıbbı Bitkiler: Ticari önemli bitkiler). In VI. Ornamental Plants Congress, Antalya, Türkiye, (p.123).

13. Statement

As the corresponding author and co-author of the following journal publications, I hereby verify that all the findings/results presented in this thesis and the associated scientific publications have not been previously used to obtain any Ph.D. degree and will not be used for such purposes in the future.

Kondak, S., Janovszky, P., Szőllősi, R., Molnár, Á., Oláh, D., Adedokun, O. P., Dimitrakopoulos, P. G., Rónavári, A., Kónya, Z., Erdei, L., Galbács, G., & Kolbert, Z. (2024). Nickel oxide nanoparticles induce cell wall modifications, root anatomical changes, and nitrosative signaling in ecotypes of Ni hyperaccumulator *Odontarrhena lesbiaca*. Environmental Pollution, 341, 122874. https://doi.org/10.1016/j.envpol.2023.122874.

Dr. Zsuzsanna Ördögné Kolbert
Associate Professor
Department of Plant Biology
Faculty of Science and Informatics
University of Szeged, Szeged, Hungary

Kondak, S., Kondak, D., Kabadayi, O., Erdei, L., Rónavári, A., Kónya, Z., Galbács, G., & Kolbert, Z. (2024). Current insights into the green synthesis, in planta characterization and phytoeffects of nickel nanoparticles and their agricultural implications. Environmental Research, 119665. https://doi.org/10.1016/j.envres.2024.119665.

Dr. Zsuzsanna Ördögné Kolbert
Associate Professor
Department of Plant Biology
Faculty of Science and Informatics
University of Szeged, Szeged, Hungary

Oliveira, H. C., Seabra, A. B., **Kondak, S.,** Adedokun, O. P., & Kolbert, Z. (2023). Multilevel approach of plant-nanomaterial relationship: from cells to living ecosystems. Journal of Experimental Botany, erad107. http://dx.doi.org/10.1093/jxb/erad107.

Dr. Zsuzsanna Ördögné Kolbert
Associate Professor
Department of Plant Biology
Faculty of Science and Informatics
University of Szeged, Szeged, Hungary

Szőllősi, R., Molnár, Á., **Kondak, S.,** & Kolbert, Z. (2020). Dual effect of nanomaterials on germination and seedling growth: Stimulation vs. phytotoxicity. Plants, 9(12), 1745. https://doi.org/10.3390/plants9121745.

Dr. Zsuzsanna Ördögné Kolbert
Associate Professor
Department of Plant Biology
Faculty of Science and Informatics
University of Szeged, Szeged, Hungary